R-99-13

Compilation of data for the analysis of radionuclide migration from SFL 3-5

Kristina Skagius, Michael Pettersson, Marie Wiborgh
Kemakta Konsult AB

Yngve Albinsson, Stellan Holgersson
Department of Nuclear Chemistry, CTH

December 1999

Svensk Kärnbränslehantering AB
Swedish Nuclear Fuel
and Waste Management Co
Box 5864
SE-102 40 Stockholm Sweden
Tel 08-459 84 00
+46 8 459 84 00
Fax 08-661 57 19
+46 8 661 57 19

ISSN 1402-3091
SKB Report R-99-13

Compilation of data for the analysis of radionuclide migration from SFL 3-5

Kristina Skagius, Michael Pettersson, Marie Wiborgh
Kemakta Konsult AB

Yngve Albinsson, Stellan Holgersson
Department of Nuclear Chemistry, CTH

December 1999

Keywords: safety assessment, LILW, deep repository, data, uncertainty.

Abstract

A preliminary safety assessment of the deep repository for long-lived, low and intermediate level waste, SFL 3-5, has been made. This report contains a compilation of data selected for the calculations of the migration of radionuclides and toxic metals from the waste to the biosphere. It also contains the data needed for the next step, which is to calculate dose to man from the far-field release figures.

In the preliminary safety assessment it is assumed that SFL 3-5 is located in connection to the deep repository for spent fuel. This makes it possible to utilise site-specific information derived within the safety assessment of the deep repository for spent fuel, SR 97, for the sites Aberg, Beberg and Ceberg. When information from SR 97 is utilised, the values selected are as far as possible those proposed as a '*reasonable estimate*' for the migration calculations in SR 97. The selection of values for parameters specific for the calculation of migration from the SFL 3-5 repository is in general on the pessimistic side. The uncertainty in the selected values is discussed and if possible also quantified.

Sammanfattning

En preliminär säkerhetsanalys har utförts av ett djupförvar för långlivat, låg- och medelaktivt avfall, SFL 3-5. Denna rapport sammanställer valda data att användas i beräkningarna av transport av radionuklider och miljöfarliga metaller från avfallet till biosfären. Rapporten redovisar också data för att beräkna dos till människa från ett utsläpp av radionuklider till biosfären.

Den preliminära säkerhetsanalysen utgår från antagandet att SFL 3-5 lokaliseras till samma plats som djupförvaret för använt bränsle. Därigenom kan platsspecifik information som tagits fram för säkerhetsanalysen av djupförvaret för använt bränsle användas. Säkerhetsanalysen för djupförvaret för använt bränsle benämns SR 97 och de tre hypotetiska platserna som ingår i SR 97 benämns Aberg, Beberg och Ceberg. När data från SR 97 utnyttjas så väljs i möjligaste mån de värden som för beräkningarna i SR 97 har angivits som '*rimliga uppskattningar*'. För parametrar specifika för SFL 3-5 beräkningarna är de valda värdena i huvudsak åt det pessimistiska hållet. Osäkerheterna i valda data diskuteras och i den mån det är möjligt görs en kvantitativ uppskattning.

Summary and overview

A preliminary safety assessment of the deep repository for long-lived, low and intermediate level waste, SFL 3-5, has been made. This report contains a compilation of data selected for the calculations of the migration of radionuclides and toxic metals from the waste to the biosphere. It also contains the data needed for the next step, which is to calculate dose to man from the far-field release figures.

The SFL 3-5 repository can be built as a part of the deep repository for spent fuel or completely separate. However, in the preliminary safety assessment it is assumed that SFL 3-5 is located in connection to the deep repository for spent fuel. This makes it possible to utilise site-specific information derived within the safety assessment of the deep repository for spent fuel, SR 97, for the sites Aberg, Beberg and Ceberg.

The composition of the groundwater and the hydrology at the sites as well as the water composition and hydraulic conditions in the near field are discussed as a background to the selection of data for the migration calculations. These data are compiled in Tables 1 to 4 below, either in terms of the actual values selected or as a reference to the table in the report where the selected values are given. A reference is also given to the section in the report where the selection of the values are discussed and motivated. When information from SR 97 is utilised, the values selected are as far as possible those proposed as a '*reasonable estimate*' for the migration calculations in SR 97. The selection of values for parameters specific for the calculation of migration from the SFL 3-5 repository is in general on the pessimistic side. The uncertainty in the selected values is discussed and if possible also quantified.

Table 1 Compilation of *source term* data selected for the calculations of the migration of radionuclides and toxic metals from SFL 3-5 in Aberg, Beberg and Ceberg.

Parameter	SFL 3	SFL 4	SFL 5	Reference
Radionuclide inventory	Table 6-3	Table 6-3	Table 6-3	Section 6.2
Quantity of toxic metals (kg)	Table 6-4	Table 6-4	Table 6-4	Section 6.3
Cadmium	990			
Lead	19 965		108 592	
Beryllium			300	
Element solubility	Table 7-1	Table 7-1	Table 7-1	Section 7.1.1
Element solubility affected by isosaccharinic acid, ISA	Table 7-6			Section 7.3.2 and Appendix 3
Isotope dilution factor				Section 7.1.2
Nickel			100	
Zirconium			1 000	
Corrosion rate (μm/year)				Section 7.1.4
Steel	1		1	
Zircalloy	0.01		0.01	

Table 2 Compilation of *near-field migration* data selected for the calculation of the migration of radionuclides and toxic metals from SFL 3-5 in Aberg, Beberg and Ceberg.

Parameter	Aberg	Beberg	Ceberg	Reference
Sorption distribution coefficient, K_d (m^3/kg)	Saline GW	Saline and non-saline GW	Non-saline GW	Section 5.3
Concrete	Table 7-4	Table 7-4	Table 7-4	Sections 7.2.1 and 7.2.2
Gravel	Table 7-5	Table 7-5	Table 7-5	Section 7.2.3
Effect of ISA	None	None	None	Section 7.3.2 and Appendix 3
Specific water flow (m/year)				Section 8.1
SFL 3, enclosure	10^{-4}	10^{-5}	10^{-6}	
SFL 3, gravel backfill	0.31	$3.1 \cdot 10^{-2}$	$3.1 \cdot 10^{-3}$	
SFL 4, gravel backfill	3.8	0.38	$3.8 \cdot 10^{-2}$	
SFL 5, enclosure	10^{-4}	10^{-5}	10^{-6}	
SFL 5, gravel backfill	0.32	$3.2 \cdot 10^{-2}$	$3.2 \cdot 10^{-3}$	
Effective diffusivity (m^2/s)				Section 8.2
Structural concrete	$1 \cdot 10^{-11}$	$1 \cdot 10^{-11}$	$1 \cdot 10^{-11}$	
Porous concrete	$1 \cdot 10^{-10}$	$1 \cdot 10^{-10}$	$1 \cdot 10^{-10}$	
Gravel backfill	$6 \cdot 10^{-10}$	$6 \cdot 10^{-10}$	$6 \cdot 10^{-10}$	
Porosity (%)				Section 8.2
Structural concrete	15	15	15	
Porous concrete	30	30	30	
Gravel backfill	30	30	30	

Table 3 Compilation of *far-field migration* data selected for the calculation of the migration of radionuclides and toxic metals from SFL 3-5 in Aberg, Beberg and Ceberg.

Parameter	Aberg	Beberg	Ceberg	Reference
Advective water travel time (years)	10	40	900	Section 9.1.1
Flow wetted surface area (m^2/m^3 water)	770	10 000	1 000	Section 9.1.2
Peclet number	10	10	10	Section 9.2
Diffusion porosity in the rock matrix (%)				Section 9.3
Anions	0.05	0.05	0.05	
Other species	0.5	0.5	0.5	
Effective diffusivity in the rock matrix (m^2/s)	Table 9-3, saline GW	Table 9-3, saline and non-saline GW	Table 9-3, non-saline GW	Section 9.4
Penetration depth into the rock matrix (m)	2	2	20	Section 9.3
Sorption distribution coefficients, K_d (m^3/kg)	Table 7-5, saline GW	Table 7-5, saline and non-saline GW	Table 7-5, non-saline GW	Section 9.5 and Section 7.2.3

Table 4 Compilation of data selected for the calculation of *dose* and the *concentration of toxic metals in the biosphere* caused by the release from SFL 3-5 in Aberg, Beberg and Ceberg.

Parameter	Aberg	Beberg	Ceberg	Reference
Biosphere recipient	Coast-open, Coast-archipelago, Well	Agricultural land, Peatland, Well	Peatland, Well	Section 10.1
Ecosystem-specific dose conversion factor (Sv/Bq)	Tables 10-2 and 10-3	Tables 10-2 and 10-3	Tables 10-2 and 10-3	Section 10.2
Recipient data, i.e. area, depth, volume, water exchange, density, porosity	Table 10-4	Table 10-4	Table 10-4	Section 10.3

The calculations of the near-field transport require data concerning the liberation of radionuclides and toxic metals in the waste as well as data related to the transport of these species in the engineered barriers in the repository. To calculate the liberation from the waste, the initial inventory of radionuclides and toxicants is given as well as potential restrictions in element solubility (Table 1). SFL 3 contains cellulose that may degrade to isosaccharinic acid, ISA, thereby affecting the solubility of certain elements. Metal waste in SFL 5 contains both radioactive and stable isotopes of nickel and zirconium. This isotope dilution could reduce the solubility of radioactive nickel and zirconium. For metal waste with neutron induced activity, the liberation of radionuclides will be determined by the corrosion of the metal. It is therefore suggested that the annual fraction of the initial inventory that is released from the metals due to corrosion is given by the mean corrosion time of the waste. The mean corrosion time is estimated from the average thickness of the metals exposed to corrosion and the expected corrosion rate of Zircalloy and steel.

The near-field migration calculation requires data on sorption, porosity and diffusivity in concrete and in gravel backfill, as well as data on the water flow in the concrete encapsulation in SFL 3 and SFL 5 and in the gravel backfill in all three repository parts. The selected values of these parameters are compiled in Table 2. Sorption data are selected considering the salinity of the groundwater at the three sites as well as changes in water composition due to leaching of the concrete. The concentration of ISA in the waste packages is estimated to be too low to have any effect on element sorption. The water flow in the near-field barriers is derived based on results from regional hydrology modelling of the three sites and a generic modelling of the near-field hydrology. These modelling results are described in Chapter 4 and in Appendices 1 and 2.

The model applied for calculation of the migration in the far field is a one-dimensional model for migration along a single flow path in the geosphere. The flow related input parameters to the model are the advective water travel time, the flow wetted surface area and the Peclet number. In addition, the model requires data on sorption, diffusivity and diffusion porosity in the rock matrix as well as the maximum allowed diffusion depth into the rock matrix. The values selected for these parameters are compiled in Table 4. The values of the advective water travel time and the flow wetted surface area are selected based on results of a regional hydrology modelling of the three sites and

site specific data from SR 97 on the flow wetted surface area. The Peclet number is also selected in accordance with the values used in SR 97. The values of the remaining parameters are the same as those selected as a '*reasonable estimate*' in SR 97.

The data selected for the dose calculations and for the estimation of the concentration of toxic metals at the ground surface are compiled in Table 4. The calculation of dose is made by applying ecosystem-specific dose conversion factors, EDF's, to the calculated release of radionuclides from the far field. The results from the regional hydrology modelling are used to determine the discharge areas on the ground surface for water passing the location of the repository. The classification of the three sites into different ecosystems that is made in SR 97 is then used to identify the ecosystem in the discharge area. The regional hydrology modelling show no release to any of the wells presently located in the areas. Despite this a well is selected as biosphere recipient at all sites, since it can not be excluded that wells in the future will be founded at the location of the release areas. The EDF's derived within SR 97 are selected for the dose calculations. Recipient data in terms of area, volume, depth, water exchange rate, density and porosity are needed to convert the release of toxic metals from the far field to a concentration of these metals in the biosphere recipient. The recipient data selected are the same as those used in SR 97 to calculate the ecosystem-specific dose conversion factors.

Contents

1 Introduction

1.1 Aim and background

A preliminary safety assessment of the repository for long-lived low and intermediate level waste, SFL 3-5, has been made. As a part of this assessment, the migration of radionuclides and chemotoxic metals from the SFL 3-5 repository to the biosphere is evaluated. The aim of this report is to compile and motivate the input data used for modelling the transport of radionuclides and other substances in the near field and the far field, and for transforming the release of radionuclides from the far field to dose to man.

1.2 Structure of report

In Chapter 2, the input data needed for modelling the migration of radionuclides and toxic metals in the near field and the far field and for estimating the consequences of the release to the biosphere are identified. A brief description of the SFL 3-5 repository is given in Chapter 3 and the waste to be deposited is described in Chapter 6. The results of hydrology calculations are discussed in Chapter 4 as a background to the selection of input data to the migration calculations. The water chemistry is important since it affects several parameters determining the migration of radionuclides in the near field and the far field. The expected water composition is therefore discussed in Chapter 5. In Chapters 7 and 8, the chemical and physical data for the near field are compiled. This includes solubility and sorption of radionuclides as well as data related to the materials used in the repository and the water flow through the SFL 3-5 repository. Far-field migration data are given in Chapter 9, and finally data needed for determining the consequences of the release to the biosphere are summarised in Chapter 10.

The evaluation of flow and transport parameters in the far field of SFL 3-5 in Aberg, Beberg and Ceberg are given in Appendices 1 and 2. The results given are the advective travel times for water in the geosphere and the location of the release points in the biosphere. The waste in SFL 3 contains organic materials that can form complexing agents. The effect of the complexing agent isosaccharinic acid, ISA, on sorption and solubility in SFL 3 is discussed in Appendix 3. The effect of heat generated by the decay of radionuclides on the temperature in the repository is evaluated in Appendix 4.

2 Models and data requirements

The calculations of the migration of radionuclides and other toxicants than radionuclides from the SFL 3-5 repository to the biosphere are carried out by two models in series, the near-field model COMP24 and the far-field model FARF31. The near-field model is used to calculate the migration in the engineered barriers by advection and diffusion, and the output is the release rate of radionuclides and toxicants from the engineered barriers to the water in the surrounding rock. The far-field model is used to calculate transport by advection in the geosphere, with the output from the near-field model as input and the release rate of radionuclides and other toxicants from the geosphere to the biosphere as a result. The release rate of radionuclides from the geosphere to the biosphere is converted to dose by the use of ecosystem-specific dose conversion factors.

2.1 Near-field model

COMP24 is a compartment model that can handle migration by both diffusion and advection and it also includes chain decay. This model is a further development of the model COMP23 (Romero *et al.,* 1995) that is used in SR 97 for the near-field modelling of radionuclide transport from the deep repository for spent fuel (SKB, 1999). The basic information needed for setting up the model and selecting input data for the calculations concerns:

- Geometry and material composition of waste packages and near-field barriers. The geometry is needed for dimensioning of the compartments and the composition of materials will affect the selection of physical and chemical data affecting the transport in the compartments.

- Water chemistry in near-field barriers. The water composition will affect the solubility and sorption coefficients of radionuclides and other toxicants, and possibly also the diffusivity of some species. The water chemistry is dependent on the composition of the materials in the repository, but also on the groundwater composition at the actual site.

- Near-field hydrology. The near-field hydrology will determine the magnitude and the direction of the water flow in the different near-field barriers. It is dependent on the properties of the near-field barriers and on the hydrological situation at the actual site.

The input data required for carrying out the calculations are:

- The initial inventory of radionuclides and other toxicants in the waste. This is the source term for the near-field migration.

- Dissolution rates and solubilities of radionuclides and other toxicants. The dissolution rate and the solubility may in some cases limit the source term for the near-field migration.

- Sorption coefficients for radionuclides and other toxicants on materials in the waste packages and near-field barriers.

- Transport parameters in terms of magnitude and direction of water flow, porosity and diffusivity in waste packages and near-field barriers.

2.2 Far-field model

FARF31 is a one-dimensional model for migration along a single flow path in the geosphere (Norman and Kjellbert, 1990). This model is also used for calculations of the radionuclide migration in the geosphere in the SR 97 analysis of the deep repository for spent fuel (SKB, 1999). The model considers advection and dispersion along a single path and diffusion into and sorption in the rock matrix transverse the path. It also takes chain decay into account. The basic information needed for selecting input data to the far-field calculations concerns the hydrogeology and the groundwater chemistry at the actual sites.

The direct input parameters to the model are:

- The advective travel time for water in the geosphere. This is a theoretical quantity used in the transfer of results from calculations with hydro models to transport models. It could be seen as the transport time in the geosphere for a particle moving with the same velocity as the water without interacting with the rock.

- The Peclet number

- The flow-wetted surface area per volume of water

- The rock matrix porosity and the maximum penetration depth into the rock matrix

- The effective diffusivity in the rock matrix

- The sorption coefficient for radionuclides and other toxicants in the rock matrix

2.3 Dose calculations

Nordlinder *et al.* (1999) have applied a biosphere model (Bergström *et al.,* 1999) to derive ecosystem-specific dose conversion factors, EDF, for the ecosystems at the three sites included in SR 97. These factors give the dose to a critical group in Sv/year resulting from a release to the actual ecosystem of 1 Bq/year of each nuclide. With the help of maps, each site is divided into squares, 250x250 m in size. Each square is classified based on the dominating type of ecosystem within the square. The EDF that should be used is then given by the classification of the square corresponding to the location where the discharge of radionuclides from the geosphere occurs.

The information required for the conversion of the radionuclide release rate from the geosphere to dose to a critical group is then:

- The release rate of radionuclides from the geosphere
- The location of the discharge area on the ground surface for groundwater passing through the location of the repository
- The ecosystem at the discharge point and the EDF for this ecosystem

The release of radionuclides to a well is also illustrated. The water capacity and the EDF for the wells are therefore also needed.

2.4 Evaluation of release of other toxicants than radionuclides

The release of other toxicants than radionuclides from SFL 3-5 is also calculated and the results are given as the concentration in the primary recipient in the biosphere. The ecosystems and wells in question are the same as those used for estimating the radiological dose.

The data required for evaluation of the release of toxicants other than radionuclides are:

- The release rate of toxicants from the geosphere
- The primary recipient for the toxicants released from the geosphere
- The recipient volume or water turn over in the recipient
- The water capacity of wells at the three sites

3 The SFL 3-5 repository concept

3.1 Repository location and layout

The deep repository for long-lived low and intermediate level waste, SFL 3-5, can be built as a part of the deep repository for spent fuel or completely separate. In the preliminary safety assessment it is assumed that SFL 3-5 is a part of the deep repository for spent fuel. Layouts for the repositories in Aberg, Beberg and Ceberg have been proposed by Munier *et al.* (1997). In those layouts the same access ramp will be used, but the position of the SFL 3-5 repository will be about 1 km downstream of the nearest canister position in the spent fuel repository.

The position of the SFL 3-5 repository at the three different sites is required for calculations of the water flow in the repository and for evaluating water travel times and discharge points for water leaving the repository (Appendices 1 and 2). The co-ordinates for the edges of the SFL 3-5 repository have been estimated from the layouts proposed in Munier *et al.* (1997) and are given in Table 3-1. It should be noted that an older layout of the SFL 3-5 repository is used in Munier *et al.* (1997). The repository area is larger in the present layout of SFL 3-5. Effects of this discrepancy in repository area will most likely be small in relation to the effects of uncertainties in hydrogeological parameter values used in the calculations.

Table 3-1 Co-ordinates for the position of the SFL 3-5 repository in Aberg, Beberg and Ceberg (derived from information in Murnier *et al.*, 1997).

Site	RAK		Depth below surface (m)	Local co-ordinates	
	E	N		E	N
Aberg	6365262	1556216	300	3800	6300
	6365331	1556304	300	3850	6400
	6365443	1556229	300	3975	6350
	6365374	1556141	300	3925	6250
Beberg	1617390	6696540	360		
	1617390	6696690	360		
	1617260	6696690	360		
	1617260	6696540	360		
Ceberg	1664600	7044400	375		
	1664740	7044390	375		
	1664750	7044540	375		
	1664610	7044550	375		

Based on the results from the prestudy of the SFL 3-5 repository (Wiborgh, 1995) a modification of the layout of the SFL 3-5 repository was made. The present layout of the SFL 3-5 repository is shown in Figure 3-1. The repository consists of two parallel rock vaults, SFL 3 and SFL 5, surrounded by transport tunnels. These transport tunnels will be used as deposition tunnels for decommissioning waste, SFL 4.

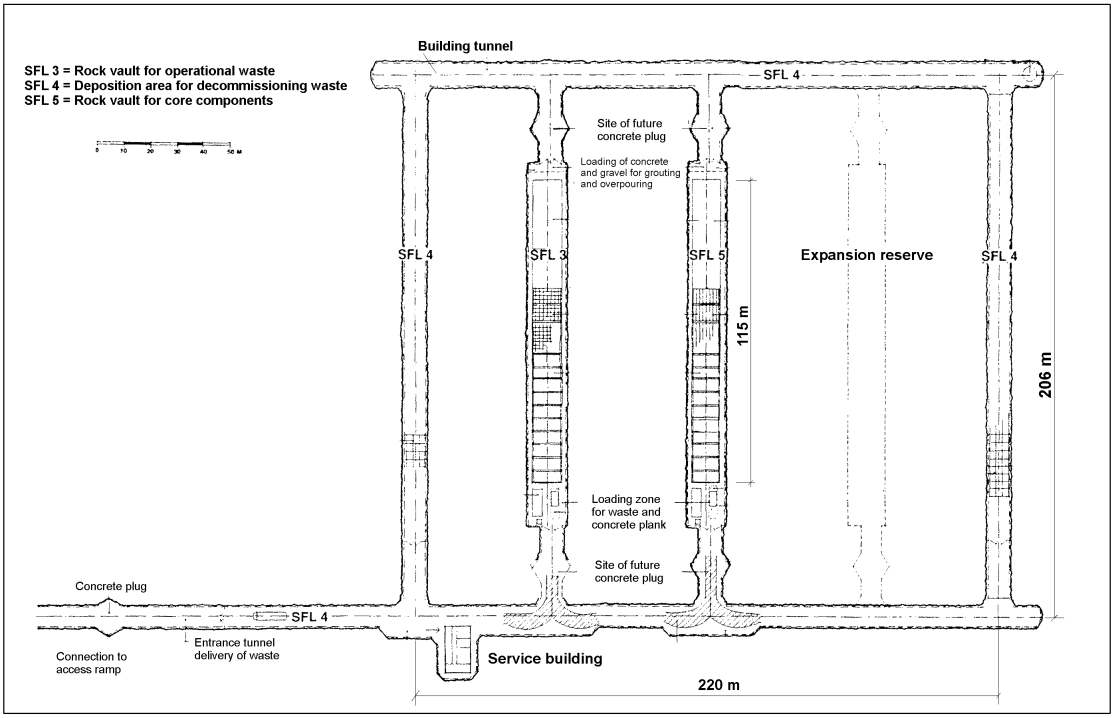

Figure 3-1 The SFL 3-5 repository layout.

3.2 SFL 3 and SFL 5

The SFL 3 and SFL 5 are identical in design (see Figures 3-1 and 3-2). The rock vaults are 133 m long, 14 m wide and have a height of about 19 m. The vaults contain a concrete building that is founded on a 0.5 m thick layer of gravel. The concrete building is 114.6 m long, 10.8 m wide and 10.7 m high. It is divided into three sections and each section is in turn divided into smaller compartments by inner walls transverse to the length of the building (see Figure 3-3). The bottom plate of the building is 0.5 m thick and the thickness of both outer and inner walls is 0.4 m.

The waste packages are piled in the compartments in the concrete building and porous concrete is added in order to fill up the voids between the waste packages and the concrete walls. A lid of pre-fabricated concrete elements and a layer of concrete that is cast on top of the elements cover each section. The thickness of the lid is 0.6 m.

At repository closure, the rock vaults are backfilled with gravel. The dimensions and volumes of different construction materials in SFL 3 and SFL 5 are summarised in Table 3-2.

Table 3-2 Dimensions and volume of construction materials used in SFL 3 and SFL 5.

Material	Volume (m^3)	Thickness (m)
Structural concrete	3190	
- bottom plate	620	0.5
- lid	680	0.6
- outer walls	1020	0.4
- inner walls	870	0.4
Shotcrete	~ 500	
- roof	~ 250	0.05-0.1
- walls	~ 250	0.03-0.05
Porous concrete [a)]	~ 800	
Gravel backfill	21000	
- foundation		0.5
- outside concrete walls		1.6
- above concrete lid		7-8

a) Volume available for porous concrete inside the compartments if all waste packages are containers or moulds. The volume of porous concrete will be larger in SFL 3 since it also will contain waste drums.

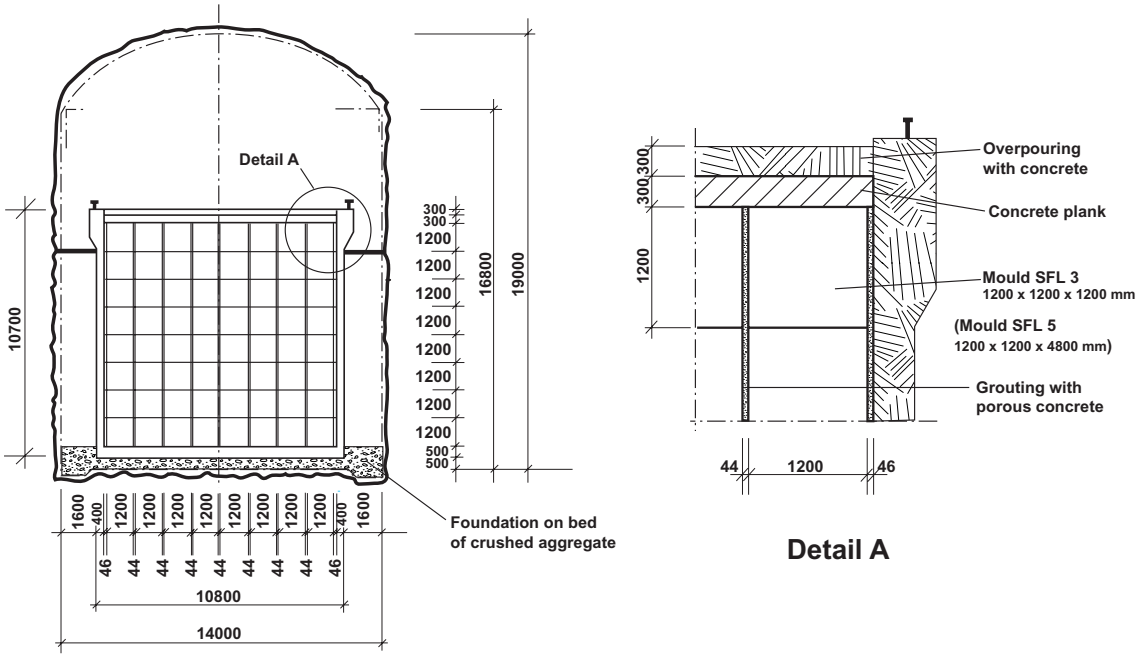

Figure 3-2 Cross-section perpendicular to the main axis of the SFL 3 and SFL 5 tunnels.

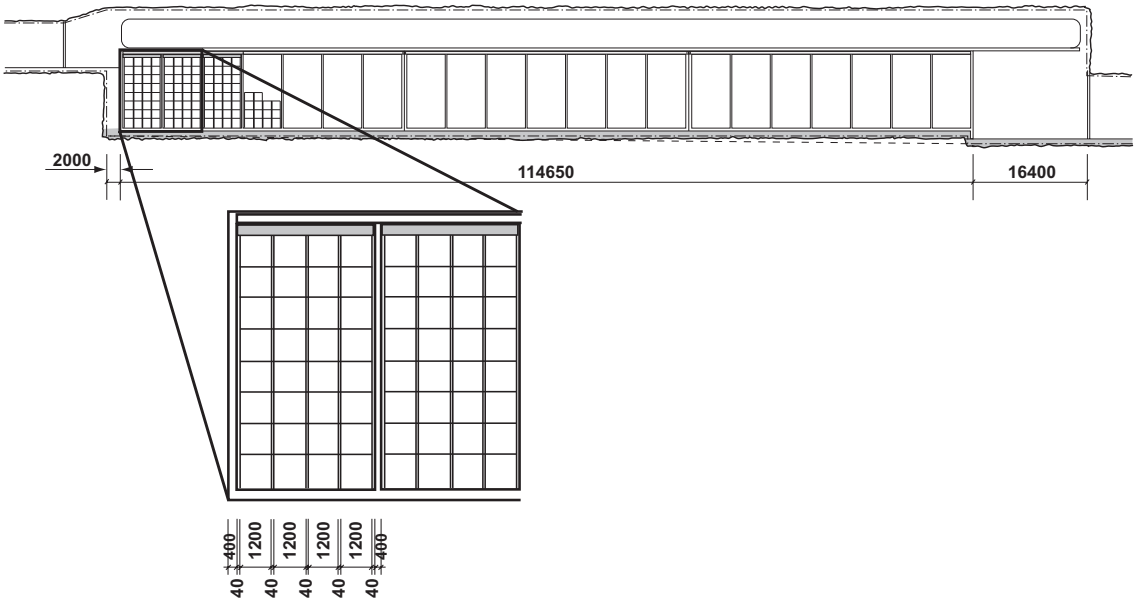

Figure 3-3 Cross-section along the main axis of the SFL 3 and SFL 5 tunnels.

3.3 SFL 4

Surrounding the SFL 3 and SFL 5 tunnels is the rectangular SFL 4 tunnel (see Figure 3-1). The tunnel has a total length of approximately 900 m, a width of 8 m, and a height of 6.5 m. A cross section of the tunnel is shown in Figure 3-4.

Steel containers with the waste are placed directly on a 20 cm thick layer of reinforced concrete, which covers a bed of packed gravel. Approximately 650 m of the tunnel is needed for depositing the estimated waste volume. When deposition is completed, the tunnel will be backfilled with approximately 30 000 m^3 of gravel.

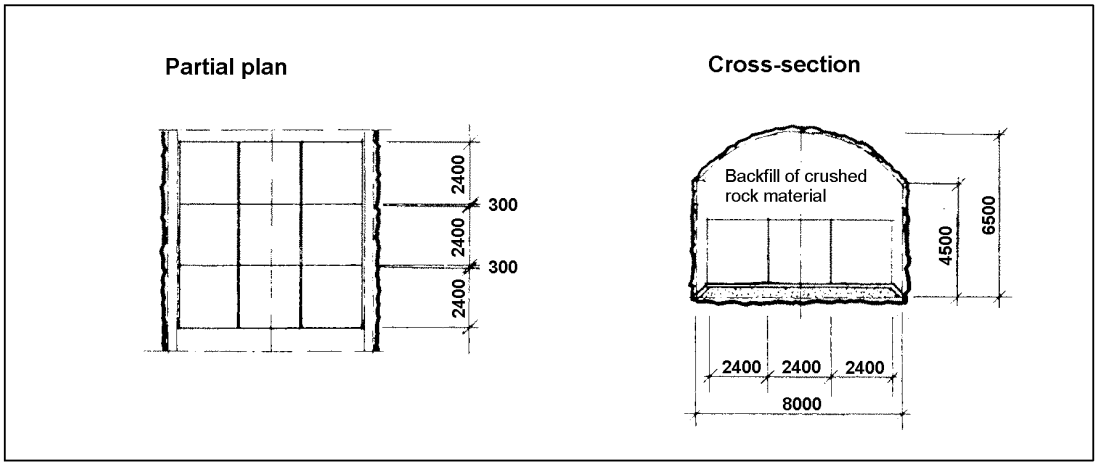

Figure 3-4 Cross-section of the SFL 4 tunnel.

4 Hydrology

The water flow in the different near-field barriers in SFL 3-5 has been studied by performing a generic hydrogeological modelling (Holmén, 1997). The results are given as multiples of the prescribed regional specific flow in the rock for different directions of the regional flow relative the tunnel system.

The regional hydrogeological models set up for Aberg, Beberg and Ceberg within the safety assessment of the deep repository for spent fuel, SR 97, have been used to estimate the flow direction and specific groundwater flow at the proposed location of the SFL 3-5 repository at these sites (see Appendices 1 and 2). These regional hydrogeological models were also used to estimate other parameters required as input to the far-field migration modelling (see Chapter 9).

4.1 Specific groundwater flow and flow direction

The regional hydrogeological modelling carried out for the SFL 3-5 repository location in Aberg, Beberg and Ceberg is described in Appendices 1 and 2. The calculated size and direction of the groundwater flow in the repository area are given in Table 4-1.

Table 4-1 Calculated specific groundwater flow and flow direction in the SFL 3-5 repository area in Aberg, Beberg and Ceberg (Appendices 1 and 2).

	Specific flow (l/m^2,year)			Flow direction (° from horizontal) [1)]		
	Aberg	Beberg	Ceberg	Aberg	Beberg	Ceberg
Mean	27	3	0.04	-31	-6	-1
Minimum	6	2	0.04	-84	-9	-18
Maximum	64	4	0.05	11	-2	17

[1)] A negative flow direction corresponds to a flow directed downwards relative the horizontal plane

4.2 Water flow in near-field barriers

The generic modelling of the water flow in the near-field barriers of SFL 3-5 was carried out as a part of a larger study on the flow of groundwater in closed tunnels (Holmén, 1997). The SFL 3 and SFL 5 parts were modelled as tunnels containing a concrete encapsulation, representing the concrete building and its interior, and a surrounding flow barrier. The encapsulation was defined as a homogeneous medium with a hydraulic conductivity 10 times that of the rock mass surrounding the tunnels. The flow barrier was also defined as a homogeneous medium with a varying hydraulic conductivity. In the case where the flow barrier consisted of gravel the hydraulic conductivity was set to 10^5 times that of the rock mass. The SFL 4 tunnel was assumed to be either empty or filled with gravel and was modelled as a homogeneous medium. When filled with gravel, the hydraulic conductivity was set to 10^4 times that of the rock mass.

The water flow in the different parts of the repository was calculated for different directions of the groundwater flow. The results are given in terms of a factor between the flow in the repository barriers and the regional specific groundwater flow. This factor for the total flow in the different near-field barriers in SFL 3-5 is given in Table 4-2 for some different directions of the groundwater flow and the above given values of the relative hydraulic conductivity. The total flow is defined as the total amount of water that has entered the barrier.

Table 4-2 Factor between the total flow in the near-field barriers in SFL 3-5 and the regional specific groundwater flow (from Holmén, 1997).

Flow direction	SFL 3		SFL 4	SFL 5	
	Encapsulation	Backfill	Backfill	Encapsulation	Backfill
Horizontal, along SFL 3 and SFL 5	1	6 000	48 000	1	6 200
Horizontal, at right angle to SFL 3 and SFL 5	0.6	3 000	56 000	0.7	3 100
Vertical	1.8	5 800	11 000	1.8	5 900

The hydraulic conductivity in the rock in the repository area is of the order of (Appendices 1 and 2):

10^{-7} m/s in Aberg

10^{-8} m/s in Beberg, and

10^{-10} m/s in Ceberg.

The expected hydraulic conductivity in intact structural concrete is of the order of 10^{-12} to 10^{-11} m/s (Höglund and Bengtsson, 1991). The hydraulic conductivity in concrete that to some extent contains penetrating cracks is expected to be of the order of 10^{-8} m/s. This is based on a theoretical evaluation that shows that the overall conductivity is lower than 10^{-9} m/s for fully penetrating cracks with apertures of 10 μm or less every metre and lower than 10^{-7} m/s for fully penetrating cracks with apertures of 100 μm or less every ten metres (Höglund and Bengtsson, 1991).

The hydraulic conductivity of coarse gravel is about $10^{-2} – 10^{-1}$ m/s and of sand and gravel about $10^{-5} – 10^{-2}$ m/s (de Marsily, 1986). Freeze and Cherry (1979) give the hydraulic conductivity of gravel in the range of $10^{-3} – 1$ m/s and of clean sand of approximately $10^{-6} – 10^{-2}$ m/s. A value of 10^{-4} m/s is here considered as a representative value for a gravel backfill.

The results given in Table 4-2 are for a conductivity contrast of 10 between the concrete encapsulation and the rock and for a conductivity contrast of 10^5 between the gravel backfill and the rock in SFL 3 and SFL 5. These contrasts in conductivity are not in agreement with the conductivity contrasts obtained using the expected conductivity in gravel backfill, concrete encapsulation and rock at the three sites. However, results from flow calculations in a single tunnel with barriers with varying conductivity show that

the flow in the encapsulation is inversely proportional to the contrast in conductivity between the gravel backfill and the concrete encapsulation. This is valid as long as the gravel backfill is sufficiently permeable, i.e. the conductivity in the backfill is equal to or greater than 1 000 times the conductivity in the rock (Holmén, 1997). This condition is met for all three sites. Furthermore, the contrast in conductivity between the gravel backfill and the concrete encapsulation is in agreement with that used in the flow calculations. This means that the results given in Table 4-2 can be used to calculate the flow in the encapsulation in SFL 3 and SFL 5 at all three sites. In addition, the results in Holmén (1997) indicate that the total flow in the gravel backfill is approximately constant for a conductivity in the backfill that is equal to or greater than 1 000 times that in the rock. This is the case at all three sites and the results in Table 4-2 can then also be used to calculate the water flow in the gravel backfill in SFL 3 and SFL 5.

The long SFL 4 tunnel that surrounds SFL 3 and SFL 5 can act as a hydraulic cage when the regional flow is horizontal or nearly horizontal and the conductivity in the SFL 4 tunnel is at least 100 times higher than in the rock mass (Holmén, 1997). This means that the water flow in SFL 3 and SFL 5 as well as in SFL 4 may be affected by the conductivity in the SFL 4 tunnel. The flow calculations were carried out for a contrast in conductivity of 10^4 between the SFL 4 tunnel and the rock. This corresponds to the situation at Beberg while this conductivity contrast is 10^3 in Aberg and 10^6 in Ceberg. However, the same calculation results are also used for Aberg and Ceberg. For Ceberg with an expected conductivity contrast higher than 10^4, this means that the flow in the barriers in SFL 3 and SFL 5 is overestimated, while the flow in SFL 4 is not affected. For Aberg with an expected conductivity contrast lower than 10^4, this may mean that the water flow in the barriers in SFL 3 and SFL 5 are underestimated by at most about 40%. The water flow in SFL 4 is overestimated by the same order of magnitude (Holmén, 1997).

5 Temperature and water chemistry

5.1 Temperature

The average temperature gradient in Aberg is estimated to be 15.0°C/km, and a mean temperature of 14.6°C has been measured at a depth of 500 m (Ahlbom *et al.*, 1995). In Beberg, the average temperature gradient is estimated to be 12.7°C/km, and measurements in bore holes gave a mean temperature of 11.6°C at a depth of 500 m in the rock mass (Ahlbom *et al.*, 1995). The mean temperature at a depth of 500 m in Ceberg is 10.9°C, and the temperature gradient is 15.5°C/km (Ahlbom *et al.*, 1995). Based on these values the mean temperature at the proposed depth of the SFL 3-5 repository at the three sites is estimated to be about 11.6°C at 300 m depth in Aberg, about 10.9°C at 360 m depth in Beberg and about 9°C at 375 depth in Ceberg.

Heat will be generated in the waste in SFL 3-5 due to loss of energy as the radionuclides decay. Radioactive decay of ^{60}Co and ^{63}Ni in SFL 5 will dominate the heat generation. The effect of heat generation due to radioactive decay on repository temperature has been evaluated (Appendix 4). The calculations show that the increase in average temperature in the repository and 20 m out in the surrounding rock 100 years after repository closure is less than 3°C. The temperature inside the waste will be negligibly higher than the average temperature in the repository and surrounding rock.

The heat generated in SFL 3 and SFL 4 is about 10 % of the heat generated in SFL 5. It can therefore be concluded, that the increase in temperature in SFL 3-5 is small and the influence on the long-term properties of the barriers and the water flow is negligible.

5.2 Groundwater chemistry

Four types of reference groundwater have been defined for SR 97 (Laaksoharju *et al.,* 1998). These waters represent the chemical composition of groundwater from four, near vertical and deep bore hole sections in Aberg, Beberg and Ceberg. In Aberg this groundwater is saline while it is non-saline in Ceberg. In Beberg both saline and non-saline groundwater are present. Two reference waters, one saline and one non-saline, are therefore defined for Beberg. The composition of the reference waters is given in Table 5-1.

Table 5-1 Chemical composition of reference waters in Aberg, Beberg and Ceberg (Laaksoharju *et al.*, 1998).

Groundwater components	Unit	Aberg saline	Beberg 1 saline	Beberg 2 non-saline	Ceberg non-saline
Bore hole		KAS02	BFI01	KFI07	KGI04
Date of measurement		88-05-04	86-10-27	80-11-19	82-07-04
Depth	m	528	436	508	384
Drilling water content	%	0.19	0.02	–	11.03
Na^+	mg/l	2 100	1 700	275	105
K^+	mg/l	8	13	2	2
Ca^{2+}	mg/l	1 890	1 650	142	21
Mg^{2+}	mg/l	42	110	17	1
Sr^{2+}	mg/l	35	21	–	–
Fe^{2+}	mg/l	0.24	–	1.80	0.05
Mn^{2+}	mg/l	0.29	0.82	0.13	0.01
HCO_3^-	mg/l	10	47	278	18
SO_4^{2-}	mg/l	560	370	49	0.1
Cl^-	mg/l	6 410	5 500	555	178
I^-	mg/l	–	0.12	–	0.14
Br^-	mg/l	40	32	–	–
F^-	mg/l	1.5	1.2	1.5	3.2
HS^-	mg/l	0.15	<0.01[1)]	–	<0.01[1)]
NH_4^+ calculated as N	mg/l	0.03	0.35	0.09	0.01
NO_3^- calculated as N	mg/l	<0.010[1)]	<0.005[1)]	<0.002[1)]	0.009
NO_2^- calculated as N	mg/l	<0.001[1)]	0.005	0.010	<0.001[1)]
$PO_{4.tot}$ calculated as P	mg/l	0.005	0.005	0.040	0.008
SiO_2 calculated as Si	mg/l	4.1	5.4	5.6	4.7
DOC (dissolved organic carbon)	mg/l	1	–	6	2
Eh[2)]	mV	-308	–	-250	-202
pH[2)]		7.7	7.0	7.9	9.3

[1)] *below the detection limit*
[2)] *see Laaksoharju et al., 1998*

5.3 Near-field water chemistry

The development of the water composition in the near-field barriers in SFL 3-5 is discussed by Karlsson *et al.* (1999). The expected water composition after water saturation as well as the development in a longer time perspective is given for both a saline and a non-saline intruding groundwater (Aberg and Ceberg reference water). The aspects of the water composition that are of importance for the selection of chemical data for the modelling of radionuclides and other toxicants in the near-field barriers are summarised below.

The waste in SFL 3 contains organic materials, and an increase in the content of dissolved organic matter in the near-field water in SFL 3 is anticipated. Part of the waste generated organic substances are similar in character to natural dissolved organic substances, but other parts may form strong complexes with some of the radionuclides. This is further discussed in Section 7.3.

5.3.1 SFL 3 and SFL 5

In SFL 3 and SFL 5, where large amounts of concrete is present, the water composition inside the concrete enclosure and in the surrounding gravel backfill will be affected by both leaching of the concrete and the composition of the intruding groundwater. The expected conditions and ranges in water composition of the important elements are given in Table 5-2. These water compositions are expected to remain for time periods of the order of hundreds of thousands of years after saturation provided that the groundwater chemistry does not change (Karlsson *et al.,* 1999).

Table 5-2 Expected water composition in the near-field barriers in SFL 3-5 for a saline and a non-saline intruding groundwater. Compiled from Karlsson *et al.,* (1999)

	Concrete enclosure, SFL 3 and 5 and waste packages, SFL 4		Gravel fill, SFL 3, 4 and 5	
	Saline water	**Non-saline water**	**Saline water**	**Non-saline water**
Redox	Reducing conditions		Reducing conditions	
pH	13.1 $\rightarrow$ 12.5[a]	13.1 $\rightarrow$ 12.5[a]	7.7 – 12.5[b]	9.3 – 12.5[b]
Important cations				
Na^+ (mmol/l)	91	28 $\rightarrow$ 5[a]	91	5
K^+ (mmol/l)	83 $\rightarrow$ 0.2[a]	83 $\rightarrow$ 0.05[a]	0.2	0.05
Ca^{2+} (mmol/l)	1 $\rightarrow$ 20[a]	1 $\rightarrow$ 20[a]	$\leq$ 47	$\leq$ 0.5
Mg^{2+} (mmol/l)	$\leq$ 0.02	$\leq$ 0.02	$\leq$ 2	$\leq$ 0.04
Important anions				
Cl^- (mmol/l)	181	5	181	5
$CO_3^{2-}{}_{tot}$ (mmol/l)	0.1	0.1	$\leq$ 0.2	$\leq$ 0.3
SO_4^{2-} (mmol/l)	6	0.001	6	0.001
Complexing agents				
ISA (mmol/l)	< 0.1[c]	< 0.1[c]		
Colloids (mg/l)	< 0.05	< 0.05	< 0.05	< 0.05

[a] The arrow $\rightarrow$ shows how the water will change with time

[b] Possible range of pH in the water in the gravel fill

[c] inside waste packages with cellulose in SFL 3, see Section 7.3 and Appendix 3

Redox

The oxygen entrapped in the repository at repository closure will soon be consumed by reactions such as steel corrosion, oxidation of ferrous iron and sulphides and decomposition of organic material and reducing conditions will be created in the near-field barriers (Karlsson *et al.*, 1999).

pH

In the concrete enclosure pH may initially be high, above pH = 13. Leaching of alkali hydroxides and portlandite will lead to a decrease in pH, but as long as portlandite is remaining in solid phase pH will be maintained at about 12.5. When the cement phase is

depleted of portlandite dissolution of calcium silicate hydrate begins. A gradual reduction of pH to about 10 occurs during this dissolution phase (Karlsson *et al.*, 1999).

Experiments have shown that it will take of the order of 2 000 porewater exchange cycles before portlandite is depleted and pH falls below 12.5 (Engkvist *et al.,* 1996). Depletion by water flowing through the concrete enclosure only would mean that it will take many millions of years to remove all portlandite from the concrete in SFL 3 and SFL 5. This is due to the low water flow through the concrete. Removal of portlandite by diffusion can be faster, but it will still take several thousands of years up to hundreds of thousands of years before the leaching front has reached the interior of the concrete enclosure (Karlsson *et al.,* 1999).

Leaching of alkali hydroxides and portlandite from the concrete enclosure will increase the pH in the surrounding gravel backfill. However, this high pH can be neutralised by dissolution of silicate minerals in the backfill by hydrolysis reactions and precipitation of secondary minerals, such as CSH-phases, CASH-phases and zeolites. Some simple mass balance calculations indicate that neutralisation of all hydroxide from the concrete in SFL 3 and SFL 5 would be possible without exceeding a reaction depth of 50 μm in the fill material (Karlsson *et al.*, 1999). In addition, the kinetics of the silica dissolution seems to be faster than the leaching rate of OH^- (Karlsson *et al.,* 1999). These results indicate that the gravel backfill could have high enough buffering capacity to neutralise OH^- leached from the concrete. No enhanced pH would then be expected outside the near field of the SFL 3 and SFL 5. However, in the gravel backfill the pH would vary in the range between the pH of the ambient groundwater and pH 12.5, depending on time and distance from the concrete.

Important cations

The sodium concentration in the concrete enclosure will be determined by the sodium concentration in the intruding groundwater (Karlsson *et al.*, 1999). However, since the sodium concentration in cement pore water is higher than in non-saline groundwater, the sodium concentration in the concrete enclosure in a non-saline groundwater environment may during a short initial period be determined by the alkali hydroxides in the cement before these are leached out.

The concentration of potassium inside the concrete will initially be determined by the alkali hydroxides in the cement (Karlsson *et al.*, 1999). Leaching of the alkali hydroxides will lower the concentration of potassium down to that of the ambient groundwater.

The concentration of calcium in the concrete enclosure is controlled by the pH and the solubility of portlandite. The magnesium concentration is determined by the solubility of brucite ($Mg(OH)_2$) (Karlsson *et al.*, 1999).

The sodium and potassium concentration in the gravel backfill is determined by the ambient groundwater (Karlsson *et al.*, 1999). The potassium concentration might be slightly enriched due to the supply from the concrete enclosure, but this effect is assessed to be marginal because of the dilution volume and rather fast water exchange in the backfill.

The concentration of calcium in the backfill is controlled by the ambient groundwater. Geochemical reactions induced by OH^- leached from the concrete might possibly lead to depletion (Karlsson *et al.*, 1999).

Important anions (except OH^-)

The chloride and sulphate concentration in the concrete enclosure is controlled by the ambient groundwater. Sulphate and, to some extent, chloride can be taken up by the cement, but the effect on the concentration in the concrete enclosure is assessed to be small (Karlsson *et al.*, 1999).

The carbonate concentration in the concrete enclosure is determined by the solubility of calcite and the concentration of calcium ions (Karlsson *et al.*, 1999).

The concentration of chloride and sulphate in the gravel backfill is controlled by the ambient groundwater (Karlsson *et al.*, 1999).

The carbonate – bicarbonate concentration in the backfill might possibly be lower than the ambient groundwater due to depletion by geochemical reactions induced by OH^- leached from the concrete (Karlsson *et al.*, 1999).

Complexing agents

Certain waste types in SFL 3 contain cellulose, which can degrade under alkaline conditions to isosaccharinic acid, ISA. The concentration of ISA in these waste packages has been calculated to be equal to or less than 0.1 mM (see Section 7.3 and Appendix 3).

Colloids

Groundwaters and particularly deep groundwaters are very poor in colloids. The measurements that have been done indicate concentrations around 20-45 µg/l (Laaksoharju *et al.*, 1995). The reason for this low concentration is that deep groundwater is strongly mineralised, i.e. contain a lot of dissolved salts. The mineral particles are generally negatively charged, so the positive ions in the groundwater are of the greatest importance for the stability of the colloids. Trivalent ions such as Fe^{3+} and Al^{3+} are present in much too low concentrations in the groundwater to be of importance, but there are plenty of divalent ions such as Ca^{2+}. Ideally, the concentration of the calcium ion Ca^{2+} in the water should be higher than 10^{-4} mol/l (4 mg/l) (Laaksoharju *et al.*, 1995). Other ions such as Na^+, K^+ and Mg^{2+} contribute towards keeping down the colloid concentrations.

The cement could also give rise to particles, but the concentration of cations is high, which keeps down the colloid concentrations. One conclusion from a study of a natural analogue for cement in Maqarin in Jordan (Smellie *et al.*, 1999) is that the colloid concentration is very low in the strongly mineralised water and there is no colloid production observed. Colloids could possibly be formed when pH drops at the front of a pH plume, for example, due to silica supersaturation. However, it is here assumed that SFL 3-5 will not cause any increase in the colloid concentration beyond what can

normally occur in groundwater at a depth of 300 metres on the investigated sites. This assumption is based on the results from Maqarin and the fact that the composition of the groundwater ultimately controls the stability of the colloids.

5.3.2 SFL 4

The waste deposited in SFL 4 is not stored in a concrete enclosure. Instead, the waste packages, steel containers, will be piled on a concrete pavement and gravel will be used to backfill SFL 4. The walls may presumably be lined with shotcrete. The waste in the packages contains small amounts of concrete. To withstand the load from the gravel backfill in the tunnel the waste packages have to be backfilled. In a practical point of view, concrete (cement grout) seems to be the most likely choice of backfill.

With concrete as backfill in the waste packages the water composition inside the waste packages after water penetration will be similar to the water chemistry in the concrete enclosure in SFL 3 and SFL 5. One possible exception is that the depletion of portlandite from the cement in the concrete will be faster because of shorter diffusion distances and larger water exchange in SFL 4 than in the concrete enclosures in SFL 3 and SFL 5. However, portlandite should still remain in the concrete for very long time periods and it is therefore assumed that the porewater chemistry in the concrete backfill in the waste packages are similar to the water chemistry in the concrete enclosures in SFL 3 and SFL 5 (Table 5-2). From this it is also expected that the water composition in the tunnel backfill is similar to that in the backfill in SFL 3 and SFL 5 (Table 5-2).

6 Waste characteristics

6.1 Waste types and volumes

Neutron activated and surface contaminated steel components are the dominating waste types that will be allocated to SFL 3-5. The materials used in the packaging are steel and concrete. The estimated quantities of different materials in the waste and in the packaging are given in Tables 6-1 and 6-2, respectively (Lindgren *et al.,* 1998).

Table 6-1 Estimated quantities of materials in SFL 3-5 waste.

Material	Quantity of material (tonnes)			
	SFL 3	SFL 4	SFL 5	Total
Metals				
Aluminium	82			82
Brass and copper	2			2
Cadmium	1			1
Chromium			5	5
Hafnium			4	4
Inconel			2	2
Lead	4			4
Stainless steel	71	4 720	1 650	6 441
Boron steel		1 260	17	1 277
Carbon steel	80	3 190	280	3 550
Thorium metal	2			2
Zircalloy	3		30	33
Others [a)]	0.1		0.3	0.4
Organic materials				
Resin	230			230
Paper/wood	5			5
Textile/rags	20			20
Plastic/rubber	130			130
Unspecified	1			1
Concrete				
Concrete/Cement [b)]	2 580	880		3 460
Others [c)]	84			84

[a)] *Zinc and titanium in SFL 3 and beryllium in SFL 5*

[b)] *Cement/concrete in solidified waste as well as contaminated concrete*

[c)] *Ashes, glass, ferrocyanide precipitates etc*

Table 6-2 Estimated quantities of materials in SFL 3-5 packaging.

Material	Quantity of material (tonnes)			
	SFL 3	SFL 4	SFL 5	Total
Lead	20		110	130
Carbon steel [a)]	820	1 000	440	2 260
Stainless steel	20		930	950
Concrete	5 000		7 300	12 300
Concrete (backfill)	700		10 400	11 100

[a)] Including reinforcement

6.2 Radionuclide inventory

The radionuclide inventory in SFL 3, SFL 4, and SFL 5 at year 2040 is given in Table 6-3. The estimate of the radionuclide content is based on a combination of measurements, calculations and assumptions. Radionuclides with a half-life less than approximately two years and radionuclides with very long half-life, being more or less stable, and with expected small content have been excluded from the inventory list. A detailed description of how the radionuclide inventory has been estimated is given in Lindgren *et al.* (1998).

Half-lives as given by the ICRP (1983) were used in the calculations of the activity content of the waste in SFL 3-5 in year 2040. More recent information (Firestone *et al*., 1998) gives other half-lives for some of the radionuclides in the waste (see Table 6-3). The radionuclides with largest difference in reported half-lives are ^{79}Se and ^{108m}Ag. Smaller differences in half-life are reported for e.g. ^{63}Ni, ^{93m}Nb and ^{93}Mo. Half-lives from Firestone *et al*. (1998) are used in the calculations of radionuclide transport from SFL 3-5.

Table 6-3 Radionuclide inventory[a)] (Bq) in SFL 3-5 at year 2040.

Radionuclide	Half-life (years) ICRP (1983)	Half-life (years) Firestone *et al.* (1998)	SFL 3	SFL 4	SFL 5	Total
H-3	12	12	$3.2 \cdot 10^{12}$	$4.3 \cdot 10^{9}$	$2.5 \cdot 10^{15}$	$2.5 \cdot 10^{15}$
Be-10	$1.6 \cdot 10^{6}$	$1.5 \cdot 10^{6}$	$1.2 \cdot 10^{7}$	$1.6 \cdot 10^{4}$	$1.4 \cdot 10^{11}$	$1.4 \cdot 10^{11}$
C-14	$5.7 \cdot 10^{3}$	$5.7 \cdot 10^{3}$	$3.5 \cdot 10^{13}$	$2.7 \cdot 10^{10}$	$1.7 \cdot 10^{14}$	$2.0 \cdot 10^{14}$
Cl-36	$3.0 \cdot 10^{5}$	$3.0 \cdot 10^{5}$	$2.1 \cdot 10^{10}$	$1.6 \cdot 10^{7}$	$2.5 \cdot 10^{11}$	$2.7 \cdot 10^{11}$
K-40	$1.3 \cdot 10^{9}$	$1.3 \cdot 10^{9}$	$1.0 \cdot 10^{9}$	not calc.	not calc.	$1.0 \cdot 10^{9}$
Fe-55	2.7	2.7	$9.3 \cdot 10^{12}$	$2.7 \cdot 10^{13}$	$9.6 \cdot 10^{14}$	$1.0 \cdot 10^{15}$
Co-60	5.3	5.3	$3.6 \cdot 10^{14}$	$2.7 \cdot 10^{13}$	$8.1 \cdot 10^{15}$	$8.5 \cdot 10^{15}$
Ni-59	$7.5 \cdot 10^{4}$	$7.6 \cdot 10^{4}$	$1.6 \cdot 10^{14}$	$2.7 \cdot 10^{10}$	$1.4 \cdot 10^{15}$	$1.5 \cdot 10^{15}$
Ni-63	96	$1.0 \cdot 10^{2}$	$2.2 \cdot 10^{16}$	$5.3 \cdot 10^{12}$	$1.2 \cdot 10^{17}$	$1.4 \cdot 10^{17}$
Se-79	$6.5 \cdot 10^{4}$	$1.1 \cdot 10^{6}$	$4.6 \cdot 10^{8}$	$6.4 \cdot 10^{6}$	$4.5 \cdot 10^{7}$	$5.1 \cdot 10^{8}$
Sr-90	29	29	$2.3 \cdot 10^{12}$	$1.6 \cdot 10^{11}$	$5.6 \cdot 10^{11}$	$3.1 \cdot 10^{12}$
Zr-93	$1.5 \cdot 10^{6}$	$1.5 \cdot 10^{6}$	$2.1 \cdot 10^{10}$	$2.7 \cdot 10^{7}$	$2.2 \cdot 10^{12}$	$2.3 \cdot 10^{12}$
Nb-93m	14	16	$6.0 \cdot 10^{12}$	$2.7 \cdot 10^{10}$	$8.0 \cdot 10^{13}$	$8.6 \cdot 10^{13}$
Nb-94	$2.0 \cdot 10^{4}$	$2.0 \cdot 10^{4}$	$4.9 \cdot 10^{11}$	$2.7 \cdot 10^{8}$	$4.7 \cdot 10^{12}$	$5.1 \cdot 10^{12}$
Mo-93	$3.5 \cdot 10^{3}$	$4.0 \cdot 10^{3}$	$2.4 \cdot 10^{11}$	$1.3 \cdot 10^{8}$	$1.8 \cdot 10^{12}$	$2.0 \cdot 10^{12}$
Tc-99	$2.1 \cdot 10^{5}$	$2.1 \cdot 10^{5}$	$5.8 \cdot 10^{11}$	$8.0 \cdot 10^{9}$	$3.2 \cdot 10^{11}$	$9.1 \cdot 10^{11}$
Pd-107	$6.5 \cdot 10^{6}$	$6.5 \cdot 10^{6}$	$1.1 \cdot 10^{8}$	$1.6 \cdot 10^{6}$	$1.1 \cdot 10^{7}$	$1.3 \cdot 10^{8}$
Ag-108m	$1.3 \cdot 10^{2}$	$4.2 \cdot 10^{2}$	$1.2 \cdot 10^{12}$	$1.6 \cdot 10^{9}$	$9.6 \cdot 10^{9}$	$1.2 \cdot 10^{12}$
Cd-113m	14	14	$5.7 \cdot 10^{9}$	$9.6 \cdot 10^{8}$	$1.5 \cdot 10^{9}$	$8.2 \cdot 10^{9}$
Sn-126	$1.0 \cdot 10^{5}$	$1.0 \cdot 10^{5}$	$5.7 \cdot 10^{7}$	$8.0 \cdot 10^{5}$	$5.6 \cdot 10^{6}$	$6.3 \cdot 10^{7}$
Sb-125	2.8	2.8	$6.6 \cdot 10^{11}$	$2.7 \cdot 10^{12}$	$1.4 \cdot 10^{10}$	$3.3 \cdot 10^{12}$
I-129	$1.6 \cdot 10^{7}$	$1.6 \cdot 10^{7}$	$3.4 \cdot 10^{7}$	$4.8 \cdot 10^{5}$	$3.4 \cdot 10^{6}$	$3.8 \cdot 10^{7}$
Cs-134	2.1	2.1	$3.9 \cdot 10^{10}$	$1.6 \cdot 10^{12}$	$7.9 \cdot 10^{8}$	$1.6 \cdot 10^{12}$
Cs-135	$2.3 \cdot 10^{6}$	$2.3 \cdot 10^{6}$	$5.7 \cdot 10^{8}$	$8.0 \cdot 10^{6}$	$5.6 \cdot 10^{7}$	$6.3 \cdot 10^{8}$
Cs-137	30	30	$3.4 \cdot 10^{13}$	$1.6 \cdot 10^{12}$	$5.7 \cdot 10^{12}$	$4.2 \cdot 10^{13}$
Ba-133	11	11	$2.9 \cdot 10^{10}$	$2.7 \cdot 10^{8}$	$2.9 \cdot 10^{8}$	$3.0 \cdot 10^{10}$
Pm-147	2.6	2.6	$2.5 \cdot 10^{10}$	$1.4 \cdot 10^{12}$	$5.1 \cdot 10^{9}$	$1.5 \cdot 10^{12}$
Sm-151	90	90	$2.3 \cdot 10^{11}$	$4.8 \cdot 10^{9}$	$2.7 \cdot 10^{10}$	$2.6 \cdot 10^{11}$
Eu-152	13	14	$1.5 \cdot 10^{12}$	$1.1 \cdot 10^{8}$	$1.7 \cdot 10^{8}$	$1.5 \cdot 10^{12}$
Eu-154	8.8	8.6	$4.8 \cdot 10^{11}$	$1.6 \cdot 10^{11}$	$1.1 \cdot 10^{11}$	$7.6 \cdot 10^{11}$
Eu-155	5.0	4.8	$5.2 \cdot 10^{10}$	$1.1 \cdot 10^{11}$	$1.4 \cdot 10^{10}$	$1.8 \cdot 10^{11}$
Ho-166m	$1.2 \cdot 10^{3}$	$1.2 \cdot 10^{3}$	$8.3 \cdot 10^{10}$	$1.1 \cdot 10^{8}$	$7.3 \cdot 10^{8}$	$8.4 \cdot 10^{10}$
Pb-210	22	22	$2.7 \cdot 10^{11}$	< 1	< 1	$2.7 \cdot 10^{11}$
Ra-226	$1.6 \cdot 10^{3}$	$1.6 \cdot 10^{3}$	$3.8 \cdot 10^{11}$	< 1	< 1	$3.8 \cdot 10^{11}$
Ac-227	22	22	$1.4 \cdot 10^{6}$	< 1	4.5	$1.4 \cdot 10^{6}$
Th-229	$7.3 \cdot 10^{3}$	$7.3 \cdot 10^{3}$	$1.4 \cdot 10^{2}$	< 1	< 1	$1.4 \cdot 10^{2}$
Th-230	$7.7 \cdot 10^{4}$	$7.5 \cdot 10^{4}$	$1.8 \cdot 10^{5}$	2.4	$7.3 \cdot 10^{1}$	$1.8 \cdot 10^{5}$
Th-232	$1.4 \cdot 10^{10}$	$1.4 \cdot 10^{10}$	$1.1 \cdot 10^{10}$	< 1	< 1	$1.1 \cdot 10^{10}$
Pa-231	$3.3 \cdot 10^{4}$	$3.3 \cdot 10^{4}$	$2.5 \cdot 10^{6}$	< 1	7.9	$2.5 \cdot 10^{6}$
U-232	72	69	$4.4 \cdot 10^{6}$	$8.0 \cdot 10^{2}$	$4.2 \cdot 10^{3}$	$4.4 \cdot 10^{6}$
U-233	$1.6 \cdot 10^{5}$	$1.6 \cdot 10^{5}$	$3.1 \cdot 10^{4}$	< 1	$1.3 \cdot 10^{1}$	$3.1 \cdot 10^{4}$
U-234	$2.4 \cdot 10^{5}$	$2.5 \cdot 10^{5}$	$7.8 \cdot 10^{8}$	$2.7 \cdot 10^{4}$	$2.4 \cdot 10^{5}$	$7.8 \cdot 10^{8}$
U-235	$7.0 \cdot 10^{8}$	$7.0 \cdot 10^{8}$	$6.4 \cdot 10^{9}$	$5.3 \cdot 10^{2}$	$3.7 \cdot 10^{3}$	$6.4 \cdot 10^{9}$
U-236	$2.3 \cdot 10^{7}$	$2.3 \cdot 10^{7}$	$8.1 \cdot 10^{7}$	$8.0 \cdot 10^{3}$	$5.6 \cdot 10^{4}$	$8.1 \cdot 10^{7}$
U-238	$4.5 \cdot 10^{9}$	$4.5 \cdot 10^{9}$	$4.6 \cdot 10^{10}$	$1.1 \cdot 10^{4}$	$7.5 \cdot 10^{4}$	$4.6 \cdot 10^{10}$
Np-237	$2.1 \cdot 10^{6}$	$2.1 \cdot 10^{6}$	$1.8 \cdot 10^{8}$	$1.1 \cdot 10^{4}$	$7.9 \cdot 10^{4}$	$1.8 \cdot 10^{8}$
Pu-238	88	88	$3.7 \cdot 10^{11}$	$1.1 \cdot 10^{8}$	$5.9 \cdot 10^{8}$	$3.7 \cdot 10^{11}$
Pu-239	$2.4 \cdot 10^{4}$	$2.4 \cdot 10^{4}$	$2.3 \cdot 10^{12}$	$8.9 \cdot 10^{6}$	$6.2 \cdot 10^{7}$	$2.3 \cdot 10^{12}$
Pu-240	$6.5 \cdot 10^{3}$	$6.6 \cdot 10^{3}$	$1.8 \cdot 10^{12}$	$1.8 \cdot 10^{7}$	$1.3 \cdot 10^{8}$	$1.8 \cdot 10^{12}$
Pu-241	14	14	$4.4 \cdot 10^{12}$	$2.7 \cdot 10^{9}$	$4.6 \cdot 10^{9}$	$4.4 \cdot 10^{12}$
Pu-242	$3.8 \cdot 10^{5}$	$3.7 \cdot 10^{5}$	$1.2 \cdot 10^{9}$	$8.0 \cdot 10^{4}$	$5.6 \cdot 10^{5}$	$1.3 \cdot 10^{9}$
Pu-244	$8.3 \cdot 10^{7}$	$8.1 \cdot 10^{7}$	$1.8 \cdot 10^{2}$	< 1	< 1	$1.8 \cdot 10^{2}$
Am-241	$4.3 \cdot 10^{2}$	$4.3 \cdot 10^{2}$	$5.0 \cdot 10^{12}$	$2.7 \cdot 10^{7}$	$6.3 \cdot 10^{8}$	$5.0 \cdot 10^{12}$
Am-242m	$1.5 \cdot 10^{2}$	$1.4 \cdot 10^{2}$	$2.0 \cdot 10^{9}$	$2.7 \cdot 10^{5}$	$1.6 \cdot 10^{6}$	$2.0 \cdot 10^{9}$
Am-243	$7.4 \cdot 10^{3}$	$7.4 \cdot 10^{3}$	$8.5 \cdot 10^{9}$	$8.0 \cdot 10^{5}$	$5.6 \cdot 10^{6}$	$8.5 \cdot 10^{9}$
Cm-243	29	29	$1.7 \cdot 10^{9}$	$5.3 \cdot 10^{5}$	$1.8 \cdot 10^{6}$	$1.7 \cdot 10^{9}$
Cm-244	18	18	$4.4 \cdot 10^{10}$	$8.0 \cdot 10^{7}$	$1.9 \cdot 10^{8}$	$4.4 \cdot 10^{10}$
Cm-245	$8.5 \cdot 10^{3}$	$8.5 \cdot 10^{3}$	$7.7 \cdot 10^{7}$	$8.0 \cdot 10^{3}$	$5.6 \cdot 10^{4}$	$7.7 \cdot 10^{7}$
Cm-246	$4.7 \cdot 10^{3}$	$4.7 \cdot 10^{3}$	$2.1 \cdot 10^{7}$	$2.1 \cdot 10^{3}$	$1.5 \cdot 10^{4}$	$2.1 \cdot 10^{7}$

[a)] derived with half-lives from ICRP (1983)

6.3 Toxic metals

The waste packages in SFL 3 and SFL 5 contains toxic metals such as cadmium, lead and beryllium. The total estimated quantity of toxic metals is given in Table 6-4 (Lindgren *et al.,* 1998).

Table 6-4 Estimated quantities of toxic metals in SFL 3-5.

Material	Quantity of material (kg)			
	SFL 3	SFL 4	SFL 5	Total
Cadmium	990			990
Lead - waste	3 965			3 965
Lead - packaging	16 000		108 592	124 592
Beryllium			300	300

6.4 Data uncertainties

The uncertainties in the estimates of waste volumes and radionuclide inventory are discussed in Lindgren *et al.*, (1998). Since most of the waste allocated to SFL 3-5 are not yet produced, the waste volumes and radionuclide inventory are based on prognoses concerning the future operation of the waste producing plants and the decommissioning of these facilities. Naturally, this will introduce uncertainties in the waste volumes and radionuclide inventory.

To estimate the radionuclide inventory, available information on the radionuclide content in already produced waste is used as far as possible. However, for many of the radionuclides such information is lacking, especially for radionuclides that are difficult to measure. To be able to estimate the inventory of these radionuclides, correlation factors to 'key' radionuclides are used. Two sets of general correlation factors are defined, one set for activation products in metal components and one set for radionuclides deposited on the surface of materials. These two sets are used to estimate the radionuclide content for all types of waste where information is lacking.

To define these correlation factors, measured and calculated data for waste produced in Sweden, and to some extent also in other countries, are used. These data give rise to correlation factors that vary over a wide range for many radionuclides, often orders of magnitude. This is not unexpected since the correlation factors are dependent on conditions during reactor operation. In the case of surface contamination, the relationships between different radionuclides, and thereby also the correlation factors, are affected by e.g. reactor type, chemistry of the primary coolant, fuel leakage, and impurities in the fuel and the corroding materials. In the case of induced activity, the correlation factors are primarily dependent on material composition, occurrence of impurities, irradiation times and neutron fluxes. These circumstances illustrate the uncertainties associated with the simplified approach of using general correlation factors for all waste as well as the potential uncertainty in the correlation factors selected.

7 Near-field chemical data

7.1 Dissolution of radionuclides and other toxicants

Sorption is expected to be the major process that affects the concentration of radionuclides and other toxicants in the near-field water in SFL 3-5. However, for some elements the solubility is so low that that it will, in addition to sorption, limit the element concentration in the pore water and thereby determine the source term release. In that aspect, also coprecipitation and the content of inactive elements might be of importance. The rate of dissolution of radionuclides from the waste is difficult to assess and in general an instantaneous dissolution of radionuclides not being solubility-limited has to be assumed in radionuclide release calculations. One possible exception is the dissolution of neutron-induced activity in metal waste in SFL 5 that can be limited by the corrosion rate of the metals (Wiborgh, 1995). The above mentioned aspects of the dissolution of radionuclides and other toxicants from the waste in SFL 3-5 are discussed in the following subsections.

7.1.1 Solubility in concrete pore water

The solubility of elements is dependent of the water chemistry. Important factors are pH, redox conditions and the presence of complexing agents. This section discusses the potential solubility of different elements in an alkaline and reducing water, which is representative of the waste environment in the repository SFL 3-5 (see section 5.3).

The effect of complexing agents in SFL 3-5 on solubility is discussed later in this chapter (section 7.3). However, it can be concluded that the concentration of CO_3^{2-} will be low due to the low solubility of $CaCO_3$ in concrete pore water ($[CO_3^{2-}] \sim 10^{-4}$ M, Table 5-2). The complexation of the metals with carbonate is therefore expected to be negligible as compared to complex formation with hydroxide (a relatively high concentration caused by the high pH).

Wiborgh (1995) compiled solubility data from the literature for various elements in concrete pore waters (pH=12-13.5). These data, together with additional data found in the literature are used to select solubility data for the cementitious environment in SFL 3-5. The solubility of the actinides is mostly based on a crystalline solubility-limiting phase. For the other elements, the solubility is based on an amorphous hydroxide-limiting phase. The selected solubility data are compiled in Table 7-1.

Caesium and Strontium

The quantities of caesium and strontium are small compared with the amount of water in the repository. Since the solubility of caesium and strontium is high, no solubility limit is considered.

Radium, cadmium, nickel, beryllium, iron, cobalt and lead

The solubility of radium is expected to be even higher than that of strontium due to the fact that the alkaline-earth metals exhibit less and less tendency to hydrolyse as the atomic number increases (Baes and Mesmer, 1976). Therefore, in similarity to strontium, no solubility limit is considered

Cadmium hydroxide is fairly soluble in the low pH range (pH<10), but reaches a minimum solubility of less than $3 \cdot 10^{-7}$ M at pH ≈ 11. Above pH 12, the solubility increases with increasing pH to about 10^{-5} M at pH 13.5 (Baes and Mesmer, 1976). However, with the stability constants obtained for the higher hydroxide complexes by Dyrssen and Lumme (1962), the solubility would be as high as 10^{-3} M at pH 13.5. This value is chosen as the maximum solubility of cadmium in the cementitious environment in SFL 3-5.

Nickel has a low solubility in alkaline media, with a minimum solubility of $3 \cdot 10^{-8}$ M at pH 12-12.5. The solubility of nickel increases below pH 12 and above 12.5. However, the solubility does not exceed 10^{-7} M for the relevant range of pH values (Pilkington and Stone, 1990; Holgersson *et al.*, 1999), why this value of the solubility is selected.

Beryllium has a low solubility in neutral or slightly basic media. The minimum solubility is $2 \cdot 10^{-7}$ M. The solubility is however strongly enhanced by the formation of $Be(OH)_3^-$ and $Be(OH)_4^{2-}$ when pH exceeds 9. At pH 13.5, the solubility of beryllium reaches $1 \cdot 10^{-3}$ M (Baes and Mesmer, 1976). No anions but the hydroxide ions present in the groundwater or the pore water of concrete have an effect on the solubility of beryllium (Smith and Martell, 1976). Therefore, a solubility of 10^{-3} M is selected.

Iron(II) has a minimum solubility of $<10^{-6}$ M at pH 10.5. The solubility increases to 10^{-5} M at pH 13 (Baes and Mesmer, 1976), which is the value selected.

Cobalt has a lesser tendency to form anionic hydroxide species. The minimum solubility is thus maintained in the pH region of 10-12.5 at a value of $<10^{-6}$ M (Baes and Mesmer, 1976). At pH 13.5 the solubility have increased to 10^{-5} M (Baes and Mesmer, 1976), why this value is chosen as the solubility of cobalt in the cementitious environment in SFL 3-5.

The solubility of lead is strongly dependent on the pH conditions. The solubility of $Pb(OH)_2$ has been measured by Pokric and Pucar (1973) giving aqueous lead concentrations of about 10^{-6} M at pH 13.5. This value is selected as the solubility of lead.

Americium, curium and promethium

Trivalent americium and curium are strongly solubility limited in concrete-influenced water in the repository. A compilation of experimental data for actinides gives a solubility of Am of 10^{-10} M in the pH range 11 to 13, without stating the solid phase (Ewart *et al.*, 1992). Calculations with $Am(OH)_3$ as the highest hydroxide complex and with crystalline $Am(OH)_3$ as the limiting phase from the NEA-OECD (1995) compilation of data results in a solubility decrease from 10^{-5} M at pH 7 to less than

10^{-10} M in the pH range of 11.5 – 13.5. No evidence for anionic hydroxide complexes is given by these two references. Measurements of the maximum stability of Pm in solution (as an analogue for trivalent actinides) gave a value of $9 \cdot 10^{-8}$ M at pH 13.5 (Holgersson *et al.*, 1999). This value is appreciably higher than those values mentioned above and it may not reflect equilibrium conditions. However, it is the value selected as the maximum solubility of trivalent actinides in the cementitious environment in SFL 3-5.

Technetium, zirconium, thorium, protactinium, uranium, neptunium and plutonium

Measurements have demonstrated that tetravalent technetium has a low solubility in neutral to alkaline media (Eriksen *et al.,* 1992). The solubility in the repository is expected to be 10^{-7} M.

The solubility of zirconium is affected by the formation of anionic hydroxo species. The minimum solubility is less than 10^{-10} M at pH 5 to 6, but increases slowly to $1 \cdot 10^{-4}$ M at pH 13.5. The solubility is based on ZrO_2 as the limiting phase (Baes and Mesmer, 1976). Measurement by Kulmala and Hakanen (1993) shows a much lower solubility in concrete water (below 10^{-8} M), thus indicating that the negative zirconium hydroxide complex does not exist. However, since the negative Zr-OH complexes are still not proven to not exist, we have chosen a solubility limit of 10^{-4} M at pH 13.5.

The redox conditions in the repository are expected to stabilise the tetravalent state of the actinides Th, Pa, U, Np and Pu. Although the pH is high, no enhancement of the solubility of the tetravalent actinides is expected because of their reluctance to form negatively charged hydroxide complexes (Engkvist, 1993, Albinsson *et al.,* 1996). Since the carbonate concentration is low in cementitious systems, actinide oxide or hydroxide solids will limit the solubility. However, data on the solubility of the hydroxides are virtually non-existent and most calculations are based on data for the oxides.

Thorium has a very limited solubility in neutral to alkaline solutions. In their compilation of data, Baes and Mesmer calculate the solubility of crystalline ThO_2 to be about $3 \cdot 10^{-10}$ M for pH > 5 with $Th(OH)_4$ as the highest hydroxide complex. Ewart *et al.* (1992) report a solubility of about $3 \cdot 10^{-9}$ M for the pH range 8 – 13, without stating the limiting solid phase. Measurements of the solubility of microcrystalline ThO_2 gave values of $1 \cdot 10^{-10}$ M at pH 13.2 and $5 \cdot 10^{-10}$ M at pH 12.5 (Wierczinski *et al.,* 1998). Measurements of the maximum stability of thorium in solution at pH 13.5 resulted in a value of $5 \cdot 10^{-9}$ M (Holgersson *et al.*, 1999).

Protactinium also has a very limited solubility in neutral to alkaline waters. From data compiled by Baes and Mesmer (1986) the solubility of crystalline PaO_2 can be calculated to be below 10^{-10} M for pH > 9.5 with $Pa(OH)_3^+$ as the highest hydroxide complex. Ewart *et al*. (1992) give $5 \cdot 10^{-10}$ M as an estimated solubility of Pa at pH 12.5, without stating the limiting solid phase.

For uranium hydrolysis the references are somewhat divergent. Baes and Mesmer (1986) states that the fifth, anionic hydroxide complex is formed. This results in a minimum solubility of crystalline UO_2 of 10^{-12} M at pH 5. With rising pH the solubility

increases to 10^{-5} M at pH 13.5. Ewart *et al.* (1992) gives a solubility of uranium hydroxide of $2 \cdot 10^{-7}$ M in the pH range 5 – 13 and draws the conclusion that the absence of a solubility increase with pH supports the non-existence of a fifth hydroxide complex. From the NEA-OECD (1992) database for uranium the solubility of crystalline UO_2 can be calculated to be $4 \cdot 10^{-10}$ M in the pH range 2 – 10. Due to the fifth hydroxide complex the solubility rises to $1 \cdot 10^{-8}$ M at pH 13.5.

Tetravalent neptunium hydrolysis data are scarce. Ewart *et al.* (1992) report a value of $1 \cdot 10^{-8}$ M for the solubility in the pH range 8 – 13 without giving the limiting solid phase.

Plutonium has a limited solubility in neutral to alkaline waters. From Baes and Mesmer (1986) the solubility of crystalline PuO_2 can be calculated to be higher than $1 \cdot 10^{-3}$ M in the entire pH range. Such high values are very doubtful and this can perhaps illustrate the unreliability in earlier data. More recent investigations that are cited by Ewart *et al.* (1992) give a Pu solubility of 10^{-10} M in the pH range 9 – 13, but also here without specifying the limiting solid phase.

From this survey it is clear that the hydrolysis behaviour of all tetravalent actinides are similar. Thorium is therefore selected as a model for the hydrolysis-controlled solubility of all tetravalent actinides. Based on the measurements by Holgersson *et al.* (1999) a solubility of $5 \cdot 10^{-9}$ M is therefore selected as the maximum solubility limit for all tetravalent actinides in the cementitious environment in SFL 3-5.

Niobium

According to Kulmala and Hakanen (1993), niobium will dissolve only as pentavalent ions and the solubility will be limited to 10^{-9} M. However, measurements by Baker *et al.* (1994) indicated a higher solubility, around 10^{-6} M, at very high pH's (around pH 13.5). Conservatively, the higher solubility of 10^{-6} M is selected for the cementitious environment in SFL 3-5.

Table 7-1 Selected solubility of elements in concrete porewater, pH = 12-13.5 and reducing conditions.

Ox. state	Element	Solubility (M)
M(II)	Be, Cd	10^{-3}
	Fe, Co	10^{-5}
	Ni	10^{-7}
	Pb	10^{-6}
M(III)	Am, Cm, Pm	$9 \cdot 10^{-8}$
M(IV)	Tc	10^{-7}
	Zr	10^{-4}
	Th, Pa, U, Np, Pu	$5 \cdot 10^{-9}$
M(V)	Nb	10^{-6}

7.1.2 Isotope dilution

The waste to be stored in SFL 3-5 will contain both radioactive and stable isotopes of the same element. This could be of importance when considering the effects of solubility limits since the solubility of the radioactive isotopes will be further reduced if stable isotopes of the same element are present.

The waste in SFL 5 comprises internal parts from the reactors. These metals (e.g. stainless steel containing nickel as alloying material and Zircalloy containing zirconium) have been exposed to irradiation. The amount of the radioactive isotopes ^{59}Ni and ^{63}Ni in relation to the total amount of nickel in stainless steel can be estimated from data in Lindgren *et al.* (1998). The results for the most activated stainless steel components in the SFL 5 waste are given in Table 7-2. The reported content of nickel as alloying material in different types of stainless steel is 10 to 13 % by weight. The results in Table 7-2 is based on the assumption of a nickel content of 10 % by weight. In one of the waste types the relative content of ^{59}Ni is above 6 % by weight while the relative content of ^{59}Ni in the remaining waste types as well as the average relative content in all waste types is below 1 % per weight. The relative content of ^{63}Ni is of the order of 0.1 % by weight or less.

A corresponding estimate of the amount of the radioactive isotope ^{93}Zr in relation to the total amount of zirconium in Zircalloy from data in Lindgren *et al.* (1998) results in a relative content of ^{93}Zr of 0.08 % by weight.

The ratios of radioactive to stable isotopes of nickel and zirconium that were used in the prestudy of the SFL 3-5 repository (Wiborgh, 1995) are 0.01 for nickel and 0.001 for zirconium. The updated waste characterisation does not imply any changes in these values. This means that an isotope dilution factor of 100 for radioactive nickel and 1 000 for radioactive zirconium can be used to reduce the solubility of radioactive nickel and zirconium in the water in the waste packages in SFL 5.

Table 7-2 Amount of ^{59}Ni and ^{63}Ni in relation to the total amount of Ni in the most activated stainless steel components in the waste in SFL 5. The content of Ni in stainless steel is 10% by weight (data from Lindgren *et al.*, 1998).

Waste component	Stainless steel (kg)	Content (g) of		Weight% of total Ni	
		Ni-59	Ni-63	Ni-59	Ni-63
Core grid, BWR	108 000	$7.5 \cdot 10^4$	$1.1 \cdot 10^4$	0.70	0.10
Moderator tank, BWR	288 000	$1.3 \cdot 10^5$	$1.9 \cdot 10^4$	0.44	0.07
Core spray, BWR	77 400	$1.3 \cdot 10^3$	$2.0 \cdot 10^2$	0.02	0.00
Control rods, BWR	379 312	$5.9 \cdot 10^4$	$1.0 \cdot 10^4$	0.15	0.03
Transition pieces, BWR	1 750	$2.9 \cdot 10^2$	49	0.17	0.03
PRM detectors and tubes, BWR	11 286	$7.5 \cdot 10^4$	$1.4 \cdot 10^3$	6.67	0.12
Burnable absorbers, PWR	2 155	$8.9 \cdot 10^2$	$1.6 \cdot 10^2$	0.41	0.07
Internal parts, PWR	331 623	$4.2 \cdot 10^4$	$5.7 \cdot 10^3$	0.13	0.02
Total	*1 199 526*	*$3.8 \cdot 10^5$*	*$4.8 \cdot 10^4$*	*0.32*	*0.04*

7.1.3 Coprecipitation and adsorption on corrosion products

Large amount of metal waste, mainly different qualities of steel, will be stored in SFL 3-5. With time, the metals will corrode and the corrosion products that will be formed in largest quantities are different oxides/hydroxides of iron. Such compounds are well known to adsorb and coprecipitate other metal ions present in solution. The effect of coprecipitation with ferric iron could reduce the solubility of nickel to about 0.14 times the solubility of a corresponding pure nickel precipitate (Wiborgh, 1995).

When the groundwater is mixed with the alkaline water in the SFL 3-5 repository precipitation of calcite/aragonite ($CaCO_3$) may take place (Karlsson *et al.,* 1999). Trace elements present as divalent cations may coprecipitate with calcite/aragonite by replacing calcium in the crystal lattice. Also the recrystallisation of different cement minerals may capture radionuclides, but little is known on this subject. This potential effect is therefore disregarded in the quantitative estimates of radionuclide release as well as the potential effects of coprecipitation with calcite/aragonite.

Coprecipitation and adsorption on corrosion products can have some impact on the source concentration of radionuclides in SFL 3-5. However, these effects are difficult to quantify and might not be so important in SFL 3-5 in relation to sorption on cement/concrete. It is therefore suggested that the potential effects of coprecipitation and sorption on corrosion products are discussed in the safety assessment, but not included in the quantitative estimates of the radionuclide release.

7.1.4 Corrosion limited release of induced activity

The waste in SFL 5 consists of different metal components from the reactors and neutron activation products in the metals dominate the radionuclide content in the waste categories with the highest total activity (Lindgren *et al.,* 1998). This means that the

corrosion rate of the metals might influence the concentration of these activation products in the water in the waste packages.

The major types of metals present in the waste are stainless steel, carbon steel, boron steel, and Zircalloy. The waste categories containing Zircalloy components contain the highest activity of ^{93}Zr, but only a small amount of the remaining activation products compared to the waste categories containing stainless steel (Lindgren *et al.,* 1998). The release of ^{93}Zr can therefore be considered as being determined by the corrosion of Zircalloy, while the remaining activation products are determined by the corrosion of steel.

For the quantitative analyses of radionuclide migration from SFL 3-5 it is suggested that a corrosion-limited release is assumed for those activation products that have a negligible contribution to the total activity in the metal component from surface contamination. Assuming that these activation products are evenly distributed in the metal components exposed to corrosion, the annual fraction of the initial inventory that is released from the metals due to corrosion is given by the mean corrosion time of the waste. The mean corrosion time is estimated from the average thickness of the metals exposed to corrosion and the expected corrosion rate of Zircalloy and steel. These corrosion rates are (Wiborgh, 1995):

1 μm/year for all steel grades (stainless, carbon and boron), and

0.01 μm/year for Zircalloy.

7.2 Sorption in near-field barriers

The materials acting as sorbents in the near-field barriers are concrete and a backfill of crushed rock or gravel. Carbol and Engkvist (1997) have compiled sorption coefficients on granite in the far-field rock to be used in the calculations of radionuclide migration in the performance assessment of spent fuel disposal in a deep underground repository (SKB, 1999). These sorption coefficients can be used for the backfill material in SFL 3-5 as well. Some nuclides of interest for SFL 3-5 is not of importance in the performance assessment of spent fuel disposal, and is therefore not included in Carbol and Engkvist (1997). Sorption data on granite for these nuclides have been taken from other references or by using analogies to other nuclides.

Sorption data for concrete are selected based on information from batch sorption experiments found in the literature and by using chemical analogies between nuclides. Dependent on the site, the water in the repository can be saline or non-saline and dependent on the time of radionuclide release the concrete can be in different stages of portlandite leaching. Experimental data in the literature are almost entirely for sorption on fresh concrete in non-saline water. No data are available on sorption on leached concrete and for many of the nuclides of interest in SFL 3-5 data on sorption on fresh concrete in saline waters are lacking. Leaching of concrete in non-saline water will not affect the sorbent. Enough mineral surfaces will remain which can take up radionuclides. The changes in the composition of the water phase can be more

important. The pH will drop and the ionic strength decrease. The expected change in pH (see Table 5-2) will not significantly affect the sorption, but differences in ionic strength can be of importance for elements that sorbs by ion exchange (i.e. Cs, Be, Sr, Ba and Ra). A lower ionic strength means less competition from other ions and hence, stronger sorption. The difference between sorption on concrete in non-saline and saline water is also related to the difference in ionic strength. A saline intruding groundwater can give rise to slightly higher sodium and, with time, potassium concentrations in the water in the concrete and thereby a slightly lower sorption of elements that sorbs by ion exchange.

Based on the circumstances stated above, only one set of sorption coefficients, K_d-values, is defined for the quantitative analysis of radionuclide migration. This data set is mainly based on the data available on sorption on fresh concrete in non-saline water. For most of the elements the data selected are expected to be representative for both non-saline and saline conditions. When experimental data are available for both saline and non-saline water, the selected K_d is based on data for saline water if those are lower than for non-saline water. The data selected are used for sorption on concrete regardless of non-saline or saline water in the repository and are compiled in Table 7-3.

7.2.1 Sorption on concrete, anions

In this section, sorption coefficients for anions on concrete are discussed and in the next section, sorption coefficients for cations. Relevant literature is cited, and the selected sorption coefficient for each element is given. The selected sorption coefficients for all elements on concrete at pH 13.5 are compiled in Table 7-3.

Chlorine (Cl)

Chlorine is a negative ion with low sorption. However, there are indications that chlorine is retarded in concrete, probably by other chemical processes than pure sorption (Baker *et al.,* 1994, Holgersson and Albinsson, 1999, and Sarott *et al.,* 1992). Sarott *et al.* (1992) have obtained sorption values around 0.02 m^3kg^{-1} from measured diffusion profiles in cement discs. The concentrations of chlorine were in the range 10^{-5} to 10^{-7} M. Sorption measurement by Baker *et al.* (1994) and Holgersson and Albinsson (1999) at higher Cl^- concentrations indicate sorption values below 10^{-2} m^3kg^{-1} that are increasing with time. Taking these investigations into account a sorption value of $6 \cdot 10^{-3}$ m^3kg^{-1} is chosen.

Iodine (I)

The aqueous chemistry of iodine is complicated, especially at very low concentrations. Here it is assumed that iodine is present as I^-. Many investigations of the sorption behaviour of iodine in cement paste have been reported (Andersson *et al.,* 1981, Allard *et al.,* 1984, Atkinson and Nickerson, 1988, and Atkins and Glasser, 1990). The studies indicate low, but measurable sorption. All the investigations give K_d -values above $3 \cdot 10^{-3}$ m^3kg^{-1}, why this value is chosen.

Molybdenum (Mo)

Molybdenum probably exists as an anion, MoO_4^{2-} under reducing conditions. Low sorption is expected, and there are almost no data available. A K_d-value of $6 \cdot 10^{-3}$ m^3kg^{-1} is chosen in accordance with actual measurements made by Holgersson and Albinsson (1999).

Selenium (Se)

Under the reducing conditions expected in the repository, selenium will probably exist predominantly as anionic species (SeO_4^{2-}, SeO_3^{2-}, HSe^-). Thus low sorption is expected. Since no adequate sorption measurements are available, a K_d-value of $6 \cdot 10^{-3}$ m^3kg^{-1} in analogy with molybdenum is selected.

Carbon (C)

Carbon in the form of carbonate will precipitate as $CaCO_3$ in concrete systems. A K_d-value of 0.2 m^3kg^{-1} is selected (Bayliss *et al.,* 1988 and Allard *et al.,* 1991), although this is not a sorption process but rather a precipitation process. For other forms of carbon, e.g. organic compounds like methane etc., a $K_d = 0$ is selected.

7.2.2 Sorption on concrete, cations

Tritium (H)

Tritium will probably exist as tritiated water, why no sorption is expected. A $K_d = 0$ is selected.

Caesium (Cs) and Silver (Ag)

Several investigations have shown that sorption of caesium increases with decreasing ionic strength and thereby lower pH, and that the sorption on concrete mainly takes place on the ballast (Ewart *et al.,* 1985, Andersson *et al.,* 1981, Hietanen *et al.,* 1984, Allard *et al.,* 1984). A K_d of 0.001 m^3kg^{-1} has been obtained on fresh cement paste in saline water (Andersson *et al.,* 1981). This value is selected, provided that the Cs-concentration is below 10^{-5} M (Ewart *et al.,* 1985). This weak sorption is then mainly due to the high salinity of the water. K_d values for Cs sorption on cement paste and concrete in non-saline waters are higher, but of the same order of magnitude (Holgersson *et al.,* 1998, Allard *et al.,* 1984).

No sorption values for Ag are found in the open literature. It is assumed that silver is predominantly in the +1 state, or possibly as Ag^0. The sorption is therefore assumed to be weak and, as for Cs, to take place mainly on the ballast material. The same K_d-value of 0.001 m^3kg^{-1} as for Cs is then chosen.

Nickel (Ni), Cobalt (Co), Iron (Fe), Palladium (Pd) and Cadmium (Cd)

Much of the sorption data for nickel that are reported in the literature might not be relevant for sorption only since the sorption measurements can have been disturbed by precipitation processes. The K_d-value selected for Ni is based on the results of two investigations (Pilkington and Stone, 1990, and Holgersson *et al.,* 1998). In the first study there seems to have been some problem with filtration and solid to liquid ratio effects. We have chosen the sorption values obtained with centrifugation (Holgersson *et al.,* 1998) rather than the ones obtained with filtration, due to the possibility of sorption onto filters, which would render higher K_d's. A K_d -value of 0.04 m^3kg^{-1} is chosen as realistic, although higher values have been obtained by others (Hietanen *et al.,* 1984, Pilkington and Stone, 1990, and Bradbury and Van Loon, 1998 (original reference Sarott, 1996)).

There are few measurements on the sorption of cobalt and iron on cementitious material, but it is expected to be similar to nickel. The only sorption study that could be found was experiments that have been carried out at the Chalmers University and are reported in Wiborgh (1995), Appendix C. The measured K_d-values on crushed concrete and cement was in the range 0.2-0.4 m^3kg^{-1}.

The major aqueous species of palladium and cadmium is likely to be $Pd(OH)_2^0$ and $Cd(OH)_2^0$, respectively, and the sorption behaviour is likely to be analogous to nickel.

Due to the expected similarity in sorption behaviour, the K_d value selected for Co, Fe, Pd and Cd is the same as the value selected for Ni, i.e. $K_d = 0.04$ m^3kg^{-1}.

Lead (Pb)

Data for lead sorption are reported by Bayliss *et al.* (1988). The experiments were carried out with two different cement phases and lead concentrations in the range 10^{-3} to 10^{-9} M. Phase separation had a major impact on the sorption values obtained and filtering was included in all sorption measurements. The measured K_d-values were between 0.1 and >5 m^3kg^{-1} and, usually, sorption increased with time. Since filtration was used as a separation method, we choose the lower value obtained, $K_d = 0.1$ m^3kg^{-1}.

Tin (Sn)

Tin is, under the slightly reducing conditions obtained in the repository, probably present in the tetravalent state. Since it readily forms strong hydroxy complexes, a strong sorption is expected. Bayliss *et al.* (1989) reported sorption values in the range 0.6 to 60 m^3kg^{-1} depending on the type of filter that was used, indicating that tin exists in a range of colloidal sizes. Baker *et al.* (1994) reported even higher K_d-values than that using about 20 times lower concentration of tin ($6 \cdot 10^{-8}$ M Sn). Taking into consideration the problems with solubility and the formation of colloids, a K_d-value of 0.5 m^3kg^{-1} is chosen.

Strontium (Sr), Radium (Ra), Barium (Ba) and Beryllium (Be)

Sorption of the alkaline earth elements is generally rather low. These metal ions are weakly hydrolysed, but some of them can form anionic hydroxide species in highly alkaline medium.

The sorption property of strontium is related to the concentration of calcium as a competitive ion. No difference between saline and non-saline waters is therefore expected since the calcium concentration in concrete is determined by the concrete and not by the salinity of the intruding groundwater (see Table 5-2). A K_d-value of 0.001 m^3kg^{-1} is chosen based on data reported in the literature (Allard *et al.,* 1991, Hietanen *et al.,* 1984, Ewart *et al.,* 1985, and Atkinsson and Nickerson, 1988).

There is not much information available in the literature on the sorption of radium on cementitious material. Bayliss *et al.* (1989) reports a K_d-value of 0.05 m^3kg^{-1}. This value is selected for sorption of radium.

Barium sorption values are expected to be in-between those of Sr and Ra. An analogy is made with Sr, which exhibits about the same K_d for concrete as for granite in saline groundwater. A K_d-value of 0.007 m^3kg^{-1} is chosen for barium sorption on concrete based on measurements of barium sorption on granite in saline waters (Kulmala and Hakanen, 1995 and Byegård *et al.,* 1995).

Beryllium is expected to behave similar to radium and $K_d = 0.05$ m^3kg^{-1} is selected to represent sorption of beryllium on concrete.

Niobium (Nb)

The strong hydrolysis should cause a high sorption of niobium. Pilkington and Stone (1990) report sorption values between 0.5 and 80 m^3kg^{-1} and Kulmala and Hakanen (1993) report data in the range 0.2 to 120 m^3kg^{-1}. Baker *et al.* (1994) obtained K_d-values around 40 m^3kg^{-1}, using very low concentrations of Nb ($<10^{-12}$ M). Taking into consideration the large variations in these investigations a K_d-value of 0.5 m^3kg^{-1} is chosen.

Actinium (Ac), Americium (Am), Curium (Cm), Promethium (Pm), Samarium (Sm), Europium (Eu), Holmium (Ho)

These actinides and lanthanides will be in the trivalent state. For the actinides a K_d-value of 1 m^3kg^{-1} is selected based on measurements on sorption of Am on crushed cement (Bayliss *et al.,* 1996, and Allard *et al.,* 1984). The K_d-value for these actinides and lanthanides is probably higher as indicated by some investigations (Allard *et al.,* 1984). Bayliss *et al.* (1996) had a very low starting concentration, and thus no precipitation, why this value is chosen.

For the lanthanides (Pm, Sm, Eu, Ho) only sorption values for Pm was found (Holgersson *et al.,* 1998). In the investigation by Holgersson *et al.* (1998), care was taken to avoid precipitation, and the K_d-values obtained were >20 m^3kg^{-1}. Because of

uncertainties in determination of very high K_d-values and because of the large similarity in chemical behaviour of the lanthanides, a K_d-value of 5 m^3kg^{-1} is selected for all the lanthanides.

Antimony (Sb)

Antimony is probably trivalent under reducing conditions. No sorption data have been found in the literature, why we use Pm as an analogue and choose a K_d of 5 m^3kg^{-1}. This is a very crude assumption, but as we see it, the only possible one to make.

Thorium (Th), Protactinium (Pa), Uranium (U), Neptunium (Np), Plutonium (Pu)

These actinides are probably in the tetravalent state under reducing conditions, and they are strongly hydrolysed. Actually, the $An(OH)_4$ species are completely dominating in this region. For some of these actinides an $An(OH)_5^-$ species has been reported in older literature, but it seems that all later investigations have ruled out this species as unimportant or non-existing. Due to the redox chemistry of Pu and the expected low Eh, a fraction of the dissolved Pu is likely to be trivalent. This will not affect the sorption to any great extent, since trivalent actinides also have strong sorption on cementitious material. The sorption data are mainly based on the investigation of Bayliss *et al.* (1996) in which the sorption of U and Np on cement was investigated. Very high sorption values were obtained, in consistency with most of the sorption investigations on cement or other materials at high pH (Jakobsson *et al.,* 1998, Holgersson *et al.,* 1998, Bradbury and Sarott, 1994, Allard *et al.,* 1991, Bayliss *et al.,* 1996, Ewart *et al.,* 1988, Ewart and Tasker, 1987, Allard and Andersson, 1987, and Allard *et al.,* 1984). The K_d-values obtained are usually above 10 m^3kg^{-1}. Because of uncertainties in determination of very high K_d-values and because of the large similarity in chemical behaviour of these actinides, a K_d-value of 5 m^3kg^{-1} is selected for all of the tetravalent actinides.

Technetium (Tc), Zirconium (Zr)

Technetium is tetravalent under reducing conditions. There are very few investigations of the sorption of Zr and Tc under reducing conditions on cement, but these elements are expected to be completely hydrolysed. Thus, in analogy with the tetravalent actinides the sorption would be high. The only value that could be found in the open literature is a K_d of 0.5 m^3kg^{-1} for Zr (Kulmala and Hakanen, 1993) and values in the range 0.01 m^3kg^{-1} (oxidising condition) to 5 m^3kg^{-1} (reducing conditions) for Tc (Allard, 1985, and Bayliss *et al.,* 1992). Therefore we have chosen a K_d of 0.5 m^3kg^{-1} as a reasonable value for both Zr and Tc.

Table 7-4 Selected sorption coefficients on concrete at pH 13.5 for non-saline and saline intruding groundwater.

Ox. state[1)]	Element	K_d (m^3/kg)	Comment
M(I)	H	0	As water molecules
	Cs	0.001	Based on data for saline water
	Ag	0.001	In analogy with Cs
M(II)	Ni	0.04	Based on data for non-saline water
	Co, Fe, Pd, Cd	0.04	In analogy with Ni
	Pb	0.1	Based on data for non-saline water
	Sr	0.001	Based on data for saline water
	Ba	0.007	Based on granite data for saline water
	Ra	0.05	Based on data for non-saline water
	Be	0.05	In analogy with Ra
M(II/IV)	Sn	0.5	Based on data for non-saline water
M(III)	Am	1	Based on data for saline water
	Ac, Cm	1	In analogy with Am
	Pm	5	Based on data for non-saline water
	Sm, Eu, Ho, Sb	5	In analogy with Pm
M(IV)	Th	5	Based on data for non-saline water
	U, Np	5	Based on data for saline water
	Pa, Pu	5	In analogy with Th, U, Np
	Zr	0.5	Based on data for non-saline water
	Tc	0.5	In analogy with Zr
	C(inorg.)	0.2	Based on data for non-saline water
	C(org.)	0	No sorption
M(V)	Nb	0.5	Based on data for non-saline water
M(VI)	Mo	0.006	Based on data for non-saline water
M(-I)	Cl	0.006	Based on data for non-saline water
	I	0.003	Based on data for saline water
M(-II,IV,VI)	Se	0.006	In analogy with Mo

[1)] oxidation state for major ionic species at reducing Eh and pH 7-14

7.2.3 Sorption on granite

As stated earlier in this section, the data on sorption coefficients for sorption on backfill material is assumed to be identical to the data given by Carbol and Engkvist (1997). The selection of sorption coefficients for nuclides not included in Carbol and Engkvist (1997) are discussed below. The sorption coefficients for the elements on the backfill material that are used in the release calculations for SFL 3-5 are compiled in Table 7-5.

Iron (Fe) and Lead (Pb)

No data for iron or lead sorption on granite are available. The sorption behaviour of these elements are expected to be similar to the sorption of nickel and the K_d-values for nickel given by Carbol and Engkvist (1997) are therefore selected. These are 0.1 m^3kg^{-1} for non-saline water and 0.02 m^3kg^{-1} for saline water.

Barium (Ba)

The selected K_d-values for barium sorption on granite are 0.2 m^3kg^{-1} for non-saline water (Kulmala and Hakanen, 1995) and 0.007 m^3kg^{-1} for saline water (ibid., Byegård *et al.,* 1995).

Beryllium (Be)

No data for beryllium sorption on granite are available. Beryllium is expected to behave similar to radium and the K_d-values for radium given by Carbol and Engkvist (1997) are therefore selected. These are 0.1 m^3kg^{-1} for non-saline water and 0.02 m^3kg^{-1} for saline water.

Promethium (Pm) and Antimony (Sb)

No data for the sorption of these elements on granite are available. The K_d-value for other lanthanides given by Carbol and Engkvist (1997) are therefore selected. This value is 2 m^3kg^{-1} for both saline and non-saline water. This is a good choice for Pm, but a coarse approximation for the trivalent Sb.

Molybdenum (Mo)

Molybdenum will be present as the anion MoO_4^{2-}. Sorption data for Mo on sand and gravel in non-saline water are available (Stollenwerk, 1998). The sorption isotherm was found to be highly non-linear at lower pH and sorption decreased with increased pH, probably due to $CaMoO_4$ complex formation. For the highest pH investigated, pH = 6.5 and with a Ca concentration of 0.3 mM, the sorption isotherm was almost linear and gave a K_d -value of around 0.0001 m^3kg^{-1}. Even lower values can be expected for waters with higher Ca concentrations. A zero K_d-value for Mo is therefore selected.

Table 7-5 Selected sorption coefficients (m^3 kg^{-1}) on granite in saline and non-saline groundwater (Carbol and Engkvist, 1997).

Ox. state[1)]	Element	K_d (m^3/kg)		Comment to data not given by Carbol and Engkvist
		saline	non-saline	
M(I)	H	0	0	As water molecules
	Cs, Ag	0.05	0.5	
M(II)	Ni, Co, Cd	0.02	0.1	
	Fe, Pb	0.02	0.1	In analogy with Ni
	Pd	0.01	0.1	
	Sr	0.0002	0.01	
	Ra	0.02	0.1	
	Ba	0.007	0.2	Based on experimental data, see text
	Be	0.02	0.1	In analogy with Ra
M(III)	Am, Ac, Cm	3	3	
	Sm, Eu, Ho	2	2	
	Pm, Sb	2	2	In analogy with Sm, Eu and Ho
M(III,IV)	Pu	5	5	
M(IV)	Th, U, Np	5	5	
	Zr, Tc	1	1	
	C(inorg)	0.001	0.001	
	C(org)	0	0	No sorption
M(IV,V)	Pa	1	1	
M(V)	Nb	1	1	
M(VI)	Mo	0	0	Based on experimental data, see text
M(-I)	Cl, I	0	0	
M(-II,IV,VI)	Se	0.001	0.001	

[1)] oxidation state for major ionic species at reducing Eh and pH 7-9

7.3 Influence of complexing agents on sorption and solubilities

7.3.1 Potential complexing agents in SFL 3

The various categories of waste in SFL 3-5 will contain considerable amounts of organic material, such as ion exchange resins, plastic and rubber etc., as well as cellulose. Essentially all of the organic material, totally some 400 tonnes, will be placed in SFL 3. The degradation of the organic material under the conditions in the repository (anaerobic and pH above 12) will generate a fraction of soluble organic compounds that may have a significant influence on the solubility and adsorption behaviour of the radionuclides and thereby their releases and migration out of the repository.

In the prestudy of the SFL 3-5 disposal concept (Wiborgh, 1995) it was concluded that alkaline degradation of cellulose will yield products, mainly isosaccharinic acid (ISA) that may have great effects on solubility and sorption of certain elements. Degradation products from other organic materials in the waste are expected to have minor effects only.

In the prestudy (Wiborgh, 1995) it was also concluded that inorganic complexing agents are less important in comparison, with one exception, cyanides. Cyanides are present in some of the concrete conditioned waste from Studsvik, where Cs has been coprecipitated with ferrocyanides (copper(II)-iron-cyanide) from waste solutions (Lindgren *et al.,* 1998). The effect of cyanides as a complexing agent had been observed by Bradbury and Sarrot (1994) and equal weight was given to cyanides and cellulose in the Swiss safety assessment of a LLW and ILW repository in Wellenberg (NAGRA, 1994). However, more recent information indicates that cyanide in the form of ferrocyanide is of negligible importance as a source for complexing agents (Bradbury and Van Loon, 1998). Ferrocyanide is readily soluble at high pH and goes into solution as the hexacyanoferrate anion $Fe(CN)_6^{4-}$. This anion forms only weak complexes with metal cations and it is stable at pH > 8, provided that light is excluded. Based on this and on the fact that the estimated quantities of cyanides are only 10% of the amount of cellulose in SFL 3, cyanide is neglected as a complexing agent in SFL 3.

Another potential source for complexing agents in the repository is chemicals used as additives in concrete. No quantification has been made of the amount of concrete additives that could be expected in SFL 3-5. Furthermore, there are still uncertainties regarding the importance of concrete additives as complexing agents, but this is presently under investigation. It is therefore decided to not consider concrete additives as complexing agents until more information on this aspect is available.

7.3.2 Effects of isosaccharinic acid (ISA) on solubility and sorption

Some of the waste categories in SFL 3 contain cellulose that by alkaline degradation could yield isosaccharinic acid, ISA, in the waste containers. The concentration of ISA in the waste containers has been calculated by the use of data available in the literature on yield of ISA and on sorption of ISA on cement. These calculations are described in Appendix 3. The results indicate that the equilibrium concentration of ISA is equal to or below 0.1 mM. For such low concentrations no effect of ISA on sorption of radionuclides is expected (see Appendix 3).

However, the effects of ISA on solubilities cannot *a priori* be neglected, as indicated by experimental results (see Appendix 3). It is therefore suggested that the effect of a higher solubility in the presence of ISA is addressed in the calculations of radionuclide release from SFL 3. The solubility limits recommended are compiled in Table 7-6 (see also Appendix 3).

Table 7-6 Recommended solubility limits in concrete pore water in SFL 3.

Element	Solubility (M)	
	not affected by ISA	affected by ISA
Ni	$1 \cdot 10^{-7}$	$2 \cdot 10^{-7}$
Pm	$9 \cdot 10^{-8}$	$3 \cdot 10^{-5}$
Am, Cm	$9 \cdot 10^{-8}$	-
Pa, Np, Pu	$5 \cdot 10^{-9}$	-
Th, U	$5 \cdot 10^{-9}$	$7 \cdot 10^{-5}$

7.4 Data uncertainties

7.4.1 Solubility and sorption on concrete

The selection of solubility data is as far as possible based on experimental data and results of equilibrium calculations reported in the literature. The data are selected for the expected conditions in the repository. What regards pH, data in the whole alkaline range at pH > 10 are considered since the solubility of many of the elements is strongly dependent on pH. A pessimistic approach is used by selecting the highest of the values reported in the literature for this pH range.

Data for sorption on concrete are based on experimental data reported in the literature for sorption in fresh, i.e. non-leached, concrete in non-saline and saline water and on chemical analogies between elements. When a range in values of the sorption coefficient is found, the lowest value is pessimistically chosen for the calculations.

It is difficult to quantify the uncertainty in the selected values of radionuclide solubility and sorption on concrete. However, the range in the values reported in the literature (see Sections 7.1.1, 7.2.1and 7.2.2) gives one indication of the uncertainty in the selected values. For example, reported sorption coefficients for the lanthanides are above 20 m^3/kg and for some actinides above 10 m^3/kg, but the value proposed for these elements is 5 m^3/kg. Another indication of the uncertainty in the selected sorption data for concrete could be obtained by comparing these data with the selected data for sorption on the gravel backfill in saline waters. For most of the elements sorption on concrete is expected to be at least as large and most likely larger than sorption on granite in saline waters due to the higher pH. One exception from this concerns the sorption of caesium and silver where potassium is a competitive ion. Since the concentration of potassium is larger in concrete porewater than in saline groundwater, at least during the initial phase after repository closure, the sorption coefficient for concrete should be lower than that for the gravel backfill. Another exception concerns the sorption of inorganic carbon, since the retention of carbon rather is due to precipitation than sorption and thus strongly correlated to the presence of cement.

Comparing the sorption data proposed for the remaining elements on concrete (Table 7-4) with those for the gravel backfill in saline waters (Table 7-5) show that the

sorption coefficients for concrete in general is about a factor of 2 higher than for the gravel backfill and at most a factor of 5 higher. However, all sorption data proposed for concrete that are higher than those proposed for gravel are also equal to or lower than the maximum value in the uncertainty range for sorption on granite given by Carbol and Engkvist (1997). For the elements actinium, americium, curium, technetium and zirconium, the sorption data proposed for concrete are lower than those proposed for the gravel backfill. This illustrates the pessimistic approach used in the selection of sorption data for concrete.

7.4.2 Effects of ISA on solubility and sorption on concrete

The experimental results available indicate that the presence of isosaccharinic acid, ISA, may cause a large increase of the solubility of actinides. There are also indications that this requires a concentration of ISA of 10^{-4} M or higher. If sorption of ISA on concrete is accounted for such low concentrations of ISA could be obtained inside the waste packages. However, it can not be ruled out that the concentration of ISA locally is higher in the water in direct contact with the waste. Pessimistically it is therefore suggested to use much higher or even disregard solubility constraints for the trivalent and the tetravalent radionuclides when ISA is present.

Effects of ISA on sorption are neglected since the estimated concentration of ISA in the waste packages does not exceed 10^{-4} M. The experimental data available on sorption on cement in the presence of ISA clearly supports a threshold value of 10^{-4} M of ISA before effects on sorption occurs. The reliability in the estimated ISA concentration in the waste packages is therefore crucial.

The estimated ISA concentration in the waste packages are based on assumptions regarding the yield of ISA from degradation of cellulose and extent of ISA sorption on cement. Different experimental studies show good agreement between determined sorption isotherms, while there seems to be larger uncertainties in the experimentally determined degradation yields. This latter discrepancy has recently been observed and discussions on future actions to solve this problem are presently taking place between the waste management companies in Sweden, Switzerland and the UK.

7.4.3 Sorption on gravel backfill

The sorption coefficients proposed for the gravel backfill are the same as those proposed for the rock in the far field. These data are taken from Carbol and Engkvist (1997) where both a reasonable estimate and an uncertainty range are given. The reasonable value is selected for the analysis of migration from SFL 3-5. The potential uncertainty in making this choice is further discussed in Section 9.6.3.

8 Near-field physical data

8.1 Water flow

One input parameter to the modelling of the radionuclide migration in the near field of SFL 3-5 is the water flow in the different near-field barriers. The results of the near-field hydrology modelling (Section 4.2) can be used to calculate these flow rates when the direction and magnitude of the specific groundwater flow at the proposed location of the repository are defined.

The SFL 3-5 repository is not included in the more detailed local hydrology models of Aberg, Beberg and Ceberg used for the hydrology analyses of the deep repository for spent fuel in SR 97. Therefore, the results obtained by the regional hydrology models of the sites (see Section 4.2 and Appendices 1 and 2) have to be used to define the direction and magnitude of the groundwater flow. The results from the regional modelling indicate that the direction of the groundwater flow is close to horizontal in Beberg and Ceberg (Table 4-1). In Aberg the flow is directed slightly downwards with a mean deviation of about 30° from horizontal flow (Table 4-1).

The results of the near-field hydrology modelling show that the highest total flow in the different barriers in SFL 3 and SFL 5 is obtained for a regional horizontal flow along the SFL 3 and SFL 5 caverns (Table 4-2). A horizontal flow at right angle to SFL 3 and SFL 5 gives the highest flow in SFL 4.

Based on these results from the regional hydrology models and the near-field hydrology model, the flow direction at all sites is defined as being horizontal along the SFL 3 and SFL 5 caverns. Assuming a horizontal flow is reasonable since the regional flow has to be vertical or very close to vertical in order to give a vertical flow through the tunnels. Choosing the direction in the horizontal plane to be along SFL 3 and SFL 5 instead of at right angle to them gives the highest water flow in these caverns, but the lowest flow in SFL 4. Making this selection is conservative since the waste in SFL 3 and SFL 5 contains much higher activity than the waste in SFL 4.

Again, due to the lack of a more detailed description of the groundwater flow at the three sites, the results from the regional modelling is used as a guide to define the order of magnitude of the groundwater flow at the sites. Based on the results from the regional hydrology modelling (see Table 4-1) the following specific groundwater flows are selected:

- 10^{-2} m^3/m^2, year (= 10 l/m^2, year) in Aberg
- 10^{-3} m^3/m^2, year (= 1 l/m^2, year) in Beberg
- 10^{-4} m^3/m^2, year (= 0.1 l/m^2, year) in Ceberg.

Combining these regional specific flows with the results from the near-field hydrology modelling (Table 4-2) gives the total water flow in the concrete enclosure and the gravel backfill in SFL 3 and in SFL 5. For SFL 4 the data gives the total flow in both of the sections of the SFL 4 tunnel that are located along the direction of the flow. The total

flow in one of these sections is then half of the total flow in both sections. The so obtained total water flows in the SFL 3-5 near-field barriers are given in Table 8-1.

To compensate for potential differences in cross-sectional areas of the barriers between the hydrology model and the radionuclide migration model, the specific flow through the barriers is calculated from the total water flow and the cross-sectional area in the hydrology model. This specific flow is included in Table 8-1 and is used as input data to the modelling of migration in the near field.

Table 8-1 Total flow (m^3/year) and specific flow (m^3/m^2, year) in the near-field barriers in SFL 3-5 for a horizontal groundwater flow along SFL 3 and SFL 5 according to the near-field hydrology model.

	SFL 3		SFL 4	SFL 5	
	Enclosure	Backfill	Backfill	Enclosure	Backfill
Cross sectional area in hydrology model (m^2) [a]	100	196	64	100	196
Specific regional groundwater flow of 10 l/m^2, year representing Aberg					
Total flow (m^3/year)	10^{-2}	60	240[b]	10^{-2}	62
Specific flow (m^3/m^2, year)	10^{-4}	0.31	3.8	10^{-4}	0.32
Specific regional groundwater flow of 1 l/m^2, year representing Beberg					
Total flow (m^3/year)	10^{-3}	6	24[b]	10^{-3}	6.2
Specific flow (m^3/m^2, year)	10^{-5}	$3.1 \cdot 10^{-2}$	0.38	10^{-5}	$3.2 \cdot 10^{-2}$
Specific regional groundwater flow of 0.1 l/m^2, year representing Ceberg					
Total flow (m^3/year)	10^{-4}	0.6	2.4[b]	10^{-4}	0.62
Specific flow (m^3/m^2, year)	10^{-6}	$3.1 \cdot 10^{-3}$	$3.8 \cdot 10^{-2}$	10^{-6}	$3.2 \cdot 10^{-3}$

[a] *from Holmén (1997)*
[b] *in one of the two parallel sections of the SFL 4 tunnel*

8.2 Diffusivity and porosity

The effective diffusivity, D_e, of radionuclides and other toxicants in the near-field barriers and the porosity, ε, in the barriers are needed as input to the near-field model to calculate the migration by diffusion. The values of the porosity and effective diffusivity in the near field selected for the migration calculations are compiled in Table 8-2.

Table 8-2 Selected values of the porosity and effective diffusivity in the near-field barriers in SFL 3-5.

Material	Porosity (%)	Effective diffusivity (m^2/s)
Structural concrete	15	$1 \cdot 10^{-11}$
Porous concrete	30	$1 \cdot 10^{-10}$
Gravel backfill	30	$6 \cdot 10^{-10}$

The effective diffusivity and the porosity are correlated since the porosity and the internal pore structure determines the effective diffusivity. The effective diffusivity can be written:

$$D_e = D_0 \cdot \varepsilon \cdot \frac{\delta_D}{\tau^2} = D_0 \cdot \varepsilon \cdot GF \qquad (8.1)$$

where D_0 is the diffusivity in unconfined water, m^2/s, δ_D is the constrictivity factor that accounts for the narrowing of passages in the pore structure, τ^2 is the tortuosity factor that describes the winding of the pores compared to straight pores and GF is the geometric factor.

8.2.1 Concrete

In the safety assessment of SFR a porosity of 15 % and 30 % in structural concrete and porous concrete, respectively, was used in the radionuclide release calculations. These values were based on estimates of the porosity of fully hydrated structural concrete and porous concrete by the use of a hydration model and on the results of calculations of the porosity change due to leaching of portlandite (Höglund and Bengtsson, 1991 and Höglund, 1993). The latter calculations indicated a porosity increase from 15 to less than 16% in structural concrete and from 30 to 30.5% in porous concrete as a result of depletion of portlandite. The porosity of concrete (a mixture of Standard Portland Cement from Degerhamn in Sweden and natural silica sand) was determined by Holgersson *et al.* (1998). Using the water saturation method the porosity of a concrete slab was estimated to 15 %, but to about 6 % and 24 % evaluated from the breakthrough curve of caesium and of tritiated water, respectively. Johnston and Wilmot (1992) determined the porosity of cement grout mixtures consisting of Portland cement, silica fume and a small amount of a water reducing superplasticizer by mercury porosimetry. The porosity varied between 11 % and 22 % depending on concrete composition and water-to-solid ratio.

The effective diffusivity selected for the calculations of radionuclide migration in SFR was $3 \cdot 10^{-12}$ m^2/s for fresh structural concrete and $3 \cdot 10^{-11}$ m^2/s for aged structural concrete. These values were based on a porosity of 15 % together with the assumptions of a geometric factor of 0.01 for fresh structural concrete and 0.1 for aged structural concrete and a diffusivity in unconfined water of $2 \cdot 10^{-9}$ m^2/s (Höglund and Bengtsson, 1991). A higher value of the geometric factor in aged concrete than in fresh concrete was selected since the internal pore structure may change towards a less complex structure due to recrystallisation of the calcium silicate hydrate gel during ageing. However, it was also pointed out that a geometric factor of 0.1 for aged concrete probably is too high since this value is a reasonable value for a homogeneous porous material with distributed pore sizes (Höglund and Bengtsson, 1991).

The effective diffusivity of caesium and tritiated water evaluated from experiments on diffusion through a slab of concrete is $2 \cdot 10^{-12}$ m^2/s for caesium and $8 \cdot 10^{-12}$ m^2/s for tritiated water (Holgersson *et al.,* 1998). The effective diffusivity of tritiated water is in agreement with the value of $(7 - 11) \cdot 10^{-12}$ m^2/s obtained by Johnston and Wilmot (1992) in through diffusion experiments. Johnston and Wilmot also report the effective diffusivity of chloride (Cl^-) to be $(4 - 7) \cdot 10^{-12}$ m^2/s. Atkinson and Nickerson (1988) report an effective diffusivity of $1.8 \cdot 10^{-12}$ m^2/s for caesium and about $7 \cdot 10^{-12}$ m^2/s for iodide (I^-) from through diffusion experiments in concrete.

The geometric factor in porous concrete is expected to be higher than in structural concrete because of the higher capillary porosity. In the safety assessment of SFR a geometric factor of 0.5 was selected. This together with a porosity of 30 % and a diffusivity in unconfined water of $2 \cdot 10^{-9}$ m^2/s gives an effective diffusivity of $3 \cdot 10^{-10}$ m^2/s, i.e. one order of magnitude higher than in structural concrete (Höglund, 1993).

For the quantitative analysis of the migration of radionuclides and other toxicants in the near-field barriers in SFL 3-5 the data selected should be representative for fresh concrete and concrete depleted of portlandite. However, since the effect of portlandite leaching on porosity is negligibly small, data for fresh concrete is selected. Based on experimental data a value of $D_e = 1 \cdot 10^{-11}$ m^2/s and $\varepsilon = 15$ % is used for structural concrete. Due to the lack of experimental data on porous concrete, the same assumption is made in this work as in the safety assessment of SFR. The porosity is 30 % and the diffusivity is one order of magnitude higher than in structural concrete, i.e. $D_e = 1 \cdot 10^{-10}$ m^2/s (see Table 8-2).

In the calculations of the water flow in the concrete enclosure it is assumed that the concrete contains fully penetrating cracks and that the hydraulic conductivity is of the order of 10^{-8} m/s (see Chapter 4). According to Höglund and Bengtsson (1991) a hydraulic conductivity of $6.3 \cdot 10^{-7}$ m/s corresponds to a fully penetrating crack with an aperture of 100 μm every metre. One fully penetrating crack of the same aperture every ten metres would give a conductivity less than 10^{-7} m/s. The diffusive flux through these fractures constitute about 2% of the diffusive flux through intact concrete in the case of one fully penetrating crack every metre (conductivity = $6.3 \cdot 10^{-7}$ m/s). With one fully penetrating crack every ten metres the diffusive flux through the cracks is about 0.2% of the diffusive flux through intact concrete. These estimates show that the release by diffusion through a concrete enclosure with a hydraulic conductivity of 10^{-8} m/s is determined by the diffusion in intact concrete, i.e. transport by diffusion in the cracks is negligible.

8.2.2 Gravel backfill

The material used as backfill in the SFL 3-5 tunnels is rock that is crushed and sieved. The expected size fraction to be used is 4 – 32 mm (Karlsson *et al.,* 1999). The porosity of gravel is in the range 25 – 40 % (Freeze and Cherry, 1979). A porosity of 30 % is assumed in this study.

Furthermore, it is conservatively assumed that the geometric factor, GF, is 1. This value and the assumed porosity together with a diffusivity in unconfined water of $2 \cdot 10^{-9}$ m^2/s gives an effective diffusivity in gravel of $6 \cdot 10^{-10}$ m^2/s.

8.3 Data uncertainties

8.3.1 Water flow

The water flow in the different near-field barriers in SFL 3-5 is derived from the results of a generic hydrogeological modelling of the near field and of regional hydrogeological modelling of the SFL 3-5 repository location in Aberg, Beberg and Ceberg. The results from the regional hydrogeological modelling are used as a guide to define the order of magnitude of the groundwater flow and the flow direction at the sites. Since the intention is to illustrate the importance of the size of the groundwater flow rather than to exactly simulate the conditions at the three sites, the uncertainty in the selected values of the groundwater flow in the rock is not further discussed here. However, the values selected can be compared with the results from the hydrogeological modelling that are given in terms of minimum, maximum and mean values in Table 4-1.

The water flow in the near-field barriers is also dependent on the direction of the regional water flow and the contrasts in conductivity between the barriers and surrounding rock. The water flows selected for the migration calculations are those calculated for a horizontal flow direction, along SFL 3 and SFL 5. The results from the generic hydrology modelling of the near field show that this flow direction gives the largest flow in the gravel backfill in SFL 3 and SFL 5, but the lowest flow in SFL 4 (Holmén, 1997). Depending on the direction of the regional flow, the total flow in the SFL 4 tunnel varies by at most a factor of about 5. The total flow in the gravel backfill and in the encapsulation in SFL 3 and SFL 5 varies by less at most a factor of 2 and 3, respectively, with the direction of the regional flow (Holmén, 1997) (see Table 4-2).

The contrast in hydraulic conductivity that gives the values of the water flows selected is 10^5 between the gravel backfill and 10 between the concrete encapsulation and the rock in SFL 3 and SFL 5. As already discussed in Section 4.2, the water flows obtained with these conductivity contrasts are applicable despite that they not are in agreement with the conductivity contrasts obtained using the expected conductivity in gravel backfill, concrete encapsulation and rock at the three sites. The reason for this is that the contrast between the expected conductivity in the concrete encapsulation and the gravel backfill in SFL 3 and SFL 5 is the same (10^4) as that used in the hydrology modelling and that the contrast in the expected conductivity in the backfill and the rock is at least 1 000.

The value of the hydraulic conductivity chosen for the gravel backfill (10^{-4} m/s) is probably low considering the data reported in the literature (see Section 4.2). A higher conductivity in the backfill would result in a lower flow through the concrete encapsulation without increasing the flow in the gravel backfill (Holmén, 1997). The uncertainty in the selected value of the conductivity in the concrete is difficult to quantify. However, a higher value than that assumed (10^{-8} m/s) will be compensated by a higher conductivity in the backfill, which seems to be more probable than a higher conductivity in the concrete encapsulation. With a lower conductivity in the concrete encapsulation, the flow through the encapsulation would be lower than the selected value and the flow through the gravel backfill would be the same provided that the conductivity in the backfill is at least 10^{-4} m/s.

The conductivity contrast between the gravel backfill in SFL 4 and the rock that gives the selected water flow in the near-field barriers is 10^4. As already mentioned in Section 4.2 this corresponds to the situation at Beberg, but not in Aberg and Ceberg. The consequence for Ceberg would be that the flow in the barriers in SFL 3 and SFL 5 is overestimated, while the flow in SFL 4 is not affected. For Aberg, this may mean that that the water flow in the barriers in SFL 3 and SFL 5 are underestimated by at most about 40%, while the water flow in SFL 4 is overestimated by the same order of magnitude (Holmén, 1997).

The long SFL 4 tunnel that surrounds SFL 3 and SFL 5 can act as a hydraulic cage when the regional flow is horizontal or nearly horizontal and the conductivity in the SFL 4 tunnel is at least 100 times higher than in the rock mass. This means that a higher conductivity in the gravel backfill than the assumed 10^{-4} m/s would reduce the flow in the barriers in SFL 3 and SFL 5. A higher conductivity would also increase the flow in SFL 4, but the maximum flow is reached when the contrast in conductivity between the tunnel and surrounding rock is 10^4 times or more (Holmén, 1997).

The importance of the heterogeneity of the rock mass on the water flow in the near-field barriers was estimated by using results from calculations with a stochastic continuum model where the rock mass has properties similar to those at the Äspö HRL (Holmén, 1997). The results show that in such a rock mass, the heterogeneity leads to an increase of the total flow in SFL 4 by a factor of about 2. In SFL 3 and 5, the maximum flow in a flow barrier will increase by a factor of about 2.5 times, provided that the conductivity of the barrier is higher than that of the rock mass.

8.3.2 Diffusivity and porosity

The selected value of the effective diffusivity of species in structural concrete is conservatively chosen based on experimental data reported in the literature. However, diffusion experiments are in general performed on fresh concrete, and it is difficult to postulate the potential changes in effective diffusivity due to leaching of alkali hydroxides and portlandite. The increase in porosity due to leaching is expected to be small and of minor importance for potential diffusivity changes, but the characteristics of the pore system and thereby the geometric factor may also change with an unknown effect on the diffusivity. In addition, the ionic strength of the concrete pore water will decrease. Diffusion experiments in clays and in rock samples indicate that the effective diffusivity of anions is lower in water with low ionic strength and that cations that sorb via an ion exchange mechanism have a higher diffusivity when the water has a low ionic strength. Therefore it cannot be ruled out that the diffusivity of certain species in concrete are affected by the decrease in ionic strength of the pore water that will take place as the leaching of the concrete proceeds. However, diffusion measurements have been initiated in pieces of concrete that have been leached of all alkali hydroxide (Albinsson, personal communication, 1999), and the results of these tests may reveal the importance of ionic strength for diffusion in concrete.

The effective diffusivity in porous concrete is expected to be higher than in structural concrete because of the larger capillary porosity. Therefore a ten times higher value than in structural concrete is selected. No experimental data on diffusivity in porous concrete are available so it is difficult to assess the uncertainty in the proposed value. However,

the diffusivity in porous concrete should be lower than in a gravel backfill that has the same porosity due to the more complex pore structure in the porous concrete than in the gravel backfill.

The porosity selected for structural concrete and porous concrete are based on the results of a concrete hydration model. The porosity of interest in the migration calculations is the diffusion porosity, which not necessarily is the same as the total porosity of the material. This is indicated by porosity values evaluated from diffusion experiments, where the evaluated porosity is different depending on the diffusing species (see Section 8.2.1). However, the selected values of the effective diffusivity and porosity in structural concrete should in combination cover the potential variations in porosity without underestimating the diffusion rate or the diffusive transport capacity of the concrete. This could be seen by comparing the selected diffusivity and porosity data with diffusivity and porosity data obtained by Holgersson *et al.* (1998) from diffusion experiments (see Table 8-3). The geometric factor GF, calculated according to Eq. 8.1, is approximately a factor of 2 higher with the selected data than with the experimental data derived by Holgersson and assuming a diffusivity of $2 \cdot 10^{-9}$ m^2/s in unconfined water. This also means that the proposed effective diffusivity, in the sense of transport capacity, could represent approximately a 2 times higher porosity than the selected value without giving a geometric factor that is lower than the value obtained from the experimental data on diffusivity and porosity (see last row in Table 8-3).

Table 8-3 Comparison of experimental and selected diffusivity and porosity data for structural concrete

	D_e (m^2/s)	ε (%)	GF
Tritiated water diffusion (Holgersson *et al.*, 1998)	$8 \cdot 10^{-12}$	24	0.017[a)]
Cesium diffusion (Holgersson *et al.*, 1998)	$2 \cdot 10^{-12}$	6	0.017[a)]
Selected data	$1 \cdot 10^{-11}$	15	0.033[b)]
Selected D_e and GF derived from data in Holgersson *et al.*, (1998)	$1 \cdot 10^{-11}$	29[c)]	0.017

[a)] Calculated (Eq. 8.1) from experimental values on D_e and ε
[b)] Calculated (Eq. 8.1) from selected values on D_e and ε
[c)] Calculated (Eq. 8.1) from selected value on D_e and GF calculated from experimental data

The effective diffusivity selected for the gravel backfill is based on a porosity of 30 %, a geometric factor of 1 and a diffusivity in unconfined water of $2 \cdot 10^{-9}$ m^2/s. The porosity in the gravel backfill can be somewhat higher than the value selected (see Section 8.2.2). On the other hand, the value of the geometric factor is most certainly lower than 1 since the gravel will increase the diffusion distance as compared to the thickness or length of the backfilled space.

A single value of the diffusivity in unconfined water is selected despite that this entity is element specific. Ohlsson and Neretnieks (1997) report a measured value for tritiated water of $2.4 \cdot 10^{-9}$ m^2/s and for cesium of $2.1 \cdot 10^{-9}$ m^2/s. The remaining measured values are all equal to or below $2.0 \cdot 10^{-9}$ m^2/s with the lowest value of $1.5 \cdot 10^{-10}$ m^2/s given for Th(IV). For many of the elements no measured data were found and therefore a value of $1 \cdot 10^{-9}$ m^2/s was assumed (Ohlsson and Neretnieks, 1997). Because measured data are lacking for a large number of elements and because a mixture of measured data and

assumed data may cause anomalies between elements that chemically and physically are similar, a single value is selected for the migration calculations in the safety analysis of SFL 3-5. According to the values reported by Ohlsson and Neretnieks (1997), the selected value is on the conservative side and for the majority of elements the selected value is at most a factor of 2 higher than the value given by Ohlsson and Neretnieks (1997).

9 Far-field migration data

9.1 Travel times for water and the flow-wetted surface area

The advective travel time for water from the repository to the ground surface and the flow-wetted surface area per volume of water are needed to calculate the transport of radionuclides and toxic metals in the far field with the far-field model FARF31 (see Section 2.2). The advective travel time is a theoretical quantity used in the transfer of results from hydro models to transport models. It could be seen as the transport time in the geosphere for a particle moving with the same velocity as the water without interacting with the rock. This quantity is strongly correlated to the flow-wetted surface area per volume of water via the flow porosity. This is further discussed in Section 9.1.2.

9.1.1 Advective travel time

The advective travel times for water and the length of different flow paths from SFL 3-5 to the ground surface in Aberg, Beberg and Ceberg have been estimated using the regional hydrology model for each site (Appendices 1 and 2). The results are summarised in Table 9-1. The simulation results for Aberg are based on travel times and lengths of transport paths for nine particles released in the region proposed for the location of SFL 3-5. Two of these particles had not reached the ground surface after 25 years travel time, which was used as the upper limit for the calculations. The results for Beberg and Ceberg are based on a simulation with 36 particles released in the part of the model corresponding to the proposed location for SFL 3-5.

Table 9-1 Estimated travel times and lengths of transport paths for groundwater in Aberg, Beberg, and Ceberg.

	Travel time (years)			Length of transport paths (m)		
	Aberg	Beberg	Ceberg	Aberg	Beberg	Ceberg
Mean	13	40	906	805	1 125	1 396
Standard deviation	7	24	208	216	194	93
Minimum	7	7	653	541	757	1 238
Maximum	25	80	1 292	1 100	1 479	1 583

Based on the estimated mean values given in Table 9-1 for each site, the following values of the advective travel times for water from the repository to the ground surface are selected in the modelling of radionuclide transport in the far-field of SFL 3-5:

- 10 years in Aberg
- 40 years in Beberg
- 900 years in Ceberg

9.1.2 Flow-wetted surface area

The flow-wetted surface area affects matrix diffusion and sorption of radionuclides, and is thus an important parameter in calculating the migration of radionuclides. The capability of the rock to delay the migration of radionuclides transported with flowing water in a fracture can be expressed using an F-factor. The F-factor for a single fracture is defined as (Andersson *et al.,* 1998):

$$F_i = t_i \cdot a_{wi} = \frac{a_{wi} \cdot \varepsilon_{fi} \cdot L_i}{q_i} = \frac{a_{ri} \cdot L_i}{q_i} \qquad (9.1)$$

where a_{ri} is the flow-wetted surface area per volume of rock (m^2/m^3), a_{wi} is the flow-wetted surface area per volume of flowing water (m^2/m^3), L_i is the transport length of water in the fracture (m), t_i is the advective travel time for water in the fracture (year), q_i is the specific water flow in the fracture (m^3/m^2, year) and ε_{fi} is the flow porosity (m^3/m^3).

For a flow path composed of different fractures and with different flow, the total F-factor is the sum of the F-factors for the different fractures, and the flow-wetted surface area per volume of flowing water for the whole flow path, a_w, can be calculated as (Andersson *et al.,* 1998):

$$a_w = \frac{\Sigma F_i}{\Sigma t_i} \qquad (9.2)$$

Andersson (1999) and Andersson *et al.,* (1998) recommend a value of 1 m^2/m^3 for the flow-wetted surface area per volume of rock in Aberg and Beberg, and 0.1 m^2/m^3 in Ceberg. However, these values can not be used directly in FARF31 since the flow-wetted surface area used in this model should be based on volume of flowing water instead of volume of rock.

For a flow path with a constant porosity the flow-wetted surface area per volume of flowing water can be estimated by dividing the flow-wetted surface area per volume of rock with the flow porosity (Andersson *et al.,* 1998). The flow porosity also affects the advective travel time for water. The flow porosity used for calculating the flow-wetted surface area per volume of flowing water should therefore be identical to the flow porosity used in the hydrology models to derive the advective water travel time that is used in the migrations calculations.

The advective water travel times in Beberg and Ceberg are estimated with a constant flow porosity of 10^{-4} as input in the hydrology models (Appendix 2). This flow porosity together with recommended values of the flow-wetted surface area per volume of rock would then give the following values of flow-wetted surface area per volume of flowing water:

- $a_w = 1/10^{-4} = 10^4$ m^2/m^3 for Beberg, and
- $a_w = 0.1/10^{-4} = 10^3$ m^2/m^3 for Ceberg.

The flow porosity used in the hydrology model for estimating the water travel time in Aberg is not constant, but depends on the hydraulic conductivity in different parts of the rock. According to equations 9.1 and 9.2, the flow-wetted surface area per volume of flowing water can be calculated if the flow porosity and the corresponding water travel time are known for all parts of the rock containing the flow paths from the repository. The flow porosity, ε_{fi}, would together with the flow-wetted surface area per volume of rock, a_{ri}, give the flow-wetted surface area per volume of water for each part of the flow path, a_{wi}. From this entity and the water travel time t_i, the F-factor F_i for each part of the flow path can be calculated. The flow-wetted surface area, a_w, can then be calculated from the sum of the F-factors and the sum of the water travel times.

Neither the flow porosity nor the specific flow are given for the flow paths that are evaluated in Aberg, but the arithmetic mean value of the flow porosity is given to be $1.3 \cdot 10^{-3}$ (Appendix 1). From the reported range in conductivity used in the regional hydrology model, the lowest and the highest possible flow porosity is estimated to be $3.7 \cdot 10^{-4}$ and $2.0 \cdot 10^{-2}$, respectively.

Since the flow porosity has been varied and data on the flow porosity is missing, it is proposed that the arithmetic mean value of the flow porosity is used for estimating the flow wetted surface, a_w, to be used in the calculations of solute migration in Aberg. This would give:

$a_w = 1/1.3 \cdot 10^{-3} = 770$ m^2/m^3 for Aberg.

Using the selected values of water travel time and flow-wetted surface area per volume of flowing water, an F-factor of $8 \cdot 10^3$ (= 10·770) year/m is obtained for Aberg, $4 \cdot 10^5$ (= 40·10 000) year/m for Beberg, and $9 \cdot 10^5$ (= 900·1 000) year/m for Ceberg. The F-factors corresponding to the data used in the far-field calculations in the safety analysis of the spent fuel repository (SR 97) are summarised in Table 9-2 (Andersson, 1999). The values on advective water travel time and flow-wetted surface area that here are selected for the calculation of the migration of radionuclides from SFL 3-5 in Beberg give a value of the F-factor that well correspond to the value defined for the reasonable estimate case in SR 97. For both Aberg and Ceberg the F-factor derived for migration from SFL 3-5 lies in the range between the value defined for the pessimistic and the reasonable estimate case in SR 97. In the SITE-94 project, an F-factor in the interval $7 \cdot 10^2$ till $6 \cdot 10^6$ year/m were used, with a reference value of $7 \cdot 10^4$ year/m (Andersson *et al.,* 1998).

Table 9-2 Comparison of F-factors corresponding to data used in this study and those in SR 97.

	F-factor		
	Aberg	**Beberg**	**Ceberg**
SFL 3-5	$8 \cdot 10^3$	$4 \cdot 10^5$	$9 \cdot 10^5$
SR 97 Reasonable estimate	$1 \cdot 10^5$	$5 \cdot 10^5$	$2 \cdot 10^6$
SR 97 Pessimistic case	$8 \cdot 10^2$	$3 \cdot 10^3$	$4 \cdot 10^5$

9.2 Peclet number

Based on experimental results, Andersson (1999) and Andersson *et al.,* (1998) have proposed that a Peclets number of 10 should be used in the modelling of radionuclide migration from the deep repository for spent fuel in Aberg, Beberg, and Ceberg. The same value is used in the safety analysis of SFL 3-5.

9.3 Rock matrix porosity and maximum penetration depth

The porosity available for diffusion of radionuclides in the rock matrix is for Swedish rock of the order of 0.1 to 1 % (Ohlsson and Neretnieks, 1997). A matrix porosity of 0.5 % has been proposed for the calculations of the migration of radionuclide from the deep repository for spent fuel in Aberg, Beberg and Ceberg (Andersson, 1999 and Ohlsson and Neretnieks, 1997). The same value is therefore selected for the calculations of the migration of radionuclide from SFL 3-5.

Anions have been shown in experiments to have a lower effective diffusivity in micropores of the rock in water with a low ionic strength than in water with a high ionic strength. This phenomenon is termed anion exclusion and is explained as repulsion between the negatively charged pore surfaces and the diffusing anion. This reduces the porosity that is available for anion diffusion. Ohlsson and Neretnieks (1997) have proposed a 10 times lower effective diffusivity of anions in non-saline water than in saline water due to anion exclusion effects. In the analysis of SFL 3-5, inorganic ^{14}C, ^{36}Cl, and ^{129}I are anions that are affected by anion exclusion. Thus, the diffusion porosity for these anions is reduced to 0.05 % in non-saline water.

The maximum penetration depth into the rock matrix depends on the structure of the rock in terms of connected porosity. The same assumption is made here as in the calculations of the migration from the spent fuel repository in SR 97, namely that there is no physical limit for diffusion into the rock matrix (Andersson, 1999). Instead, for symmetry reasons, the distance between water bearing fractures in the rock limits the penetration depth. The uncertainty in this parameter is large, but an estimate can be made from the proposed flow wetted surface of 1 m^2/m^3 rock in Aberg and Beberg, and 0.1 m^2/m^3 in Ceberg. Based on the frequency of evenly spaced conductive fractures corresponding to a flow wetted surface of 1 m^2/m^3 rock, a maximum penetration depth of 2 m in Aberg and Beberg is proposed (Andersson, 1999). In Ceberg where the flow wetted surface is ten times smaller and thus the distance between fractures is ten times larger, it is proposed that the maximum penetration depth is 20 m (Andersson, 1999).

9.4 Effective diffusivity in the rock matrix

Ohlsson and Neretnieks (1997) have proposed radionuclide specific diffusion data to be used within SR 97. These data are used in the calculations of migration of radionuclides from the spent fuel repository and is also selected in the calculations of migration from SFL 3-5.

For Aberg with a high salt content in the water, diffusion data for high ionic strength are used, and for Ceberg with non-saline ground water data for low ionic strength. The groundwater in Beberg can be both saline and non-saline. In the calculations of migration of radionuclides from the spent fuel repository, data for low ionic strength is used in the 'best estimate' case (Andersson, 1999). The reason for this choice is that there probably not will be any salt water left in Beberg at the time when the radionuclides are released from the bentonite surrounding the canisters to the far-field rock. The nuclide release from the near field of SFL 3-5 will most likely take place much earlier and therefore data for both low and high ionic strengths of the water can be relevant.

The effective diffusivity selected for the far-field migration of radionuclides from SFL 3-5 are summarised in Table 9-3 for saline (high ionic strength) and non-saline (low ionic strength) water. Some of the elements of importance in the waste in SFL 3-5 are not included in the data given by Ohlsson and Neretnieks (1997). The effective diffusivity of these elements is estimated using the same method as that used by Ohlsson and Neretnieks (1997). For further explanations see footer in Table 9-3.

Ohlsson and Neretnieks (1997) have proposed a ten times lower effective diffusivity of the elements C_{inorg}, I and Cl in the rock matrix in non-saline water than in saline water. This is because they are expected as anionic species under prevailing conditions in the rock and thereby affected by ion exclusion (see Section 9.3). The element Se probably also exists as an anionic species in the groundwater (Carbol and Engkvist, 1997). However, the potential effect of ion exclusion of Se is not considered in the diffusivity data given by Ohlsson and Neretnieks (1997). The element Mo will probably also be present in anionic form (see Section 7.2.3). Ohlsson and Neretnieks (1997) do not give the effective diffusivity in the rock matrix for Mo. It is therefore assumed that an analogy between Mo and Se can be made and the effective diffusivity of Mo is set to the value for Se given by Ohlsson and Neretnieks (1997).

The ionic strength of the water is also important for the diffusion of cations that sorbs via ion exchange. At low ionic strengths, the diffusivity of these cations is higher than expected in clays and the micropores of the rock. One explanation for this is that the sorbed cations are mobile along the surface and that the driving force for this transport is the difference in the concentration of sorbed cations along the surface. At high ionic strengths, the sorption of the cations is lower and the driving force for the diffusion along the surface, the so-called surface diffusion, is thereby less. Because of this, a ten times higher effective diffusivity of the cations Cs and Sr in non-saline water than in saline water is proposed by Ohlsson and Neretnieks (1997).

Table 9-3 Radionuclide specific effective diffusivities for saline water and non-saline water (Ohlsson and Neretnieks, 1997).

Element	$D_e \cdot 10^{14}$ (m^2/s)	
	Saline	Non-saline
H	10	10
Be [a)]	2.4	2.4
C_{inorg} [b)]	5.0	0.5
C_{org} [b)]	4.0	4.0
Cl	8.3	0.83
Co	2.9	2.9
Ni	2.8	2.8
Se	4.0	4.0
Sr	3.3	33
Zr [d)]	4.0	4.0
Nb	4.0	4.0
Mo [c)]	4.0	4.0
Tc [d)]	4.0	4.0
Pd	4.0	4.0
Ag	7.1	7.1
Cd	3.0	3.0
I	8.3	0.83
Cs	8.8	88
Sm	4.0	4.0
Eu	4.0	4.0
Ho	4.0	4.0
Pb [b)]	4.0	4.0
Ra	3.7	3.7
Ac	4.0	4.0
Th	0.63	0.63
Pa	4.0	4.0
U [d)]	4.0	4.0
Np [d)]	4.0	4.0
Pu	4.0	4.0
Am	4.0	4.0
Cm	4.0	4.0

a) *D_e calculated using the same method as Ohlsson and Neretnieks (1997) from diffusivity in unconfined water according to Li and Gregory (1974)*

b) *D_e based on the same diffusivity in unconfined water ($1.0 \cdot 10^{-9}$ m^2/s) as assumed by Ohlsson and Neretnieks (1997) when data are missing*

c) *same value as for Se is assumed*

d) *values for Tc(IV), U(IV) and Np(IV)*

9.5 Sorption coefficients in the rock matrix

Sorption data proposed by Carbol and Engkvist (1997) are used in the calculations of migration of radionuclides from the deep repository for spent fuel in the safety assessment SR 97. The same data are selected for the calculations of radionuclide migration from SFL 3-5. In accordance with the discussion in Section 9.4, sorption data for high and low ionic strengths are used for Aberg and Ceberg, respectively, and both sets of data for Beberg.

The same sorption data are used both for the gravel backfill in the repository vaults and the far-field rock in the calculations of radionuclide migration from SFL 3-5. Some of the elements of importance in the waste in SFL 3-5 are not included in the data presented by Carbol and Engkvist (1997). To estimate sorption data, chemical analogies or data from other references have been used. This is further discussed in Section 7.2.3 and the selected sorption data are given in Table 7-5.

9.6 Data uncertainties

9.6.1 Flow related migration parameters

The values selected for the flow related migration parameters in the calculations of radionuclide release from SFL 3-5 are as far as possible those proposed as a *reasonable estimate* for the migration calculations in the safety assessment of the deep repository for spent fuel, SR 97. These *reasonable estimates* are given in Andersson (1999) and the intention of presenting these values is to obtain a view of how the repository would operate without making overly optimistic or pessimistic assumptions. In order to bound the impact of uncertainty in the data a *pessimistic estimate* of the parameter values is also given in Andersson (1999).

A comparison between the values selected for the SFL 3-5 calculations and the *reasonable* and *pessimistic* values proposed by Andersson (1999) is shown in Table 9-4. The advective water travel times for SFL 3-5 are selected based on results from a regional hydrology modelling considering the position of SFL 3-5 at the different sites. The so obtained water travel times are similar to or shorter than the reasonable estimate for SR 97. In Andersson (1999) it is noted that the flow porosity of 10^{-4} that is used to estimate the water travel times in SR 97 probably is 10 times too small as indicated by tracer tests. Using a flow porosity of 10^{-4} instead of 10^{-3} makes the water travel times at least a factor of 10 too short (Andersson, 1999). The selected water travel times from SFL 3-5 are based on calculations with a flow porosity of 10^{-3} in Aberg and 10^{-4} in Beberg and Ceberg. This implies that the selected advective water travel times from SFL 3-5 in Beberg and Ceberg might be a factor of 10 too short. This discrepancy will not in general affect the release of sorbing radionuclides from the geosphere, but may, dependent on their half-lives, lead to an overestimation of the release of non-sorbing radionuclides.

The flow-wetted surface area in combination with the water travel time, expressed in terms of the ‘F-factor’ or ‘F-quotient’, is important for the release of sorbing radionuclides from the geosphere. A higher ‘F-factor’ means a larger retention in the rock. The value of the flow-wetted surface area selected for the SFL 3-5 calculations are the same as that selected as a reasonable estimate for Ceberg and Beberg in SR 97 (Table 9-4), but the values of the ‘F-factor’ are lower than the reasonable estimates for SR 97 (Table 9-2). The value of the flow-wetted surface area selected for SFL 3-5 in Aberg is even lower than the pessimistic case value for Aberg in SR 97 (Table 9-4). The value of the ‘F-factor’, however, is 10 times higher in the SFL 3-5 calculations than in the pessimistic case in SR 97, but still considerably lower than the reasonable estimate (Table 9-2).

Table 9-4 Proposed values of flow related parameters for the SFL 3-5 calculations and for the far-field calculations in SR 97 according to Andersson (1999).

Parameter	Aberg	Beberg	Ceberg
Water travel time (years)			
SFL 3-5	10	40	900
SR 97; reasonable estimate	10	60	2 000
SR 97; pessimistic case	0.8	3.3	400
Flow-wetted surface area (m^2/m^3 water)			
SFL 3-5	770	10^4	1 000
SR 97; reasonable estimate	10^4	10^4	1 000
SR 97; pessimistic case	1 000	1 000	1 000
Peclet number			
SFL 3-5	10	10	10
SR 97; reasonable estimate	10	10	10
SR 97; pessimistic case	2	2	2
Max penetration in rock matrix (m)			
SFL 3-5	2	2	20
SR 97; reasonable estimate	2	2	20
SR 97; pessimistic case	0.2	0.2	2

The Peclet number and the maximum penetration depth selected for the calculations in the analysis of SFL 3-5 are the same as the values given as reasonable estimates for SR 97. The difference between the reasonable estimate and the pessimistic case value is a factor of 5 for the Peclet number and a factor of 10 for the penetration depth into the rock matrix (Table 9-4).

9.6.2 Rock matrix porosity and diffusivity

The rock matrix porosity and effective diffusivity in the rock matrix selected for the SFL 3-5 calculations are those proposed as reasonable estimates in SR 97. Ohlsson and Neretnieks (1997) estimate the uncertainty in their proposed reasonable values of the effective diffusivity to be of the order of a factor of 3 to 5 for high salinity waters and a factor of 10 for charged species in low salinity waters. They also conclude that what here is called uncertainty also includes the variability due to the inhomogeneity of the rock matrix. For the pessimistic case in SR 97, Andersson (1999) propose that the lowest reasonable diffusivity values given in Ohlsson and Neretnieks (1997) are selected regardless of water composition and that these values are divided by a factor of 10. The selection of the lowest value is motivated by the uncertainty in the quantification of the effects of surface diffusion and the uncertainty in water composition (saline versus non-saline). The reduction of this value by a factor of 10 is motivated by the uncertainty in spatial variability of porosity (Andersson, 1999).

Regarding the matrix porosity it is suggested that the reasonable estimates also are used in a pessimistic case, i.e. a porosity of 0.05% for certain anions in non-saline water and a porosity of 0.5% for the remaining species (Andersson, 1999).

As mentioned earlier in Section 9.5, the elements Se and Mo probably exist as anionic species in the groundwater. In analogy with the other anionic species, a 10 times lower

effective diffusivity would be expected in non-saline water than in saline. This is not considered neither in the proposed reasonable values for SR 97 (Se) nor in the data proposed for the calculations in the analysis of SFL 3-5 (Se, Mo). However, the consequence of a 10 times lower effective diffusivity for Se on the release of ^{79}Se from the far field will probably be negligible due to its negligibly small sorption in the rock and its long half-life. The travel time in the far-field rock will be shorter, but the maximum release rate from the far field will not be affected. This is not necessarily the case for ^{93}Mo because of a shorter half-life. A ten times lower effective diffusivity in the rock matrix could then lead to a higher release rate of ^{93}Mo in non-saline water. However, it should be noted that the migration is affected by the square root of the effective diffusivity, but is directly proportional to the advective travel time. The possibility that the travel times proposed for Beberg and Ceberg in the calculations are 10 times too short (see Section 9.6.1) would then cancel out a potential 10 times too high matrix diffusivity used for ^{93}Mo in Beberg and Ceberg where non-saline water prevail.

9.6.3 Sorption data

The sorption data that are proposed as reasonable estimates for the migration calculations in SR 97 are also used in the calculations of radionuclide migration from SFL 3-5. Carbol and Engkvist (1997) provide the uncertainty in these values of the sorption coefficient by giving an uncertainty interval. For the pessimistic case in SR 97 the lowest value in the uncertainty range is selected (Andersson, 1999). The largest difference between the reasonable estimate and the pessimistic value is obtained for Pd with a 10 times lower pessimistic value both in saline and non-saline water. For the elements Cs, Ag, Pu, Th, U and Np the pessimistic value is 5 times lower than the reasonable estimate in both saline and non-saline water. The pessimistic value for Tc is 3.3 times lower and for Am, Ac and Cm 3 times lower than the reasonable value for saline and non-saline water. For the majority of elements, Ni, Co, Cd, Sr, Ra, Sm, Eu, Ho, Zr, C_{inorg}, Pa, Nb and Se, the pessimistic value is 2 times lower than the reasonable estimate. The actual values are given in Table 12.1 in Carbol and Engkvist (1997) and in Table A.2.6.2 in Andersson (1999).

Carbol and Engkvist (1997) do not provide sorption data for all of the elements relevant for the SFL 3-5 calculations. For the elements Fe and Pb an analogy with Ni is made and the reasonable value proposed for Ni by Carbol and Engkvist (1997) is selected also for Fe and Pb. This would then imply that the difference between the pessimistic and the reasonable value for these elements is a factor of 2 both in saline and non-saline water. A pessimistic value that is 2 times lower than the reasonable value is in this way also obtained for Be assuming it analogous to Ra and for Pm and Sb that are assumed to be in analogy with Sm, Eu and Ho.

10 Biosphere data

Ecosystem-specific dose conversion factors are used to calculate dose to man from the radionuclide release to the biosphere in the analysis of the repository for spent fuel, SR 97. The three study sites Aberg, Beberg and Ceberg were divided into sub-areas (250×250 m), and each sub-area was assigned to a typical ecosystem based on the existing ecosystem type. Maps of the areas and data on water exchange and precipitation on the three sites were used to calculate the ecosystem-specific dose conversion factors, EDF (Nordlinder *et al.*, 1999).

10.1 Selection of typical ecosystems and EDF

The results from the regional hydrology modelling (Appendices 1 and 2) are used to determine what areas on the ground surface are discharge areas for water passing the location of the repository. The results for Aberg show that the water is discharged in the sea east of Ävrö and in the bay north of Ävrö. The regional hydrology model for Beberg, shows flow paths to the ground surface via the fracture zone Imundbo to discharge points with the average co-ordinates (RAK) 1617614 mE and 6697082 mN. For Ceberg, the regional hydrology model shows that the water from SFL 3-5 is discharged at the average co-ordinates (RAK) 1665678 mE and 7045041 mN.

The classification of the three sites into different ecosystems that was done in SR 97 (Nordlinder *et al.*, 1999) and the discharge areas for groundwater that has passed a repository are shown in Figures 10-1 to 10-3. At Aberg (Figure 10-1), the discharge areas are classified as archipelago and open coast. At Beberg (Figure 10-2), discharge from the repository takes place in an area classified as agricultural land, while at Ceberg (Figure 10-3) the typical ecosystem is classified as peatland. At Beberg, a peat bog is situated immediately adjacent to the agricultural land where the discharge is projected to take place. Since a peat area in general has higher EDF's than an agricultural area, the consequence of a discharge to peatland at Beberg is also examined.

Based on the results of the regional hydrology models, there will be no release of radionuclides or other toxicants to the wells present in the region of Aberg, Beberg and Ceberg today. However, it is possible that wells will be founded at the location of the release area in the future. Release to a well is therefore included in the study as an alternative scenario. For this purpose a 'mean well' is defined for each of the three sites.

This mean well is defined as a well having a capacity equal to the arithmetic mean value of the capacity of the wells present today at each of the sites. The number of wells present today at Aberg, Beberg, and Ceberg is 3, 6, and 2 respectively. The capacity of these wells is compiled in Table 10-1, together with the site specific arithmetic mean value of the capacity. Based on these data the capacity of the site-specific mean wells is set to 300 litres/hour (Aberg), 1000 litres/hour (Beberg), and 500 litres/hour (Ceberg).

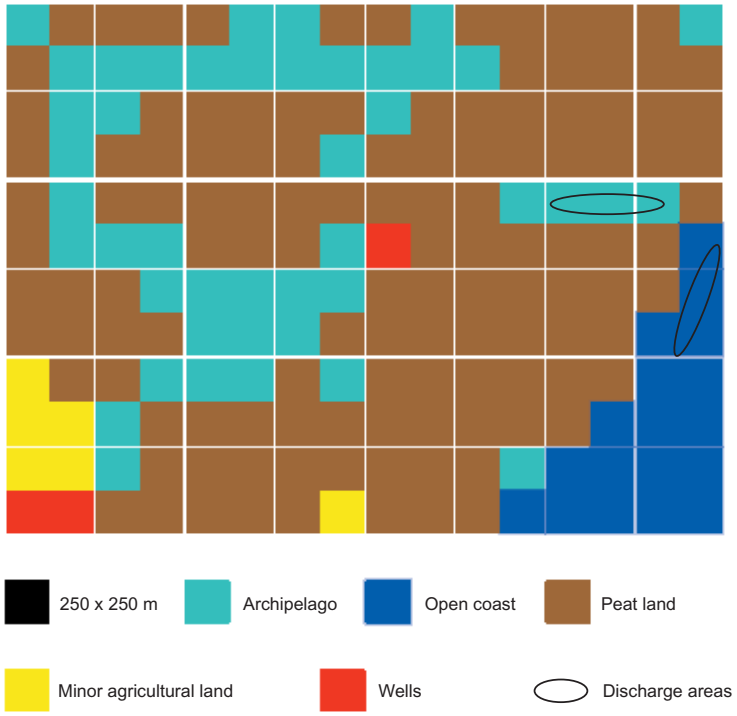

Figure 10-1 Typical ecosystems and discharge areas at Aberg.

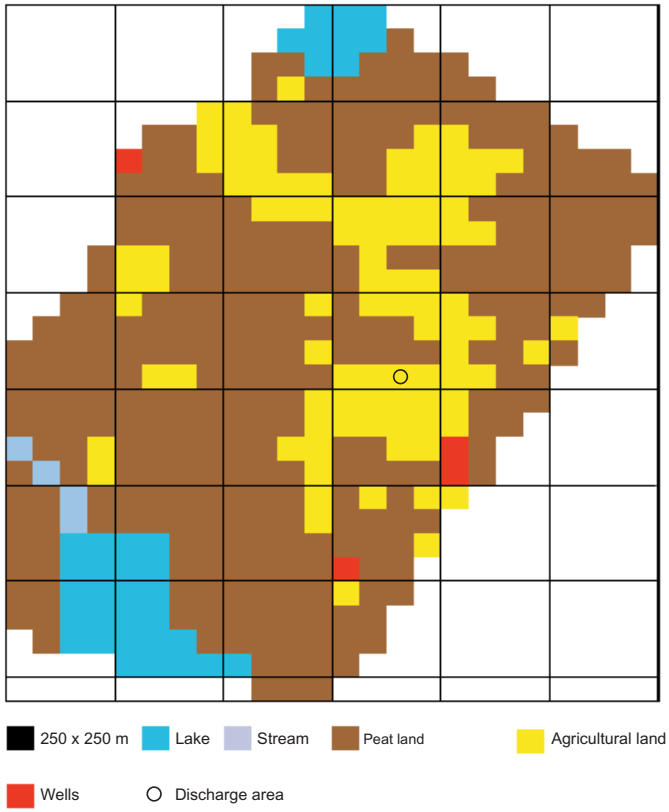

Figure 10-2 Typical ecosystems and discharge area at Beberg.

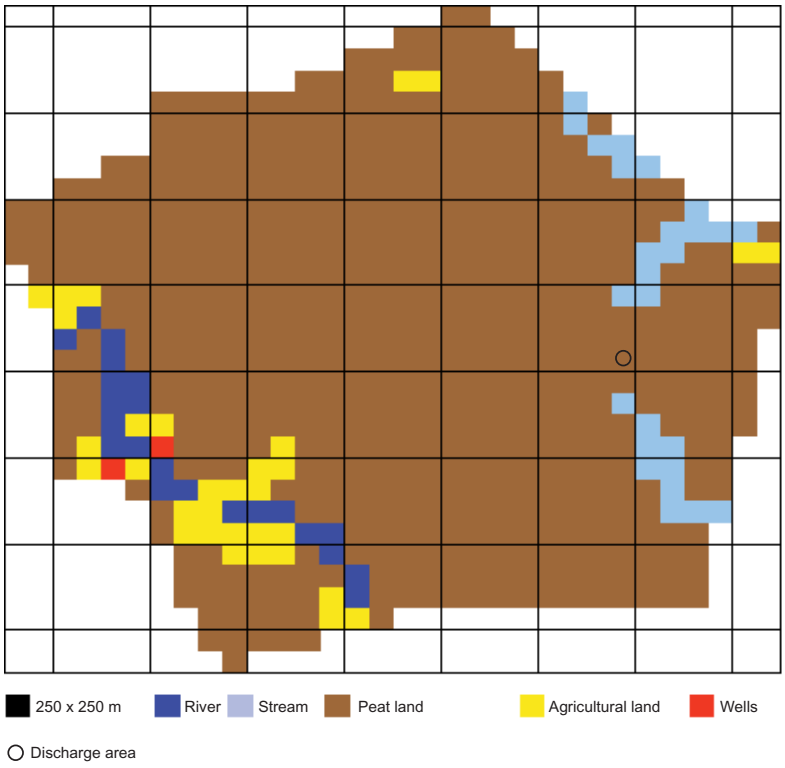

Figure 10-3 Typical ecosystems and discharge area at Ceberg.

Table 10-1 Capacity (litres/hour) of the wells in Aberg, Beberg, and Ceberg (Nordlinder *et al.*, 1999).

	Aberg	Beberg	Ceberg
Well 1	200	900	600
Well 2	300	400	400
Well 3	400	400	
Well 4		700	
Well 5		700	
Well 6		3 000	
Mean value	300	1 017	500

10.2 Ecosystem-specific dose conversion factors, EDF

Two calculation models have been used to derive the EDF's for the different ecosystems. The first model is a compartment model used for calculation of the radionuclide transfer between different parts of the ecosystem module, e.g. water, soil, sediment. The second model is used to calculate the radiation dose to man from the total quantity of radionuclides inhaled or ingested in the form of contaminated food during one year (internal exposure). The resulting EDF's are given in terms of a mean value and an uncertainty interval. The uncertainty interval is obtained by assigning an uncertainty range to the input parameters of the model. The models and the results are described in Bergström *et al.* (1999) and Nordlinder *et al.* (1999).

Since no probabilistic calculations are made for SFL 3-5, the mean values of the dose conversion factors given by Nordlinder *et al*. (1999) are selected. These are summarised in Table 10-2.

The EDF's for the mean wells are summarised in Table 10-3. For Aberg, these are the mean values of the dose conversion factors given by Nordlinder *et al.* (1999) for a well with the capacity of 300 l/hour. For Beberg and Ceberg, the EDF's for the mean wells are derived from the mean values of the dose conversion factors given by Nordlinder *et al.* (1999) for a well with the capacity of 700 l/hour in Beberg and 600 l/hour in Ceberg. This is done by compensating the EDF's for the difference in well capacity between these wells and the mean well at the site. Drinking water is not the only exposure pathway included in an EDF for 'Well'. The water is for instance also consumed by cattle and is used for irrigation of garden products. The amount of rainfall, and therefore also the amount of well water needed for irrigation, varies between the sites. Consequently, the EDF for a well with a certain capacity may not necessarily be the same for the different sites.

10.3 Recipient data

The release of toxic metals from the SFL 3-5 repository is evaluated by calculating the concentration of these metals in the primary recipient in the biosphere. To convert the release rates of these metals to concentration in the recipient some physical data are needed, such as recipient volume and water turnover in the recipient. The data selected are those used in the calculation of the ecosystem-specific dose conversion factors, EDF. These data are given by Bergström *et al.* (1999) and the values selected for calculating the concentration of toxic metals from SFL 3-5 in the different recipients are compiled in Table 10-4.

Table 10-2 Mean values of ecosystem-specific dose conversion factors (Sv/Bq) selected for recipients in Aberg, Beberg and Ceberg (Nordlinder *et al.*, 1999).

Radio-nuclide	Aberg		Beberg		Ceberg
	Coast, open	Coast, archipelago	Agricultural land	Peatland	Peatland
H-3	$1.2 \cdot 10^{-20}$	$3.2 \cdot 10^{-18}$	$1.3 \cdot 10^{-15}$	$3.6 \cdot 10^{-16}$	$2.6 \cdot 10^{-16}$
Be-10	$1.9 \cdot 10^{-18}$	$3.9 \cdot 10^{-16}$	$1.3 \cdot 10^{-14}$	$8.6 \cdot 10^{-13}$	$6.2 \cdot 10^{-13}$
C-14	$6.7 \cdot 10^{-18}$	$1.7 \cdot 10^{-15}$	$2.0 \cdot 10^{-17}$	$6.5 \cdot 10^{-15}$	$4.6 \cdot 10^{-15}$
Cl-36	$5.7 \cdot 10^{-19}$	$1.6 \cdot 10^{-16}$	$4.0 \cdot 10^{-13}$	$2.2 \cdot 10^{-11}$	$1.5 \cdot 10^{-11}$
Co-60	$3.3 \cdot 10^{-18}$	$5.1 \cdot 10^{-16}$	$5.0 \cdot 10^{-18}$	$2.8 \cdot 10^{-13}$	$2.7 \cdot 10^{-13}$
Ni-59	$9.0 \cdot 10^{-20}$	$2.2 \cdot 10^{-17}$	$1.1 \cdot 10^{-14}$	$2.7 \cdot 10^{-13}$	$1.9 \cdot 10^{-13}$
Ni-63	$2.1 \cdot 10^{-19}$	$5.2 \cdot 10^{-17}$	$7.6 \cdot 10^{-17}$	$1.6 \cdot 10^{-13}$	$1.4 \cdot 10^{-13}$
Se-79	$5.3 \cdot 10^{-17}$	$1.4 \cdot 10^{-14}$	$1.6 \cdot 10^{-12}$	$1.7 \cdot 10^{-9}$	$1.2 \cdot 10^{-9}$
Sr-90	$5.0 \cdot 10^{-18}$	$1.3 \cdot 10^{-15}$	$2.8 \cdot 10^{-14}$	$1.8 \cdot 10^{-11}$	$1.6 \cdot 10^{-11}$
Zr-93	$9.8 \cdot 10^{-19}$	$9.0 \cdot 10^{-17}$	$3.0 \cdot 10^{-15}$	$4.4 \cdot 10^{-13}$	$3.3 \cdot 10^{-13}$
Nb-94	$1.5 \cdot 10^{-18}$	$2.1 \cdot 10^{-16}$	$2.4 \cdot 10^{-13}$	$2.0 \cdot 10^{-12}$	$1.5 \cdot 10^{-12}$
Mo-93	$3.5 \cdot 10^{-19}$	$9.2 \cdot 10^{-17}$	$8.7 \cdot 10^{-13}$	$2.5 \cdot 10^{-12}$	$1.7 \cdot 10^{-12}$
Tc-99	$6.1 \cdot 10^{-19}$	$1.7 \cdot 10^{-17}$	$5.9 \cdot 10^{-14}$	$4.2 \cdot 10^{-13}$	$2.9 \cdot 10^{-13}$
Pd-107	$2.6 \cdot 10^{-20}$	$1.2 \cdot 10^{-18}$	$2.7 \cdot 10^{-15}$	$6.4 \cdot 10^{-14}$	$4.4 \cdot 10^{-14}$
Ag-108m	$4.3 \cdot 10^{-18}$	$1.1 \cdot 10^{-15}$	$1.8 \cdot 10^{-14}$	$1.9 \cdot 10^{-11}$	$1.8 \cdot 10^{-11}$
Sn-126	$3.8 \cdot 10^{-18}$	$9.9 \cdot 10^{-16}$	$1.2 \cdot 10^{-12}$	$8.6 \cdot 10^{-11}$	$6.1 \cdot 10^{-11}$
I-129	$1.1 \cdot 10^{-16}$	$1.8 \cdot 10^{-14}$	$5.0 \cdot 10^{-11}$	$3.0 \cdot 10^{-11}$	$2.1 \cdot 10^{-11}$
Cs-135	$2.9 \cdot 10^{-18}$	$7.8 \cdot 10^{-16}$	$3.1 \cdot 10^{-13}$	$2.7 \cdot 10^{-12}$	$1.8 \cdot 10^{-12}$
Cs-137	$1.8 \cdot 10^{-17}$	$4.8 \cdot 10^{-15}$	$1.7 \cdot 10^{-16}$	$3.5 \cdot 10^{-12}$	$3.1 \cdot 10^{-12}$
Sm-151	$9.1 \cdot 10^{-20}$	$5.9 \cdot 10^{-18}$	$7.0 \cdot 10^{-19}$	$6.0 \cdot 10^{-15}$	$5.7 \cdot 10^{-15}$
Ho-166m	$1.9 \cdot 10^{-18}$	$1.3 \cdot 10^{-16}$	$3.4 \cdot 10^{-14}$	$1.9 \cdot 10^{-12}$	$1.6 \cdot 10^{-12}$
Pb-210	$6.0 \cdot 10^{-16}$	$8.5 \cdot 10^{-14}$	$3.4 \cdot 10^{-15}$	$1.6 \cdot 10^{-11}$	$1.6 \cdot 10^{-11}$
Ra-226	$7.0 \cdot 10^{-17}$	$1.6 \cdot 10^{-14}$	$7.2 \cdot 10^{-12}$	$1.2 \cdot 10^{-9}$	$9.4 \cdot 10^{-10}$
Ac-227	$1.4 \cdot 10^{-15}$	$1.8 \cdot 10^{-13}$	$7.4 \cdot 10^{-16}$	$6.2 \cdot 10^{-11}$	$6.1 \cdot 10^{-11}$
Th-229	$4.0 \cdot 10^{-16}$	$1.3 \cdot 10^{-14}$	$4.6 \cdot 10^{-12}$	$7.0 \cdot 10^{-9}$	$6.5 \cdot 10^{-9}$
Th-230	$1.7 \cdot 10^{-16}$	$5.4 \cdot 10^{-15}$	$3.0 \cdot 10^{-12}$	$4.0 \cdot 10^{-9}$	$3.7 \cdot 10^{-9}$
Th-232	$1.9 \cdot 10^{-16}$	$5.9 \cdot 10^{-15}$	$3.4 \cdot 10^{-12}$	$4.4 \cdot 10^{-9}$	$4.1 \cdot 10^{-9}$
Pa-231	$4.8 \cdot 10^{-17}$	$1.3 \cdot 10^{-14}$	$6.1 \cdot 10^{-12}$	$3.5 \cdot 10^{-9}$	$2.7 \cdot 10^{-9}$
U-233	$1.1 \cdot 10^{-17}$	$2.6 \cdot 10^{-15}$	$3.7 \cdot 10^{-13}$	$6.1 \cdot 10^{-12}$	$4.3 \cdot 10^{-12}$
U-234	$1.1 \cdot 10^{-17}$	$2.5 \cdot 10^{-15}$	$3.6 \cdot 10^{-13}$	$5.9 \cdot 10^{-12}$	$4.1 \cdot 10^{-12}$
U-235	$1.0 \cdot 10^{-17}$	$2.4 \cdot 10^{-15}$	$3.4 \cdot 10^{-13}$	$5.4 \cdot 10^{-12}$	$3.7 \cdot 10^{-12}$
U-236	$1.0 \cdot 10^{-17}$	$2.4 \cdot 10^{-15}$	$3.4 \cdot 10^{-13}$	$5.5 \cdot 10^{-12}$	$3.8 \cdot 10^{-12}$
U-238	$9.7 \cdot 10^{-18}$	$2.3 \cdot 10^{-15}$	$3.1 \cdot 10^{-13}$	$5.1 \cdot 10^{-12}$	$3.5 \cdot 10^{-12}$
Np-237	$7.6 \cdot 10^{-18}$	$2.0 \cdot 10^{-15}$	$2.1 \cdot 10^{-12}$	$1.1 \cdot 10^{-10}$	$7.5 \cdot 10^{-11}$
Pu-238	$4.8 \cdot 10^{-17}$	$5.1 \cdot 10^{-15}$	$3.6 \cdot 10^{-16}$	$3.7 \cdot 10^{-11}$	$3.4 \cdot 10^{-11}$
Pu-239	$5.5 \cdot 10^{-17}$	$6.4 \cdot 10^{-15}$	$1.2 \cdot 10^{-12}$	$4.1 \cdot 10^{-10}$	$3.0 \cdot 10^{-10}$
Pu-240	$5.5 \cdot 10^{-17}$	$6.3 \cdot 10^{-15}$	$7.7 \cdot 10^{-13}$	$3.6 \cdot 10^{-10}$	$2.7 \cdot 10^{-10}$
Pu-242	$5.3 \cdot 10^{-17}$	$6.1 \cdot 10^{-15}$	$1.3 \cdot 10^{-12}$	$4.1 \cdot 10^{-10}$	$3.0 \cdot 10^{-10}$
Am-241	$2.0 \cdot 10^{-16}$	$1.6 \cdot 10^{-14}$	$6.9 \cdot 10^{-14}$	$2.0 \cdot 10^{-10}$	$2.0 \cdot 10^{-10}$
Am-242m	$1.9 \cdot 10^{-16}$	$1.5 \cdot 10^{-14}$	$6.6 \cdot 10^{-15}$	$6.3 \cdot 10^{-11}$	$6.3 \cdot 10^{-11}$
Am-243	$2.0 \cdot 10^{-16}$	$1.6 \cdot 10^{-14}$	$2.6 \cdot 10^{-12}$	$1.8 \cdot 10^{-9}$	$1.9 \cdot 10^{-9}$
Cm-244	$9.7 \cdot 10^{-17}$	$4.0 \cdot 10^{-15}$	$4.1 \cdot 10^{-18}$	$5.5 \cdot 10^{-12}$	$5.5 \cdot 10^{-12}$
Cm-245	$2.1 \cdot 10^{-16}$	$1.6 \cdot 10^{-14}$	$1.0 \cdot 10^{-12}$	$9.8 \cdot 10^{-10}$	$8.1 \cdot 10^{-10}$
Cm-246	$2.1 \cdot 10^{-16}$	$1.6 \cdot 10^{-14}$	$7.1 \cdot 10^{-13}$	$8.1 \cdot 10^{-10}$	$6.8 \cdot 10^{-10}$

Table 10-3 Mean values of ecosystem-specific dose conversion factors (Sv/Bq) for mean wells in Aberg, Beberg and Ceberg, based on data in Nordlinder *et al.*, (1999).

Radionuclide	Aberg [300 l/hour]	Beberg [1 000 l/hour]	Ceberg [500 l/hour]
H-3	$9.4 \cdot 10^{-15}$	$2.7 \cdot 10^{-15}$	$5.2 \cdot 10^{-15}$
Be-10	$4.6 \cdot 10^{-13}$	$1.3 \cdot 10^{-13}$	$2.6 \cdot 10^{-13}$
C-14	$2.4 \cdot 10^{-13}$	$7.0 \cdot 10^{-14}$	$1.4 \cdot 10^{-13}$
Cl-36	$7.3 \cdot 10^{-13}$	$2.1 \cdot 10^{-13}$	$3.7 \cdot 10^{-13}$
Co-60	$1.1 \cdot 10^{-12}$	$3.3 \cdot 10^{-13}$	$6.6 \cdot 10^{-13}$
Ni-59	$5.9 \cdot 10^{-14}$	$1.8 \cdot 10^{-14}$	$3.0 \cdot 10^{-14}$
Ni-63	$6.2 \cdot 10^{-14}$	$1.9 \cdot 10^{-14}$	$3.7 \cdot 10^{-14}$
Se-79	$2.7 \cdot 10^{-12}$	$7.7 \cdot 10^{-13}$	$1.3 \cdot 10^{-12}$
Sr-90	$1.3 \cdot 10^{-11}$	$3.7 \cdot 10^{-12}$	$7.3 \cdot 10^{-12}$
Zr-93	$3.7 \cdot 10^{-13}$	$1.1 \cdot 10^{-13}$	$2.2 \cdot 10^{-13}$
Nb-94	$3.4 \cdot 10^{-12}$	$9.8 \cdot 10^{-13}$	$1.7 \cdot 10^{-12}$
Mo-93	$2.5 \cdot 10^{-12}$	$7.7 \cdot 10^{-13}$	$1.2 \cdot 10^{-12}$
Tc-99	$5.5 \cdot 10^{-13}$	$1.6 \cdot 10^{-13}$	$2.8 \cdot 10^{-13}$
Pd-107	$2.3 \cdot 10^{-14}$	$6.6 \cdot 10^{-15}$	$1.2 \cdot 10^{-14}$
Ag-108m	$1.3 \cdot 10^{-12}$	$4.0 \cdot 10^{-13}$	$7.4 \cdot 10^{-13}$
Sn-126	$3.9 \cdot 10^{-12}$	$1.1 \cdot 10^{-12}$	$1.8 \cdot 10^{-12}$
I-129	$9.2 \cdot 10^{-11}$	$2.7 \cdot 10^{-11}$	$4.6 \cdot 10^{-11}$
Cs-135	$1.9 \cdot 10^{-12}$	$5.7 \cdot 10^{-13}$	$1.0 \cdot 10^{-12}$
Cs-137	$5.6 \cdot 10^{-12}$	$1.7 \cdot 10^{-12}$	$3.4 \cdot 10^{-12}$
Sm-151	$3.2 \cdot 10^{-14}$	$9.8 \cdot 10^{-15}$	$1.9 \cdot 10^{-14}$
Ho-166m	$2.0 \cdot 10^{-12}$	$6.1 \cdot 10^{-13}$	$1.2 \cdot 10^{-12}$
Pb-210	$1.9 \cdot 10^{-10}$	$5.6 \cdot 10^{-11}$	$1.1 \cdot 10^{-10}$
Ra-226	$1.2 \cdot 10^{-10}$	$3.4 \cdot 10^{-11}$	$6.5 \cdot 10^{-11}$
Ac-227	$3.4 \cdot 10^{-10}$	$9.8 \cdot 10^{-11}$	$2.0 \cdot 10^{-10}$
Th-229	$4.2 \cdot 10^{-10}$	$1.3 \cdot 10^{-10}$	$2.4 \cdot 10^{-10}$
Th-230	$2.1 \cdot 10^{-10}$	$6.2 \cdot 10^{-11}$	$1.2 \cdot 10^{-10}$
Th-232	$2.3 \cdot 10^{-10}$	$6.8 \cdot 10^{-11}$	$1.3 \cdot 10^{-10}$
Pa-231	$6.8 \cdot 10^{-10}$	$2.0 \cdot 10^{-10}$	$4.0 \cdot 10^{-10}$
U-233	$1.9 \cdot 10^{-11}$	$5.5 \cdot 10^{-12}$	$1.1 \cdot 10^{-11}$
U-234	$1.8 \cdot 10^{-11}$	$5.3 \cdot 10^{-12}$	$1.0 \cdot 10^{-11}$
U-235	$1.7 \cdot 10^{-11}$	$5.0 \cdot 10^{-12}$	$9.7 \cdot 10^{-12}$
U-236	$1.7 \cdot 10^{-11}$	$5.0 \cdot 10^{-12}$	$9.7 \cdot 10^{-12}$
U-238	$1.6 \cdot 10^{-11}$	$4.8 \cdot 10^{-12}$	$9.2 \cdot 10^{-12}$
Np-237	$4.7 \cdot 10^{-11}$	$1.3 \cdot 10^{-11}$	$2.5 \cdot 10^{-11}$
Pu-238	$6.6 \cdot 10^{-11}$	$2.0 \cdot 10^{-11}$	$4.0 \cdot 10^{-11}$
Pu-239	$2.2 \cdot 10^{-10}$	$6.7 \cdot 10^{-11}$	$1.3 \cdot 10^{-10}$
Pu-240	$1.8 \cdot 10^{-10}$	$5.5 \cdot 10^{-11}$	$1.1 \cdot 10^{-10}$
Pu-242	$2.3 \cdot 10^{-10}$	$7.0 \cdot 10^{-11}$	$1.3 \cdot 10^{-10}$
Am-241	$6.8 \cdot 10^{-11}$	$2.0 \cdot 10^{-11}$	$4.1 \cdot 10^{-11}$
Am-242m	$5.6 \cdot 10^{-11}$	$1.7 \cdot 10^{-11}$	$3.4 \cdot 10^{-11}$
Am-243	$1.3 \cdot 10^{-10}$	$3.9 \cdot 10^{-11}$	$7.4 \cdot 10^{-11}$
Cm-244	$3.2 \cdot 10^{-11}$	$9.8 \cdot 10^{-12}$	$1.9 \cdot 10^{-11}$
Cm-245	$1.6 \cdot 10^{-10}$	$4.8 \cdot 10^{-11}$	$9.6 \cdot 10^{-11}$
Cm-246	$1.4 \cdot 10^{-10}$	$4.2 \cdot 10^{-11}$	$8.3 \cdot 10^{-11}$

Table 10-4 General recipient data from Bergström *et al.* (1999).

	Aberg		Beberg		Ceberg
	Coast, open	Coast, archipelago	Agricultural land	Peatland	Peatland
Area (m^2) [a]	–	$1.4 \cdot 10^6$	$1 \cdot 10^4$	$1 \cdot 10^5$	$1 \cdot 10^5$
Mean depth (m) [a]	–	2.3	6.3 [b]	0.5	0.5
Volume (m^3)	$1.7 \cdot 10^8$ [a]	$3.2 \cdot 10^6$	$6.3 \cdot 10^4$	$5 \cdot 10^4$	$5 \cdot 10^4$
Mean residence time (year) [a]	0.023	0.12	–	–	–
Water discharge rate (m^3/year)	$7.5 \cdot 10^9$	$2.6 \cdot 10^7$	–	–	–
Density (kg/m^3)	–	–	2 400	100	100
Porosity (m^3/m^3)	–	–	0.30	0.90	0.90

[a] *Mean value given by Bergström et al. (1999)*
[b] *Sum of top soil, deep soil and saturated zone*

10.4 Comparison values for toxic metals

To get a measure of the consequences of the release of toxic metals from the SFL 3-5 repository it is suggested that the concentration arising in the different recipients from the release of these metals is compared with typical concentrations presently found in different types of ecosystems.

The toxic metals that are considered in the analysis of SFL 3-5 are beryllium (Be) cadmium (Cd) and lead (Pb). The Swedish Environmental Protection Agency, (Naturvårdsverket, 1999a), give the distribution of metal concentration in Swedish freshwater bodies that are unaffected by local sources of contamination. The mean values of these concentrations are given in Table 10-5. These values are applicable primarily to freshwater. The concentrations of Pb, Cd and Be in coastal waters are expected to be lower due to greater dilution. There are indications from values derived in Norway for the classification of coastal and fjord waters that the metal concentrations are a factor of 10 lower than in fresh waters. Nevertheless, it is suggested that the mean values for Swedish freshwater bodies are used as comparison values for the release to open coast and archipelago.

The concentration of Pb and Cd in Swedish arable land is reported by the Swedish Environmental Protection Agency (Naturvårdsverket, 1999b). The mean concentrations are given in Table 10-5, and it is suggested that these values are used as comparison values for the release of Pb and Cd to agricultural land. No data has been found concerning the mean concentration of Be in arable land or soil. However, the mean concentration of Be in agricultural soil in the US is reported to be 0.6 mg/kg dry weight (IPCS, 1990). This value is suggested as a comparison value for the release of Be to agricultural land since no Swedish data are available.

In a report discussing the environmental impact of burning of wood and peat typical values of the concentration of metals are given (Naturvårdsverket, 1983). The values reported for peat are given in Table 10-5 and it is suggested that these are used as comparison values for the release of Be, Cd and Pb to peatland.

For the release of the toxic metals to a well it is suggested that guideline values for drinking water are used as comparison values. The suggested values are given in Table 10-5. The values suggested for Cd and Pb are the values set by Livsmedelsverket (SLV, 1993), which are based on toxicological data from WHO (1993). As Livsmedelsverket have not set drinking water guidelines for Be, the suggested value is taken from US EPA (1996).

Table 10-5 Suggested comparison values for toxic metals released from SFL 3-5.

Recipient	Be	Cd	Pb
Open coast and archipelago (μg/l)	0.01[a)]	0.01[a)]	0.24[a)]
Agricultural land (mg/kg dw)	0.6[b)]	0.23[c)]	17.1[c)]
Peatland (mg/kg dw)	0.095[d)]	0.095-0.95[d)]	0.38-19[d)]
Well water (mg/l)	0.004[e)]	0.001[f)]	0.01[f)]

[a)] *Naturvårdsverket (1999a)*
[b)] *IPCS (1990)*
[c)] *Naturvårdsverket (1999b)*
[d)] *Naturvårdsverket (1983)*
[e)] *US EPA (1996)*
[f)] *SLV (1993)*

10.5 Data uncertainties

The uncertainty in the derived EDF's is obtained by assigning an uncertainty range to the input parameters of the model. It was found that the parameter values used to describe the biological processes such as root uptake, accumulation in fish and secretion of the nuclides to milk and meat made the biggest contribution to uncertainty. The parameter values used to describe consumption, living habits etc. made the least contribution (Bergström *et al.*, 1999).

The ecosystems peat, well and agricultural land give rise to the highest dose conversion factors. The reported uncertainty in the values of the dose conversion factors for the wells is at most a factor of 10 between the lowest and highest value, and the highest value is at most a factor of 4 higher than the mean value. The uncertainty interval for the dose conversion factors for agricultural land and peat is larger, typically two to three orders of magnitude and for some nuclides even larger. The difference between the highest and the mean value of the dose conversion factor for agricultural land in Beberg is a factor of 10 to 20 for most of the nuclides. The largest difference is given for ^{60}Co with an almost 50 times difference between the highest and the mean value. Similar intervals are given for peat in both Beberg and Ceberg with a highest value between 10 and 20 times higher than the mean value for most of the nuclides. Here, however, the largest difference is given for ^{99}Tc with a highest value that is 26 times larger than the mean value.

The selection of ecosystem representative for the discharge area for water from the repository will also affect the result. In order to define typical ecosystems the area was subdivided into 250 × 250 m squares. A square may contain several types of biotopes. In such cases, the biotope with the largest area was chosen as the typical ecosystem for

the square, but it is possible that there is a greater probability that groundwater discharge takes place to a smaller biotope.

The mean values of the dose conversion factors for the ecosystems defined for the area above the exit points of the path lines from the hydrology model are selected as the reasonable estimate in the analysis of the deep repository for spent fuel, SR 97 (Andersson, 1999). In the pessimistic case, the highest value in the uncertainty range for the EDF is chosen to display the effects of the uncertainty in these values. The effects of the uncertainty in the selection of representative ecosystem is displayed by comparing the highest value of the dose conversion factors for well, agricultural land and peat, and for each nuclide select the value that gives the highest dose (Andersson, 1999).

A similar approach is used to discuss the uncertainties in the EDF's suggested for the analysis of the release from SFL 3-5. No other recipient present in Beberg have higher dose conversion factors than those recipients suggested for the analysis (agricultural land and peatland). Using the mean values of the EDF's will for all of the radionuclides give a dose that is at most a factor of 20 lower than would be obtained with the highest values of the EDF's (see discussion above). The difference between the dose conversion factors for a well with the mean capacity and a well with the smallest capacity in the area is covered by this interval.

The highest dose rates in Ceberg is obtained for release to peat or to a well, which are the ecosystems suggested for the analysis of the release in Ceberg. Also for Ceberg, the use of the mean values of the EDF's would result in a dose that is at most 20 times lower than would be obtained with the highest value in the uncertainty range. This is the case for all nuclides apart from ^{99}Tc for which the use of the highest value in the uncertainty range would result in a 26 times higher dose rate.

In Aberg, the highest dose rates are obtained for release to peat or to a well. The well is suggested as a recipient for the release from SFL 3-5, but not a peatland since the regional hydrology modelling shows that the main discharge occurs in the sea (see Section 10.1). The consequence of not considering peat as a primary recipient for radionuclides and selecting the mean values and not the highest values of the dose conversion factors is here illustrated by comparing the different values of the dose conversion factors.

For nuclides that have a higher dose conversion factor in peat than in a well, the difference in the mean values of the dose conversion factors for the two recipients is in general a factor of about 20 or lower (see Table 10-6). For some nuclides the difference is larger: a factor of 1 000 for ^{79}Se, a factor of 49 for ^{36}Cl and a factor of 36 for ^{126}Sn. The difference between the highest value and the mean value of the dose conversion factors for peat indicates an additional factor of about 10 compared to the mean value of the dose conversion factor for the well for most of the radionuclides (Table 10-6).

For radionuclides where release to a well gives the highest dose, the difference between the highest value and the mean value of the dose conversion factor is at most a factor of about 10 (Table 10-6).

Table 10-6 The mean value of the dose conversion factor for peatland relative to that for a well with the capacity of 300 l/hour in Aberg, and the ratio between the highest value and the mean value of the dose conversion factor for the recipient with the highest dose conversion factor.

Radionuclide	Peat/Well	Well High/Mean	Peatland High/Mean
H-3, Cs-137, Sm-151, Pb-210, Ac-227, U-233, U-234, U-235, U-236, U-238,Pu-238, Cm-244	≤ 1	2	
Nb-94, I-129	< 1	~ 10	
Sr-90, Zr-93, Mo-93, Cs-135, Ho-166m, Am-242m,	≤ 2		~ 10
Tc-99	< 2		26
Be-10, Ni-63, Pd-107, Np-237, Pu-239, Pu-240, Pu-242, Am-241	3-4		~ 10
Ni-59, Pa-231, Cm-245, Cm-246	7-8		~ 10
Ag-108m, Ra-226, Th-229, Th-230, Th-232, Am-243	15-21		10-15
Sn-126	36		10
Cl-36	49		9
Se-79	1 000		10

References

Ahlbom K, Olsson O, Sehlstedt S, 1995. Temperature conditions in the SKB study sites. SKB Technical Report 95-16, Swedish Nuclear Fuel and Waste Management Co, Stockholm, Sweden.

Albinsson Y, 1999. Personal communication.

Albinsson Y, Andersson K, Börjesson S, Allard B, 1996. Diffusion of radionuclides in concrete-bentonite systems. J. of Contaminant Hydrology **21,** p. 189.

Allard B, 1985. Radionuclide sorption on concrete. NAGRA Technical Report 85-21, Wettingen, Switzerland.

Allard B, Andersson K, 1987. Chemical properties of radionuclides in cementitious environment. SKB Progress Report SFR 86-09, Swedish Nuclear Fuel and Waste Management Co, Stockholm, Sweden.

Allard B, Eliasson L, Höglund S, Andersson K, 1984. Sorption of Cs, I and Actinides in Conrete systems. SKB Technical Report 84-15, Swedish Nuclear Fuel and Waste Management Co, Stockholm, Sweden.

Allard B, Höglund S, Skagius K, 1991. Adsorption of radionuclides in concrete. SKB Progress Report SFR 91-02, Swedish Nuclear Fuel and Waste Management Co, Stockholm, Sweden.

Andersson J, Elert M, Hermansson J, Moreno L, Gylling B, Selroos J O, 1998. Derivation and treatment of the flow wetted surface and other geosphere parameters in the transport models FARF31 and COMP23 for use in safety assessment. SKB Report R-98-60, Swedish Nuclear Fuel and Waste Management Co, Stockholm, Sweden.

Andersson J, 1999. Data and data uncertainties. Compilation of data and data uncertainties for radionuclide transport calculations. SKB Technical Report TR-99-09, Swedish Nuclear Fuel and Waste Management Co, Stockholm, Sweden.

Andersson, K, Torstenfelt B, Allard B, 1981. Diffusion of Cesium in concrete. In Scientific Basis for Nuclear Waste Management, Vol 3, p 235.

Atkins M, Glasser F, 1990. Encapsulation of radioiodine in cementitious waste forms. In Scientific Basis for Nuclear Waste Management, Vol 13, p 15.

Atkinsson A, Nickerson A, 1988. Diffusion and sorption of cesium, strontium and iodine in water-saturated cement. Nuclear Technology 81, p 100.

Baes C, Mesmer R, 1976 and 1986. The hydrolysis of cations. R.E. Krieger Publishing Company, Malibar, Florida (original 1976, new print 1986).

Baker S, McCrohon R, Oliver P, Pilkington N J, 1994. The sorption of niobium, tin, iodine and chlorine onto Nirex reference vault backfill. Mat. Res. Soc. Symp. Proc. **333**, p. 719.

Bayliss S, Ewart F, Howse R, Smith-Briggs J L, Thomason H. P, Willmott H A, 1988. The solubility and sorption of lead-210 and carbon-14 in a near-field environment. In Scientific Basis for Nuclear Waste Management, Vol 11, pp 33-42.

Bayliss S, Ewart F, Howse R, Lane S, Pilkington N J, Smith-Briggs J, Williams S, 1989. The solubility and sorption of radium and tin in a cementitious near-field environment. In Scientific Basis for Nuclear Waste Management, Vol 12, p 879.

Bayliss S, Hawort A, McCrohon R, Moreton A, Oliver P, Pilkington N, Smith A, Smith-Briggs J, 1992. Radioelement behaviour in a cementitious environment. In Scientific Basis for Nuclear Waste Management, Vol 15, p 641.

Bayliss S, McCrohon R, Moreton A, Oliver P, Pilkington N J, Thomason H P, 1996. Radionuclide sorption on the Nirex reference vault backfill. BNES Conference, Manchester, UK.

Bergström U, Nordlinder S, Aggeryd I, 1999. Models for dose assessments. Modules for various biosphere types. SKB Technical Report TR-99-14, Swedish Nuclear Fuel and Waste Management Co, Stockholm, Sweden.

Bradbury M H, Sarott F-A, 1994. Sorption Databases for the Near-Field of a L/ILW Repository for Performance Assessment. NAGRA Technical Report 93-08, Wettingen, Switzerland.

Bradbury M H, VanLoon L R, 1998. Cementitious Near-Field Sorption Data Bases for Performance Assessment of a L/ILW Repository in a Palfris Marl Host Rock (CEM94:UPDATE I, june 1997)". PSI Bericht Nr. 98-01, Paul Scherrer Institut, Villigen, Switzerland.

Byegård J, Skarnemark G, Skålberg M, 1995. The use of some ion-exchange sorbing tracer cations in in-situ experiments in high saline groundwaters. Mat. Res. Soc. Symp. Proc., **353**, pp 1077-1084.

Carbol P, Engkvist I, 1997. Compilation of radionuclide sorption coefficients for performance assessment. SKB Report R-97-13, Swedish Nuclear Fuel and Waste Management Co, Stockholm, Sweden.

de Marsily G, 1986. Quantitative Hydrogeology. Academic Press, Inc., New York.

Dyrssen D, Lumme P, 1962. Acta Chem. Scand. **16**, p 1785.

Engkvist I, 1993. Diffusion and hydrolysis of some actinides. University of Gothenburg, Sweden. (Diss)

Engkvist I, Albinsson Y, Johansson Engkvist W, 1996. The long-term stability of cement – Leaching tests. SKB Technical Report 96-09, Swedish Nuclear Fuel and Waste Management Co, Stockholm, Sweden.

Eriksen T, Ndalamba P, Bruno J, Caceci M, 1992. The solubility of $TcO_2 \cdot nH_2O$ in neutral to alkaline solutions under constant pCO_2. Radiochim. Acta **58/59**, p. 67.

Ewart F T, Pugh S Y R, Wisbey S J, Woodwark D R, 1988. Chemical and microbiological effects in the near field: current status. NSS/G103, Harwell Laboratory, Oxfordshire, UK.

Ewart F T, Smith-Briggs J L, Thomason H P, Williams S J, 1992. The solubility of actinides in a cementitious near-field environment. Waste Management **12**, p. 241.

Ewart F, Tasker P, 1987. Chemical effects in the nearfield. Waste Management '87', Tuscon, Arizona, USA.

Ewart F, Terry S, Williams S, 1985. Near field sorption data for cesium and strontium. AEA Report AERE M 3452, Harwell Laboratory, Oxfordshire, UK.

Firestone R B, Baglin C M, Chu S Y F, 1998. Table of Isotopes, 8th edition, 1998 Update. John Wiley & Sons Inc, New York.

Freeze R A, Cherry J A, 1979. Groundwater. Prentice-Hall, Inc., London.

Hietanen R, Kämeräinen E, Alaluusua M, 1984. Sorption of strontium, cesium, nickel, iodine and carbonate in concrete. YJT Report YJT 84-04, Helsinki, Finland.

Holgersson S, Albinsson Y, 1999. Sorption of chlorine and molybdenium onto cement paste. In preparation.

Holgersson S, Albinsson Y, Allard B, Borén H, Pavasars I and Engkvist I, 1998. Effects of Gluco-isosaccharinate on Cs, Ni, Pm and Th sorption onto, and diffusion into cement." Radiochim. Acta, **82**, p 393 – 398.

Holgersson S, Albinsson Y, Allard B, Borén H, Pavasars I, Engkvist I, 1999. Effects of Gluco-isosaccharinate on Cs, Ni, Pm and Th sorption onto and diffusion into cement Part 2. In preparation.

Holmén J, 1997. On the flow of groundwater in closed tunnels. Generic hydrogeological modelling of nuclear waste repository SFL 3-5. SKB Technical Report TR 97-10, Swedish Nuclear Fuel and Waste Management Co, Stockholm, Sweden.

Höglund L O, Bengtsson A, 1991. Some chemical and physical processes related to the long-term performance of the SFR repository. SKB Progress Report SFR 91-06, Swedish Nuclear Fuel and Waste Management Co, Stockholm, Sweden.

Höglund L O, 1993. Long-term function of concrete grout in SFR. SKB Progress report SFR 93-01, Swedish Nuclear Fuel and Waste Management Co, Stockholm, Sweden.

ICRP, 1983. Annals of the ICRP, Radionuclide transformations, Energy and Intensity of emissions. ICRP Publication 38, Volumes 11-13, Pergamon Press, London.

IPCS, 1990. Environmental Health Criteria 106; Beryllium. International Programme on Chemical Safety, World Health Organisation, Geneva.

Jakobsson A-M, Albinsson Y, Rundberg R, 1998. Studies of surface complexation of H^+, NpO_2^+, Co^{2+}, Th^{4+} onto TiO_2 and H^+, UO_2^{2+} onto alumina. SKB Technical Report 98-15, Swedish Nuclear Fuel and Waste Management Co, Stockholm, Sweden.

Johnston H M, Wilmot D J, 1992. Sorption and diffusion studies in cementitious grouts. Waste Management, **12**, pp 289-297.

Karlsson F, Lindgren M, Skagius K, Wiborgh M., Engkvist I, 1999. Evolution of the geochemical conditions in SFL 3-5. SKB Report R-99-15, Swedish Nuclear Fuel and Waste Management Co, Stockholm, Sweden.

Kulmala S, Hakanen M, 1993. The solubility of Zr, Nb and Ni in groundwater and concrete water, and sorption on crushed rock and cement. Report YJT-93-21, Helsinki, Finland.

Kulmala S, Hakanen M, 1995. Sorption of alkaline-earth elements Sr, Ba and Ra from groundwater on rocks from TVO investigation areas. Report YJT-95-03, Helsinki, Finland.

Laaksoharju M, Degueldre C, Skårman Ch, 1995. Studies of colloids and their importance for repository assessment. SKB Technical Report TR 95-24, Swedish Nuclear Fuel and Waste management Co, Stockholm, Sweden.

Laaksoharju M, Gurban I, Skårman Ch, 1998. Summary of hydrochemical conditions at Aberg, Beberg and Ceberg. SKB Technical Report 98-03, Swedish Nuclear Fuel and Waste Management Co, Stockholm, Sweden.

Li Y H, Gregory S, 1974. Diffusion of ions in sea water and in deep-sea sediments. Geochemica et Cosmochimica Acta, Vol 38, pp 603-714.

Lindgren M, Pers K, Skagius K, Wiborg M, Broden K, Carlsson J, Riggare P, Skogsberg M, 1998. Low and intermediate level waste in SFL 3-5: Reference Inventory. Reg. No: 19.41/DL 31, Swedish Nuclear Fuel and Waste Management Co, Stockholm, Sweden.

Munier R, Sandstedt H, Niland L, 1997. Förslag till principiella utformningar av förvar enligt KBS-3 för Aberg, Beberg och Ceberg. SKB Report R-97-09, Swedish Nuclear Fuel and Waste Management Co, Stockholm, Sweden. (in Swedish)

NAGRA, 1994. Endlager für schwach- und mittelaktive abfälle (Endlager SMA)- Bericht zur langzeitsicherheit des endlagers SMA am standort Wellingberg (Geminde wolfenschiessen, NW). NAGRA Technical Report 94-06, Wettingen, Switzerland.

Naturvårdsverket, 1983. Miljöeffekter av ved- och torvförbränning. SNV PM 1708, Statens Naturvårdsverk, Solna, Sweden. (in Swedish)

Naturvårdsverket, 1999a. Bedömningsgrunder för miljökvalitet - Sjöar och vattendrag, Rapport 4913, Naturvårdsverkets förlag, Stockholm, Sweden. (in Swedish)

Naturvårdsverket, 1999b. Bedömningsgrunder för miljökvalitet- Odlingslandskapet, Rapport 4916, Naturvårdsverkets förlag, Stockholm, Sweden. (in Swedish)

NEA-OECD, 1992. Vol 1. Chemical Thermodynamics of Uranium, (H Wanner and I Forest, eds.) NORTH-Holland Elsevier Science Publishers B.V., Amsterdam, The Netherlands.

NEA-OECD, 1995. Vol. 2. Chemical Thermodynamics of Americium, (J Silva et al.) NORTH-Holland Elsevier Science Publishers B.V., Amsterdam, The Netherlands.

Nordlinder S, Bergström U, Mathiasson L, 1999. Ecosystem specific dose conversion factors for Aberg, Beberg and Ceberg. SKB Technical Report TR-99-15, Swedish Nuclear Fuel and Waste Management Co, Stockholm, Sweden.

Norman S, Kjellbert N, 1990. FARF31 – A far field radionuclide migration code for use with the PROPER package. SKB Technical Report 90-01, Swedish Nuclear Fuel and Waste Management Co, Stockholm, Sweden.

Ohlsson Y, Neretnieks I, 1997. Diffusion data in granite. Recommended values. SKB Technical Report 97-20, Swedish Nuclear Fuel and Waste Management Co, Stockholm, Sweden.

Pilkington N J, Stone N S, 1990. The solubility and sorption of nickel and niobium under high pH conditions. AEA Report NSS/R186, Harwell Laboratory, Oxfordshire, UK.

Pokric B, Pucar Z, 1973. Electrophoretic and Tyndallometric studies on the hydrolysis of lead(II) in aqueous solutions. J. Inorg. Nucl. Chem., **35**, p 1987.

Romero L, Moreno L, Neretnieks I, 1995. Fast multiple-path model to calculate radio-nuclide release from the near filed of a repository. Nucl. Technol., **112**(1), pp 89-98.

Sarott F A, 1996. Die sorption von chlor, Jod, Nickel und Americium am gemörsertem Zementstein. PSI Internal Report TM 44-96-13, Paul Scherrer Institut, Villigen, Switzerland.

Sarott F, Bradbury M, Pandelfo P, Spieler P, 1992. Diffusion and adsorption studies on hardened cement paste and the effect of carbonation on diffusion rates. Cement and Concrete Research **22**, p 439.

SKB, 1999. SR 97 – Main Report. SKB Technical Report TR-99-06, Swedish Nuclear Fuel and Waste Management Co., Stockholm, Sweden.

Smellie J (ed.), 1999. Maqarin natural analogue study. Phase III. SKB Technical Report TR-98-04, Volume I and II. Swedish Nuclear Fuel and Waste Management Co., Stockholm, Sweden.

Smith R, Martell A E, 1976. Critical Stability Constants: Vol. 4. Inorganic Complexes. Plenum Press, N.Y., USA.

Stollenwerk K G, 1998. Molybdate transport in a chemically complex aquifer: Field measurements compared with solute-transport model predictions. Water Resources Research, **34** (1998), pp 2727-2740.

SLV, 1993. Livsmedelsverkets kungörelse om dricksvatten. SLV FS 1993:35, Livsmedelsverket, Sweden. (in Swedish)

US EPA, 1996. Drinking water regulations and health advisories. EPA 822-B-96-002, US EPA Office of water, Washington DC.

WHO, 1993. Guidelined for drinking water quality. Volume 1. Recommendations. Second edition, World Health Organisation, Geneva.

Wiborgh M (Ed.), 1995. Prestudy of final disposal of long-lived low and intermediate level waste. SKB Technical Report 95-03, Swedish Nuclear Fuel and Waste Management Co., Stockholm, Sweden.

Wierczinski B, Helfer S, Ochs M, Skarnemark G, 1998. Solubility measurements and sorption studies of thorium in cement pore water. J. Alloys and Compounds **271-273**, p. 272.

Appendix 1

FLOW AND TRANSPORT FROM SFL 3-5

- ESTIMATES FROM A REGIONAL NUMERICAL MODEL

Urban Svensson
Computer-aided Fluid Engineering AB

December 1997

1 INTRODUCTION

A regional groundwater model was presented in Svensson (1997). This model covers a volume of 10 x 10 x 3 km^3 centred around the island of Äspö, see Figure 1. The reader is advised to consult the above mentioned report for a full description of the numerical model.

In the present report we will use results from the regional model to study the flow at SFL 3-5 (see Figure 1) and the flow-paths from this area.

With respect to boundary conditions, conductivity field, etc we will use the conditions described for "natural conditions" in Svensson (1997).

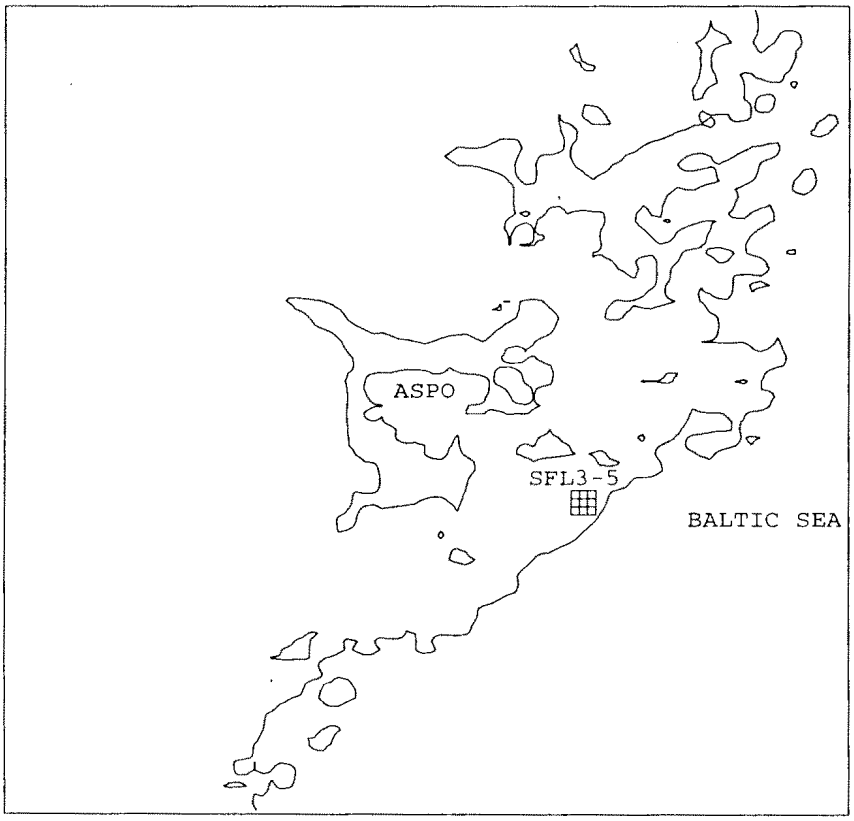

Figure 1. *Outline of regional model and position of SFL 3-5.*

2 METHOD

The basic steps in the calculation of flow-paths are as follows:

- Extract the Darcy velocities from the regional model.
- Estimate a kinematic porosity. In the present calculations we will assume that the kinematic porosity is related to the conductivity field, see Rhén et al (1997), as follows:

  $$n_e = 34.87 \times K^{0.753}$$

  This equation was used with the constraint that $n_e \leq 0.05$. This will result in an arithmetic mean kinematic porosity of 0.0013.
- Calculate a pore-velocity as $u_p = u_D / n_e$, where u_D is the Darcy velocity.
- Calculate flow paths by following a marked fluid element from a release point to one of the model boundaries. No dispersion effects (Taylor dispersion, matrix diffusion, etc) are considered in the calculation.
- The particle trajectory goes from cell centre to cell centre in the computational grid with a residence time calculated with respect to the free volume in the cell and the through-flow. When leaving a cell the particle chooses one of the directions with an outgoing flow and with a likelihood that is proportional to the flow rates. For further details see Svensson (1994).

The circulation through SFL 3-5 is estimated by simply giving the Darcian flow vector through the volume considered.

3 RESULTS

Before showing the results from the trajectory calculations, it is useful to study two figures given in Svensson (1997). The first one, see Figure 2, shows the conductivity field, including the fracture zones. As can be seen SFL 3-5 is located in a fracture zone, which means that we can expect high flow rates at this point. The second one, see Figure 3, shows the vertical flow at 200 metres depth. At SFL 3-5 the calculated upward and downward flows are more than 40 mm/year. The average kinematic porosity was above found to be 0.0013, which gives a pore-velocity of about 30 metres/year. The first rough estimate of the transport time from 300 metres depth is hence 10 years. This is for particles located in the part having a strong upward flow.

In the regional model an area of 300 x 300 metres (3 x 3 cells) is used to analyse the flow at SFL 3-5. In Table 1 the Darcy flux components for the 9 cells are given. It is found that the downward flow component is the strongest one with an average value of -4.95×10^{-10} m/s. The cells with an upward flow are found close to the Baltic Sea, which is in agreement with the distribution shown in Figure 3.

Particles were released in the 9 cells representing the SFL 3-5 location. As explained above the particles leave a cell through one of the cell-walls with an outgoing flow, with a likelihood that is proportional to the outgoing fluxes. This means that particles starting from the same position will get different flow paths. If 10 000 particles are released in the 9 cells at a depth of 300 metres we will get a distribution of ground level arrival times as shown in Figure 4. In the figure each point represents 10 particles. About 17 % of the particles had not reached ground level after 25 years. The typical travel time can from Figure 4 be estimated to 10-15 years.

The positions of 1 000 of the 10 000 particles are shown in Figure 5. Particles have been distributed randomly within their current cell in order to get an impression of the number of particles in a cell. This is the reason for the somewhat rectangular distributions seen. The figure anyway shows that most particles will end up in the discharge areas, in the Baltic Sea. Main discharge areas are located about 600 metres north of and 300 metres east of SFL 3-5.

In Table 2 the coordinates for nine particles are given for each year. The initial positions for the particles are the cell centres for the nine cells covering the SFL 3-5 area. The particles move from cell centre to cell centre and the change is thus always 100 metres in the

horizontal direction; in the vertical direction the jump may be smaller close to ground due to the high resolution grid close to ground. As can be seen in Table 2 four out of nine particles have reached ground after ten years and all but two have reached ground level after 25 years. The last line in Table 2 gives the distance travelled. The average distance can be calculated to 505 metres, from the numbers given.

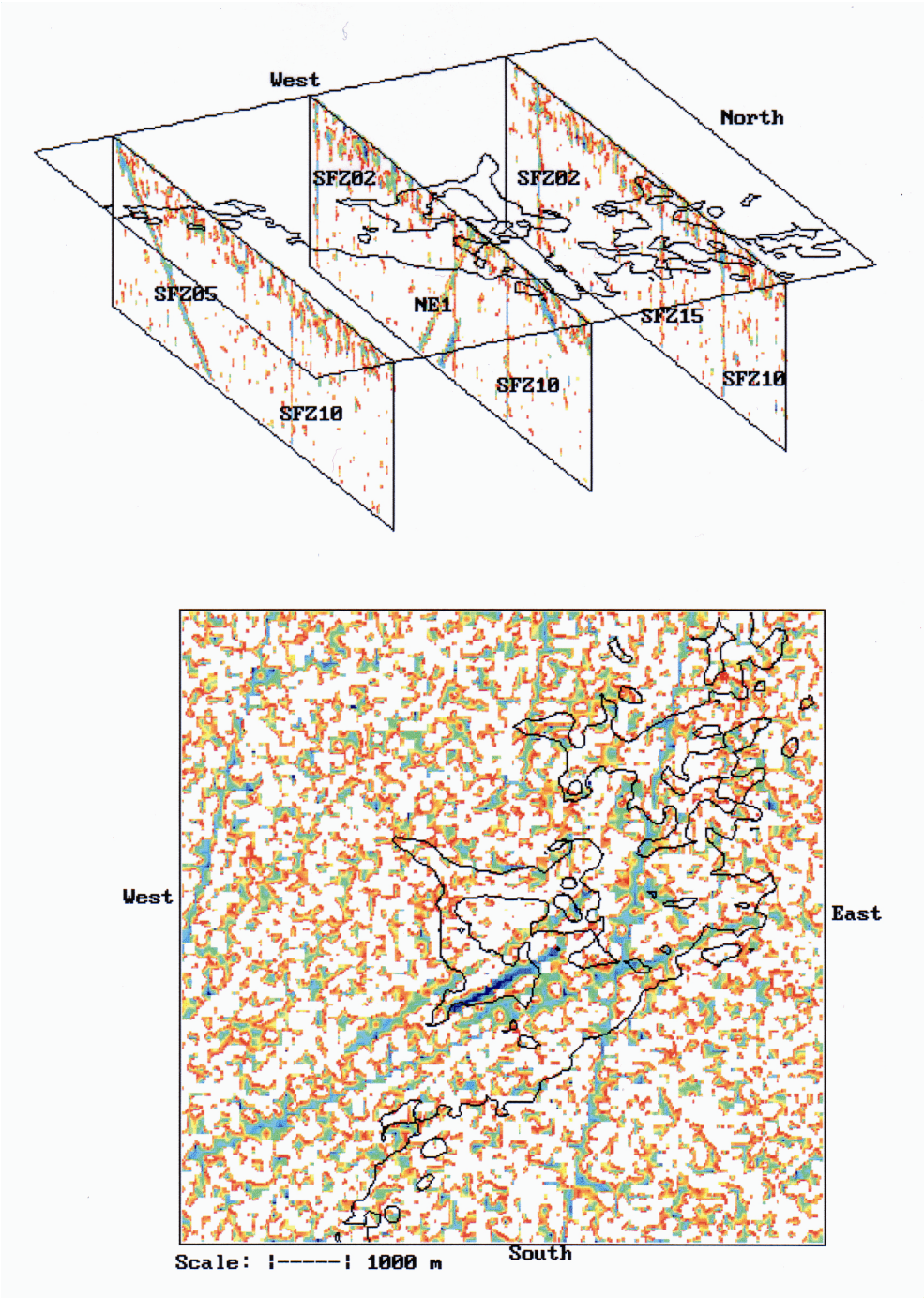

Figure 2. *Illustration of conductivity field. Perspective view (top) and horizontal section at a depth of 450 metres. Plotted conductivity interval:* $2.5\times10^{-7} \rightarrow 5.0\times10^{-5}$ *m/s.*

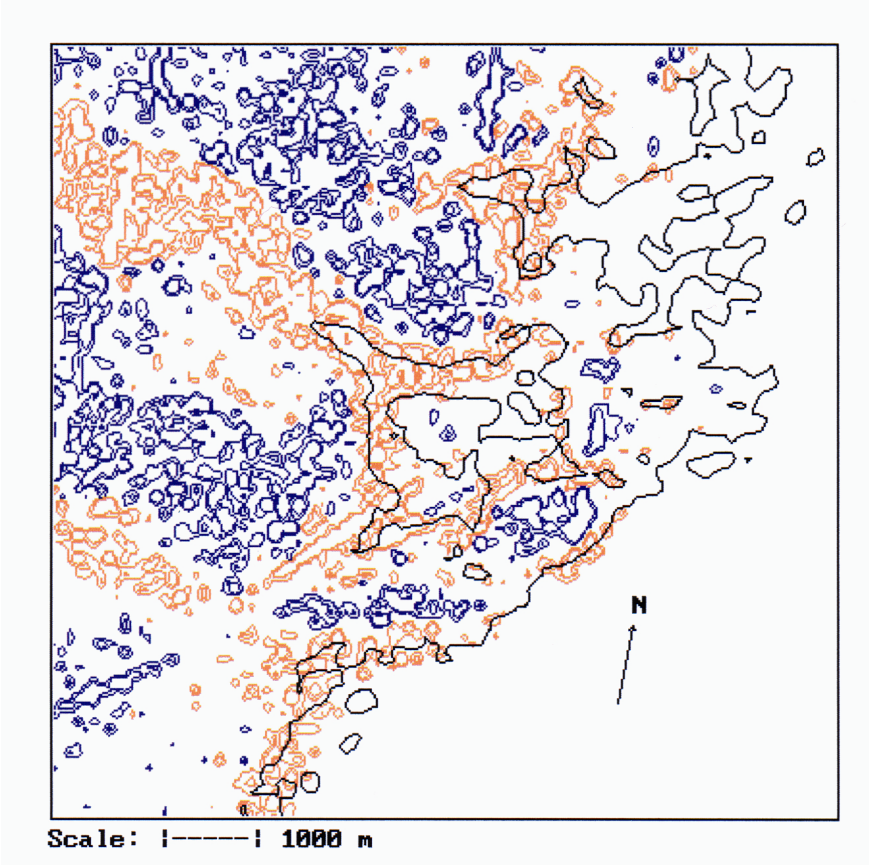

Figure 3. *Vertical flow at 200 metres depth.*
Blue colour indicates downwards and red upwards flow.
Isoline values: 20 and 40 mm/year.

Table 1. Darcy fluxes at nine positions in the SFL 3-5 area.

Position	X-coord	Y-coord	Z-coord	X-vel	Y-vel	Z-vel
1	3750	6250.	-300.	1.31E-10	-2.82E-10	-1.79E-11
2	3850.	6250.	-300.	6.82E-11	-1.54E-10	-5.64E-11
3	3950.	6250.	-300.	1.64E-10	-3.32E-10	3.33E-11
4	3750.	6350.	-300.	6.52E-10	1.53E-10	-1.17E-09
5	3850.	6350.	-300.	8.38E-10	1.09E-11	-4.96E-10
6	3950.	6350.	-300.	6.95E-10	-1.14E-10	4.65E-11
7	3750.	6450.	-300.	1.69E-10	1.05E-09	-1.73E-09
8	3850.	6450.	-300.	4.49E-10	4.27E-10	-9.47E-10
9	3950.	6450.	-300.	7.20E-10	1.38E-10	-1.15E-10
Mean	3850.	6350.	-300.	4.32E-10	9.97E-11	-4.95E-10

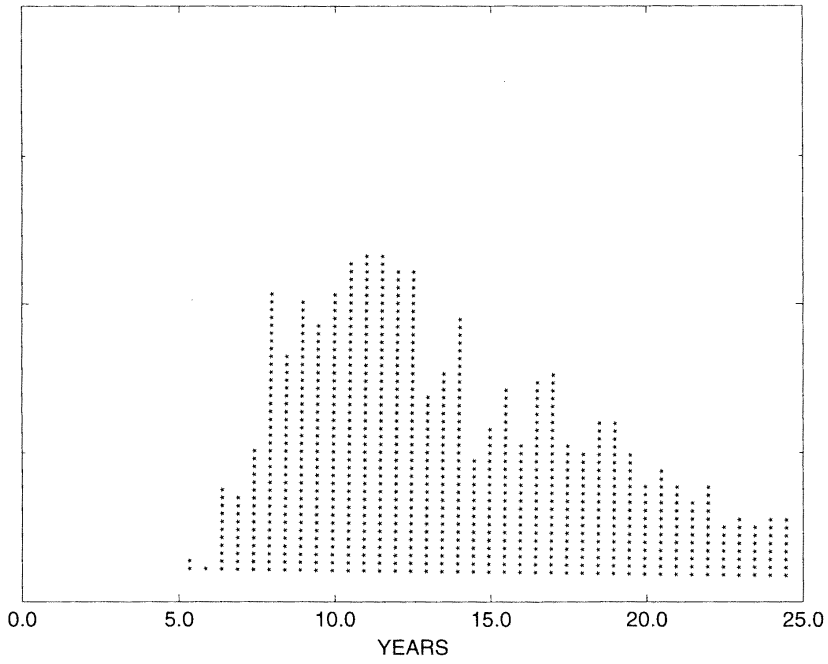

Figure 4. *Distribution of arrival times for particles reaching ground level. Each point represents 10 particles. 10 000 particles were released.*

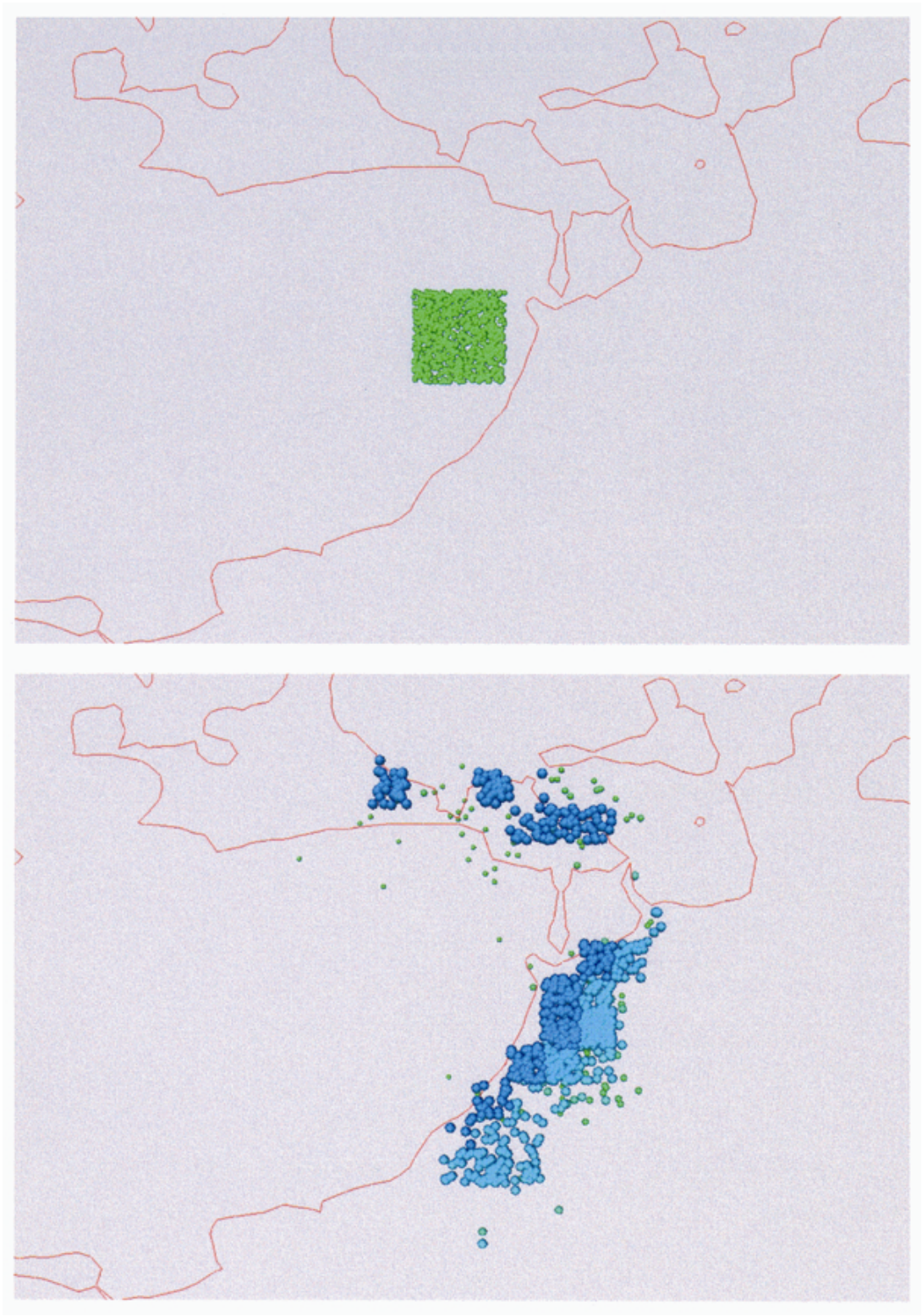

Figure 5. *Initial particle positions (top) and after 25 years. 1 000 particles are shown*

Table 2. Coordinates for nine particles during 25 years. The last line in the table gives the distance travelled.

	Particle								
	1	**2**	**3**	**4**	**5**	**6**	**7**	**8**	**9**
X-COORD	3750.	3850.	3950.	3750.	3850.	3950.	3750.	3850.	3950.
Y-COORD	6250.	6250.	6250.	6350.	6350.	6350.	6450.	6450.	6450.
Z-COORD	-300.	-300.	-300.	-300.	-300.	-300.	-300.	-300.	-300.
YEAR= 2									
X-COORD	3750.	3950.	4050.	3850.	3950.	3950.	3750.	3850.	4050.
Y-COORD	6250.	6250.	6250.	6350.	6350.	6450.	6550.	6550.	6450.
Z-COORD	-300.	-300.	-300.	-300.	-300.	-300.	-300.	-300.	-300.
YEAR= 3									
X-COORD	3750.	4050.	4150.	3950.	4050.	4050.	3750.	3950.	4150.
Y-COORD	6150.	6250.	6250.	6350.	6350.	6450.	6750.	6550.	6450.
Z-COORD	-300.	-300.	-200.	-300.	-300.	-300.	-300.	-300.	-300.
YEAR= 4									
X-COORD	3850.	4050.	4150.	3950.	4050.	4150.	3750.	4050.	4150.
Y-COORD	6150.	6250.	6250.	6350.	6350.	6450.	6750.	6550.	6450.
Z-COORD	-300.	-200.	-200.	-300.	-200.	-300.	-300.	-200.	-200.
YEAR= 5									
X-COORD	3850.	4050.	4150.	3950.	4050.	4150.	3750.	4050.	4250.
Y-COORD	6050.	6250.	6250.	6450.	6250.	6450.	6850.	6650.	6450.
Z-COORD	-300.	-100.	-200.	-300.	-100.	-200.	-300.	-200.	-200.
YEAR= 6									
X-COORD	3850.	4050.	4150.	4050.	4050.	4250.	3850.	4050.	4250.
Y-COORD	6050.	6250.	6250.	6450.	6250.	6450.	6850.	6750.	6450.
Z-COORD	-100.	-55.	-200.	-300.	-55.	-200.	-300.	-200.	-200.
YEAR= 7									
X-COORD	3950.	4050.	4150.	4150.	4150.	4250.	3950.	4050.	4250.
Y-COORD	6050.	6150.	6250.	6450.	6250.	6450.	6850.	6750.	6450.
Z-COORD	-56.	0.	-100.	-300.	-32.	-200.	-300.	-200.	-100.
YEAR= 8									
X-COORD	3950.	4050.	4150.	4150.	4250.	4250.	3950.	4150.	4250.
Y-COORD	6050.	6150.	6250.	6450.	6250.	6450.	6850.	6750.	6350.
Z-COORD	0.	0.	-100.	-200.	-12.	-100.	-300.	-200.	-58.
YEAR= 9									
X-COORD	3950.	4050.	4250.	4150.	4250.	4250.	4050.	4250.	4250.
Y-COORD	6050.	6150.	6250.	6350.	6250.	6350.	6850.	6750.	6250.
Z-COORD	0.	0.	-100.	-200.	0.	-100.	-300.	-200.	-57.
YEAR=10									
X-COORD	3950.	4050.	4250.	4150.	4250.	4250.	4050.	4250.	4250.
Y-COORD	6050.	6150.	6250.	6350.	6250.	6350.	6850.	6850.	6250.
Z-COORD	0.	0.	-57.	-200.	0.	-34.	-300.	-200.	0.
YEAR=11									
X-COORD	3950.	4050.	4250.	4150.	4250.	4250.	4050.	4250.	4250.
Y-COORD	6050.	6150.	6250.	6350.	6250.	6350.	6850.	6850.	6250.
Z-COORD	0.	0.	0.	-100.	0.	0.	-300.	-200.	0.
YEAR=12									
X-COORD	3950.	4050.	4250.	4150.	4250.	4250.	4050.	4250.	4250.
Y-COORD	6050.	6150.	6250.	6250.	6250.	6350.	6950.	6850.	6250.
Z-COORD	0.	0.	0.	-56.	0.	0.	-300.	-200.	0.
YEAR=13									
X-COORD	3950.	4050.	4250.	4250.	4250.	4250.	4050.	4350.	4250.
Y-COORD	6050.	6150.	6250.	6250.	6250.	6350.	6950.	6850.	6250.
Z-COORD	0.	0.	0.	-57.	0.	0.	-300.	-200.	0.

	Particle								
	1	**2**	**3**	**4**	**5**	**6**	**7**	**8**	**9**
YEAR=14									
X-COORD	3950.	4050.	4250.	4250.	4250.	4250.	4050.	4350.	4250.
Y-COORD	6050.	6150.	6250.	6250.	6250.	6350.	6950.	6850.	6250.
Z-COORD	0.	0.	0.	0.	0.	0.	-300.	-200.	0.
YEAR=15									
X-COORD	3950.	4050.	4250.	4250.	4250.	4250.	4050.	4350.	4250.
Y-COORD	6050.	6150.	6250.	6250.	6250.	6350.	6950.	6850.	6250.
Z-COORD	0.	0.	0.	0.	0.	0.	-300.	-200.	0.
YEAR=16									
X-COORD	3950.	4050.	4250.	4250.	4250.	4250.	4050.	4450.	4250.
Y-COORD	6050.	6150.	6250.	6250.	6250.	6350.	6950.	6850.	6250.
Z-COORD	0.	0.	0.	0.	0.	0.	-300.	-200.	0.
YEAR=17									
X-COORD	3950.	4050.	4250.	4250.	4250.	4250.	4150.	4450.	4250.
Y-COORD	6050.	6150.	6250.	6250.	6250.	6350.	6950.	6850.	6250.
Z-COORD	0.	0.	0.	0.	0.	0.	-300.	-200.	0.
YEAR=18									
X-COORD	3950.	4050.	4250.	4250.	4250.	4250.	4150.	4450.	4250.
Y-COORD	6050.	6150.	6250.	6250.	6250.	6350.	6950.	6850.	6250.
Z-COORD	0.	0.	0.	0.	0.	0.	-300.	-200.	0.
YEAR=19									
X-COORD	3950.	4050.	4250.	4250.	4250.	4150.	4150.	4450.	4250.
Y-COORD	6050.	6150.	6250.	6250.	6250.	6350.	6950.	6850.	6250.
Z-COORD	0.	0.	0.	0.	0.	0.	-300.	-200.	0.
YEAR=20									
X-COORD	3950.	4050.	4250.	4250.	4250.	4150.	4150.	4450.	4250.
Y-COORD	6050.	6150.	6250.	6250.	6250.	6350.	6950.	6850.	6250.
Z-COORD	0.	0.	0.	0.	0.	0.	-300.	-200.	0.
YEAR=21									
X-COORD	3950.	4050.	4250.	4250.	4250.	4150.	4150.	4450.	4250.
Y-COORD	6050.	6150.	6250.	6250.	6250.	6350.	6950.	6850.	6250.
Z-COORD	0.	0.	0.	0.	0.	0.	-300.	-200.	0.
YEAR=22									
X-COORD	3950.	4050.	4250.	4250.	4250.	4150.	4150.	4450.	4250.
Y-COORD	6050.	6150.	6250.	6250.	6250.	6350.	6950.	6850.	6250.
Z-COORD	0.	0.	0.	0.	0.	0.	-200.	-200.	0.
YEAR=23									
X-COORD	3950.	4050.	4250.	4250.	4250.	4150.	4150.	4450.	4250.
Y-COORD	6050.	6150.	6250.	6250.	6250.	6350.	6950.	6850.	6250.
Z-COORD	0.	0.	0.	0.	0.	0.	-200.	-200.	0.
YEAR=24									
X-COORD	3950.	4050.	4250.	4250.	4250.	4150.	4150.	4450.	4250.
Y-COORD	6050.	6150.	6250.	6250.	6250.	6350.	6950.	6850.	6250.
Z-COORD	0.	0.	0.	0.	0.	0.	-100.	-200.	0.
YEAR=25									
X-COORD	3950.	4050.	4250.	4250.	4250.	4150.	4150.	4450.	4250.
Y-COORD	6050.	6150.	6250.	6250.	6250.	6350.	6950.	6850.	6250.
Z-COORD	0.	0.	0.	0.	0.	0.	-100.	-200.	0.
DIST	412.	374.	424.	592.	510.	361.	671.	728.	469.

4 CONCLUSION

From the results presented the following conclusion can be formulated:

- SFL 3-5 is positioned in a major fracture zone. The area has strong downward and upward flow and a typical range of travel times (excluding all dispersion effects) is 7-25 years (80% of all particles will reach ground level in this time interval).

5 REFERENCES

Rhén I (ed), Gustafson G, Stanfors R, Wikberg P, 1997. Äspö HRL – Geoscientific evaluation 1997/5. Models based on site characterization 1986-1995. SKB Technical Report 97-06.

Svensson U, 1994. Refined modelling of flow and transport in the numerical model of the Äspö Hard Rock Laboratory. SKB Progress Report 25-94-12.

Svensson U, 1997. A regional analysis of groundwater flow and salinity distribution in the Äspö area. SKB Technical Report 97-09.

Appendix 2

FLOW AND TRANSPORT PARAMETERS FOR SFL 3-5

ESTIMATES FROM REGIONAL NUMERICAL MODELS FOR BEBERG AND CEBERG

Lee Hartley[1]

Maria Lindgren[2]

[1]AEA Technology, UK

[2]Kemakta Konsult AB

December 1997

SUMMARY

In this study the large-scale regional hydrogeological models set up for SR 97 in Beberg *[Hartley et al, 1998]* and in Ceberg *[Boghammar et al, 1997]* were used to evaluate transport parameters for the migration calculations in the far field of SFL 3-5. Particle tracking was for each site performed with 36 particles starting at the proposed location of SFL 3-5 according to Munier *et al. [1997]*.

In Beberg the average travel time is 40 years and the path-length 1 125 m. Corresponding figures for Ceberg is 906 years and 1 396 m.

The Darcy velocity at the location of the repository is 3 litres/year and 0.04 litres/year for Beberg and Ceberg, respectively. The direction of the flow is in both cases almost horizontal.

The final points were in both cases rather well gathered, for Beberg in the fracture zone Imundbo and for Ceberg close to the river Husån.

LIST OF CONTENT

1 INTRODUCTION

In the radionuclide migration calculations for SFL 3-5 it is necessary to have well estimated input parameters to achieve reliable results. Better background for the estimates of the transport parameters for the far field is the subject for this study.

In this study the large scale regional hydogeological models set up for SR 97 in Beberg *[Hartley et al, 1998]* and in Ceberg *[Boghammar et al, 1997]* were used for SFL 3-5. Particle tracking was in each case performed with 36 particles starting at the proposed location of SFL 3-5 according to Munier *et al. [1997]*.

Particle tracking from the location of SFL 3-5 in the two studied sites Beberg and Ceberg gives a good base when choosing the transport parameters travel time, path length and also the size and direction of the flow at the location of the repository. The final points also give valuable information when choosing the recipient for the radionuclide release.

2 PARTICLE TRACKING FROM SFL 3-5 IN BEBERG

Particle tracking from SFL 3-5 in Beberg is performed in the large-scale regional model. The numerical model used is the NAMMU-model and the case is the base case, further described in Hartley *et al. [1998]*. The location of SFL 3-5 is from the layout for a deep repository in Beberg as described in Munier *et al. [1997]*. The repository is situated at a depth of 360 m. 36 start points were chosen to represent the repository. The rock mass at the location of the repository has a conductivity of $1.6 \cdot 10^{-8}$ m/s and a porosity of $1 \cdot 10^{-4}$.

The calculated path lines show that they passes through one, two or three horizontal rock mass layers before entering the fracture zone Imundbo. Some paths cross between rock mass and the fracture zone a few times. All paths are very similar. The conductivities for the two layers above the one where the repository is located is $1.1 \cdot 10^{-8}$ m/s vertically and $1.3 \cdot 10^{-8}$ m/s horizontally in the layer above and $1.6 \cdot 10^{-7}$ m/s in the surface layer. The conductivity in the fracture zone is $6.9 \cdot 10^{-6}$ m/s. For all layers and the fracture zone the porosity is $1 \cdot 10^{-4}$. The results of the simulations are an average travel time of 40 years and a path length of 1 125 m. The Darcy velocity at the location of the repository is in average $9.7 \cdot 10^{-11}$ m/s or 3 litres/year and the direction is almost horizontal, 6 degrees below the horizon. In Figure 1 are the path lines given. It can be seen that all path lines are very similar ending in the fracture zone Imundbo. The average co-ordinates for the final points in RAK are 1617614 mE and 6697082 mN. All paths end up between 1617607-1617616 mE and 6697075-6697103 mN. Results for all paths are given in Table 1.

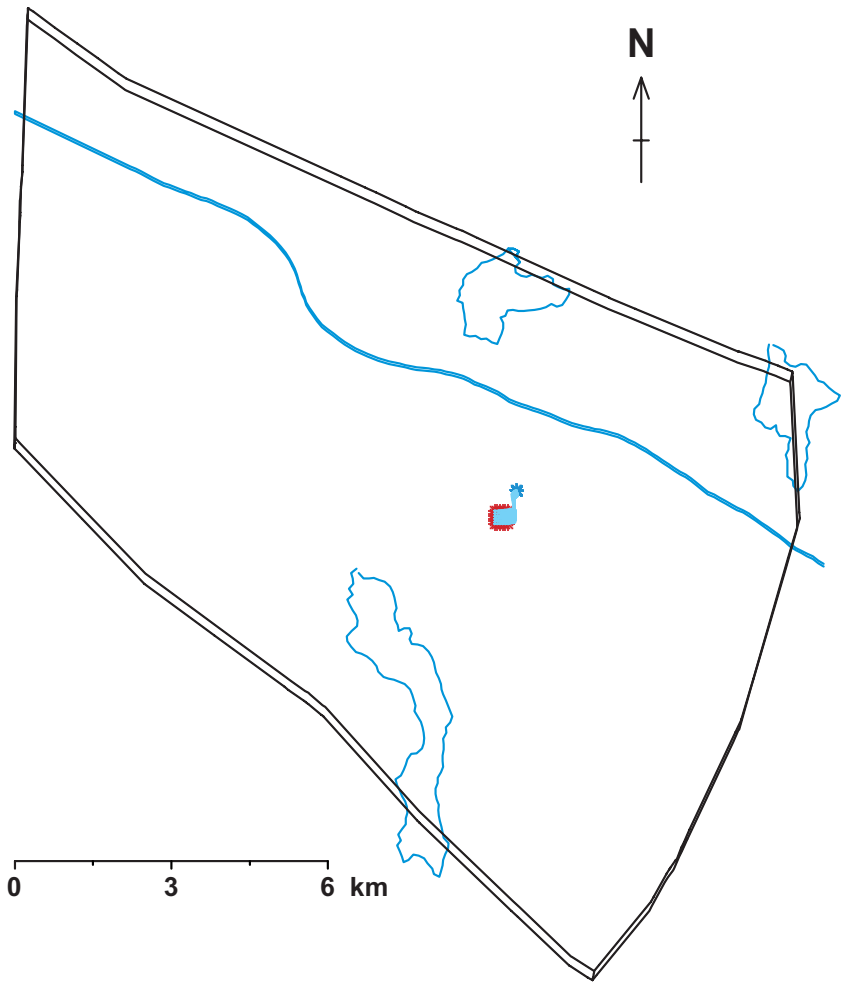

Figure 1. Initial positions (cerise stars), path lines and final points (purple stars) for all 36 particles for SFL 3-5 in Beberg. The model area for the NAMMU-model is indicated as well as three lakes and road 76.

Table 1. Results from particle tracking from SFL 3-5 in Beberg.

Path	Travel time (year)	Path length (m)	Vx (m/s)	Vy (m/s)	Vz (m/s)	Vtot (m/s)	Rotation from x-axis anti-clockwise	Dip (degrees)
1	14	956	$1.10 \cdot 10^{-10}$	$1.17 \cdot 10^{-11}$	$1.78 \cdot 10^{-11}$	$1.12 \cdot 10^{-10}$	6	-9
2	15	1 040	$1.12 \cdot 10^{-10}$	$1.33 \cdot 10^{-11}$	$1.84 \cdot 10^{-11}$	$1.15 \cdot 10^{-10}$	7	-9
3	29	1 150	$1.16 \cdot 10^{-10}$	$1.60 \cdot 10^{-11}$	$1.89 \cdot 10^{-11}$	$1.19 \cdot 10^{-10}$	8	-9
4	63	1 240	$1.19 \cdot 10^{-10}$	$1.05 \cdot 10^{-11}$	$1.88 \cdot 10^{-11}$	$1.21 \cdot 10^{-10}$	5	-9
5	80	1 370	$1.11 \cdot 10^{-10}$	$9.06 \cdot 10^{-12}$	$1.78 \cdot 10^{-11}$	$1.12 \cdot 10^{-10}$	5	-9
6	61	1 480	$1.04 \cdot 10^{-10}$	$6.97 \cdot 10^{-12}$	$1.61 \cdot 10^{-11}$	$1.06 \cdot 10^{-10}$	4	-9
7	13	916	$1.05 \cdot 10^{-10}$	$9.94 \cdot 10^{-12}$	$1.54 \cdot 10^{-11}$	$1.07 \cdot 10^{-10}$	5	-8
8	14	1 000	$1.07 \cdot 10^{-10}$	$1.05 \cdot 10^{-11}$	$1.58 \cdot 10^{-11}$	$1.09 \cdot 10^{-10}$	6	-8
9	42	1 130	$1.10 \cdot 10^{-10}$	$1.17 \cdot 10^{-11}$	$1.59 \cdot 10^{-11}$	$1.12 \cdot 10^{-10}$	6	-8
10	65	1 200	$1.09 \cdot 10^{-10}$	$1.77 \cdot 10^{-11}$	$1.60 \cdot 10^{-11}$	$1.12 \cdot 10^{-10}$	9	-8
11	75	1 340	$1.04 \cdot 10^{-10}$	$1.48 \cdot 10^{-11}$	$1.57 \cdot 10^{-11}$	$1.06 \cdot 10^{-10}$	8	-8
12	52	1 440	$1.00 \cdot 10^{-10}$	$1.19 \cdot 10^{-11}$	$1.45 \cdot 10^{-11}$	$1.02 \cdot 10^{-10}$	7	-8
13	12	876	$1.00 \cdot 10^{-10}$	$9.03 \cdot 10^{-12}$	$1.29 \cdot 10^{-11}$	$1.01 \cdot 10^{-10}$	5	-7
14	13	966	$1.01 \cdot 10^{-10}$	$8.95 \cdot 10^{-12}$	$1.29 \cdot 10^{-11}$	$1.02 \cdot 10^{-10}$	5	-7
15	51	1 100	$1.02 \cdot 10^{-10}$	$9.12 \cdot 10^{-12}$	$1.28 \cdot 10^{-11}$	$1.03 \cdot 10^{-10}$	5	-7
16	68	1 160	$1.00 \cdot 10^{-10}$	$2.14 \cdot 10^{-11}$	$1.32 \cdot 10^{-11}$	$1.03 \cdot 10^{-10}$	12	-7
17	66	1 310	$9.77 \cdot 10^{-11}$	$1.81 \cdot 10^{-11}$	$1.34 \cdot 10^{-11}$	$1.00 \cdot 10^{-10}$	11	-8
18	43	1 400	$9.55 \cdot 10^{-11}$	$1.50 \cdot 10^{-11}$	$1.26 \cdot 10^{-11}$	$9.75 \cdot 10^{-11}$	9	-7
19	10	836	$9.36 \cdot 10^{-11}$	$8.97 \cdot 10^{-12}$	$1.02 \cdot 10^{-11}$	$9.46 \cdot 10^{-11}$	5	-6
20	11	930	$9.34 \cdot 10^{-11}$	$8.48 \cdot 10^{-12}$	$9.95 \cdot 10^{-12}$	$9.43 \cdot 10^{-11}$	5	-6
21	56	1 070	$9.36 \cdot 10^{-11}$	$8.03 \cdot 10^{-12}$	$9.60 \cdot 10^{-12}$	$9.44 \cdot 10^{-11}$	5	-6
22	77	1 160	$9.17 \cdot 10^{-11}$	$2.26 \cdot 10^{-11}$	$1.03 \cdot 10^{-11}$	$9.50 \cdot 10^{-11}$	14	-6
23	55	1 290	$9.14 \cdot 10^{-11}$	$1.94 \cdot 10^{-11}$	$1.08 \cdot 10^{-11}$	$9.41 \cdot 10^{-11}$	12	-7
24	32	1 370	$9.07 \cdot 10^{-11}$	$1.65 \cdot 10^{-11}$	$1.04 \cdot 10^{-11}$	$9.28 \cdot 10^{-11}$	10	-6
25	8	796	$8.64 \cdot 10^{-11}$	$9.74 \cdot 10^{-12}$	$7.31 \cdot 10^{-12}$	$8.73 \cdot 10^{-11}$	6	-5
26	10	894	$8.53 \cdot 10^{-11}$	$9.03 \cdot 10^{-12}$	$6.79 \cdot 10^{-12}$	$8.61 \cdot 10^{-11}$	6	-5
27	59	1 040	$8.44 \cdot 10^{-11}$	$8.24 \cdot 10^{-12}$	$6.20 \cdot 10^{-12}$	$8.50 \cdot 10^{-11}$	6	-4
28	70	1 150	$8.38 \cdot 10^{-11}$	$2.18 \cdot 10^{-11}$	$7.27 \cdot 10^{-12}$	$8.69 \cdot 10^{-11}$	15	-5
29	44	1 260	$8.51 \cdot 10^{-11}$	$1.91 \cdot 10^{-11}$	$7.97 \cdot 10^{-12}$	$8.76 \cdot 10^{-11}$	13	-5
30	23	1 340	$8.58 \cdot 10^{-11}$	$1.67 \cdot 10^{-11}$	$7.84 \cdot 10^{-12}$	$8.78 \cdot 10^{-11}$	11	-5
31	7	757	$7.85 \cdot 10^{-11}$	$1.13 \cdot 10^{-11}$	$4.24 \cdot 10^{-12}$	$7.95 \cdot 10^{-11}$	8	-3
32	13	861	$7.66 \cdot 10^{-11}$	$1.05 \cdot 10^{-11}$	$3.47 \cdot 10^{-12}$	$7.74 \cdot 10^{-11}$	8	-3
33	61	1 000	$7.48 \cdot 10^{-11}$	$9.57 \cdot 10^{-12}$	$2.66 \cdot 10^{-12}$	$7.54 \cdot 10^{-11}$	7	-2
34	60	1 130	$7.63 \cdot 10^{-11}$	$1.94 \cdot 10^{-11}$	$4.04 \cdot 10^{-12}$	$7.88 \cdot 10^{-11}$	14	-3
35	34	1 230	$7.89 \cdot 10^{-11}$	$1.75 \cdot 10^{-11}$	$4.85 \cdot 10^{-12}$	$8.09 \cdot 10^{-11}$	13	-3
36	16	1 310	$8.07 \cdot 10^{-11}$	$1.57 \cdot 10^{-11}$	$4.93 \cdot 10^{-12}$	$8.24 \cdot 10^{-11}$	11	-3
Mean	40	1 130	$9.54 \cdot 10^{-11}$	$1.33 \cdot 10^{-11}$	$1.13 \cdot 10^{-11}$	$9.72 \cdot 10^{-11}$	8	-6
Stddev	24	194	$1.22 \cdot 10^{-11}$	$4.57 \cdot 10^{-12}$	$4.87 \cdot 10^{-12}$	$1.23 \cdot 10^{-11}$	3	2
Min	7	757	$7.48 \cdot 10^{-11}$	$6.97 \cdot 10^{-12}$	$2.66 \cdot 10^{-12}$	$7.54 \cdot 10^{-11}$	4	-9
Max	80	1 480	$1.19 \cdot 10^{-10}$	$2.26 \cdot 10^{-11}$	$1.89 \cdot 10^{-11}$	$1.21 \cdot 10^{-10}$	15	-2

3 PARTICLE TRACKING FROM SFL 3-5 IN CEBERG

Particle tracking from SFL 3-5 in Ceberg is performed in the large-scale regional model. The numerical model used is the NAMMU-model and the case is the base case, further described in Boghammar *et al. [1997]*. The location of SFL 3-5 is from the layout for a deep repository in Ceberg as described in Munier *et al. [1997]*. The repository is situated at a depth of 375 m. 36 start points were chosen to represent the repository. The rock mass at the location of the repository has a conductivity of $2.7 \cdot 10^{-10}$ m/s and a porosity of $1 \cdot 10^{-4}$.

Typical conductivities for the rock passed by the particles are demonstrated by a summary for the first path line. The conductivities are $2 \cdot 10^{-10}$ m/s, $2.7 \cdot 10^{-10}$ m/s, $3 \cdot 10^{-9}$ m/s, $4 \cdot 10^{-9}$ m/s, $6 \cdot 10^{-8}$ m/s, $3 \cdot 10^{-7}$ m/s and $3 \cdot 10^{-6}$ m/s. In some zones there is a small anisotropy. For the whole model the porosity is $1 \cdot 10^{-4}$. The results of the simulations are an average travel time of 906 years and a path length of 1396 m. The Darcy velocity at the location of the repository is in average $1.4 \cdot 10^{-12}$ m/s or 0.04 litres/year and the direction is almost horizontal, 0.7 degrees below the horizon. The initial positions and finial positions for the path lines are given in Figure 2. It can be seen that all particles come to Husån at almost the same place. The average co-ordinates for the final points in RAK are 1665678 mE and 7045041 mN. All paths end up between 1665656-1665703 mE and 7045013-7045072 mN. Results for all 36 path are given in Table 2.

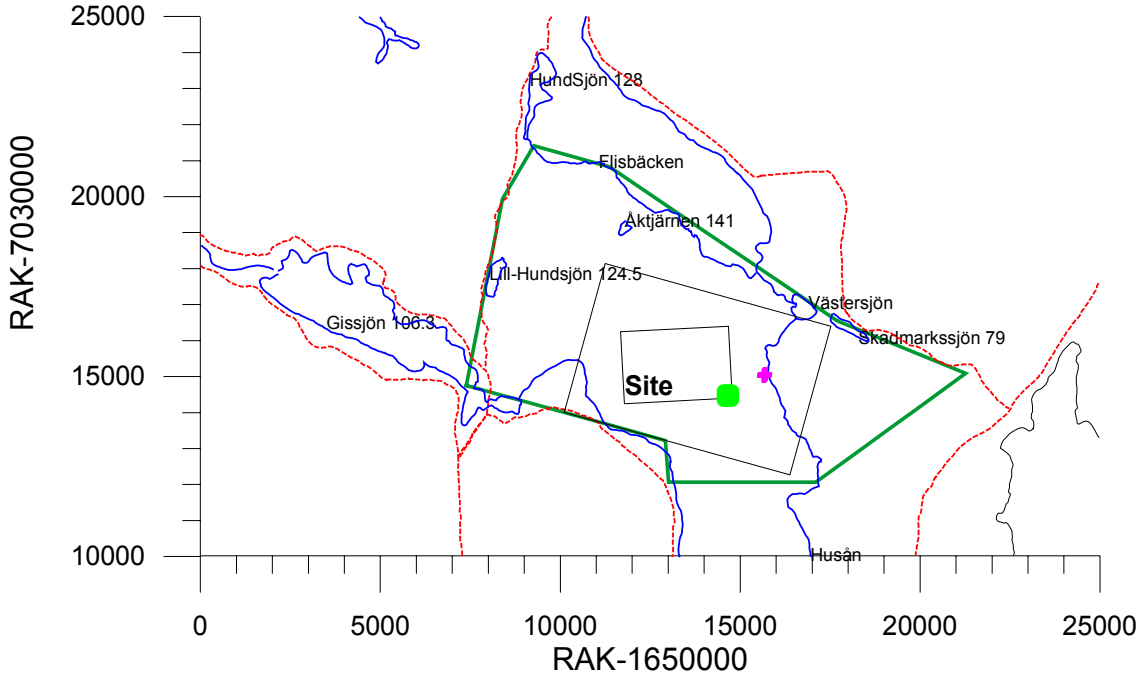

Figure 2. Initial positions (green points) and final positions (purple cross) for all 36 path lines for SFL 3-5 in Ceberg. The model area for the NAMMU-model is indicated in green and the local model area is also indicated as well as the site area.

Table 2. Results from particle tracking from SFL 3-5 in Ceberg.

Path	Travel time (year)	Path length (m)	Vx (m/s)	Vy (m/s)	Vz (m/s)	Vtot (m/s)	Rotation from x-axis anti-clockwise	Dip (degrees)
1	1 290	1 580	$1.23\cdot10^{-12}$	$-7.86\cdot10^{-14}$	$-2.93\cdot10^{-13}$	$1.27\cdot10^{-12}$	-4	13
2	1 090	1 520	$1.22\cdot10^{-12}$	$1.16\cdot10^{-13}$	$-1.64\cdot10^{-13}$	$1.23\cdot10^{-12}$	5	8
3	934	1 470	$1.23\cdot10^{-12}$	$1.13\cdot10^{-13}$	$-4.24\cdot10^{-14}$	$1.24\cdot10^{-12}$	5	2
4	817	1 410	$1.31\cdot10^{-12}$	$1.49\cdot10^{-13}$	$1.01\cdot10^{-13}$	$1.32\cdot10^{-12}$	6	-4
5	733	1 360	$1.33\cdot10^{-12}$	$1.55\cdot10^{-13}$	$2.50\cdot10^{-13}$	$1.36\cdot10^{-12}$	7	-11
6	680	1 320	$1.09\cdot10^{-12}$	$3.78\cdot10^{-13}$	$3.82\cdot10^{-13}$	$1.21\cdot10^{-12}$	19	-18
7	1 260	1 560	$1.34\cdot10^{-12}$	$-2.62\cdot10^{-14}$	$-3.28\cdot10^{-13}$	$1.38\cdot10^{-12}$	-1	14
8	1 070	1 510	$1.36\cdot10^{-12}$	$-2.88\cdot10^{-14}$	$-1.86\cdot10^{-13}$	$1.37\cdot10^{-12}$	-1	8
9	917	1 450	$1.30\cdot10^{-12}$	$1.48\cdot10^{-13}$	$-4.02\cdot10^{-14}$	$1.31\cdot10^{-12}$	6	2
10	800	1 400	$1.31\cdot10^{-12}$	$1.47\cdot10^{-13}$	$1.03\cdot10^{-13}$	$1.32\cdot10^{-12}$	6	-4
11	714	1 360	$1.33\cdot10^{-12}$	$1.60\cdot10^{-13}$	$2.52\cdot10^{-13}$	$1.36\cdot10^{-12}$	7	-11
12	659	1 330	$1.32\cdot10^{-12}$	$1.63\cdot10^{-13}$	$3.99\cdot10^{-13}$	$1.39\cdot10^{-12}$	7	-17
13	1 250	1 530	$1.34\cdot10^{-12}$	$-3.23\cdot10^{-14}$	$-3.58\cdot10^{-13}$	$1.39\cdot10^{-12}$	-1	15
14	1 050	1 470	$1.36\cdot10^{-12}$	$-3.49\cdot10^{-14}$	$-2.17\cdot10^{-13}$	$1.37\cdot10^{-12}$	-1	9
15	906	1 420	$1.44\cdot10^{-12}$	$2.29\cdot10^{-14}$	$-5.25\cdot10^{-14}$	$1.44\cdot10^{-12}$	1	2
16	796	1 370	$1.34\cdot10^{-12}$	$1.64\cdot10^{-13}$	$1.05\cdot10^{-13}$	$1.35\cdot10^{-12}$	7	-4
17	711	1 330	$1.33\cdot10^{-12}$	$1.66\cdot10^{-13}$	$2.55\cdot10^{-13}$	$1.37\cdot10^{-12}$	7	-11
18	653	1 290	$1.30\cdot10^{-12}$	$1.63\cdot10^{-13}$	$3.99\cdot10^{-13}$	$1.37\cdot10^{-12}$	7	-17
19	1 260	1 510	$1.34\cdot10^{-12}$	$-3.85\cdot10^{-14}$	$-3.90\cdot10^{-13}$	$1.39\cdot10^{-12}$	-2	16
20	1 050	1 440	$1.46\cdot10^{-12}$	$2.85\cdot10^{-14}$	$-2.36\cdot10^{-13}$	$1.48\cdot10^{-12}$	1	9
21	903	1 390	$1.45\cdot10^{-12}$	$3.20\cdot10^{-14}$	$-7.02\cdot10^{-14}$	$1.45\cdot10^{-12}$	1	3
22	794	1 340	$1.47\cdot10^{-12}$	$5.59\cdot10^{-14}$	$9.99\cdot10^{-14}$	$1.47\cdot10^{-12}$	2	-4
23	715	1 290	$1.33\cdot10^{-12}$	$1.72\cdot10^{-13}$	$2.60\cdot10^{-13}$	$1.37\cdot10^{-12}$	7	-11
24	655	1 260	$1.31\cdot10^{-12}$	$1.85\cdot10^{-13}$	$4.01\cdot10^{-13}$	$1.38\cdot10^{-12}$	8	-17
25	1 260	1 500	$1.45\cdot10^{-12}$	$-1.71\cdot10^{-15}$	$-4.21\cdot10^{-13}$	$1.51\cdot10^{-12}$	-0.1	16
26	1 060	1 440	$1.46\cdot10^{-12}$	$3.78\cdot10^{-14}$	$-2.52\cdot10^{-13}$	$1.49\cdot10^{-12}$	1	10
27	907	1 380	$1.49\cdot10^{-12}$	$6.29\cdot10^{-14}$	$-8.20\cdot10^{-14}$	$1.49\cdot10^{-12}$	2	3
28	798	1 330	$1.47\cdot10^{-12}$	$6.69\cdot10^{-14}$	$9.20\cdot10^{-14}$	$1.47\cdot10^{-12}$	3	-4
29	717	1 280	$1.47\cdot10^{-12}$	$3.03\cdot10^{-14}$	$2.57\cdot10^{-13}$	$1.49\cdot10^{-12}$	1	-10
30	664	1 250	$1.32\cdot10^{-12}$	$2.08\cdot10^{-13}$	$4.09\cdot10^{-13}$	$1.39\cdot10^{-12}$	9	-17
31	1 270	1 500	$1.43\cdot10^{-12}$	$-5.51\cdot10^{-14}$	$-4.43\cdot10^{-13}$	$1.50\cdot10^{-12}$	-2	17
32	1 070	1 440	$1.54\cdot10^{-12}$	$-7.45\cdot10^{-14}$	$-2.74\cdot10^{-13}$	$1.57\cdot10^{-12}$	-3	10
33	924	1 380	$1.49\cdot10^{-12}$	$7.41\cdot10^{-14}$	$-8.74\cdot10^{-14}$	$1.50\cdot10^{-12}$	3	3
34	813	1 330	$1.34\cdot10^{-12}$	$-9.38\cdot10^{-15}$	$8.61\cdot10^{-14}$	$1.34\cdot10^{-12}$	-0.4	-4
35	728	1 280	$1.45\cdot10^{-12}$	$-2.86\cdot10^{-14}$	$2.43\cdot10^{-13}$	$1.47\cdot10^{-12}$	-1	-10
36	675	1 240	$1.51\cdot10^{-12}$	$-5.19\cdot10^{-14}$	$4.02\cdot10^{-13}$	$1.57\cdot10^{-12}$	-2	-15
Mean	906	1 400	$1.37\cdot10^{-12}$	$7.05\cdot10^{-14}$	$1.55\cdot10^{-14}$	$1.40\cdot10^{-12}$	3	-1
Stddev	208	93	$9.70\cdot10^{-14}$	$1.02\cdot10^{-13}$	$2.71\cdot10^{-13}$	$8.77\cdot10^{-14}$	5	11
Min	653	1 240	$1.09\cdot10^{-12}$	$-7.86\cdot10^{-14}$	$-4.43\cdot10^{-13}$	$1.21\cdot10^{-12}$	-4	-18
Max	1 290	1 580	$1.54\cdot10^{-12}$	$3.78\cdot10^{-13}$	$4.09\cdot10^{-13}$	$1.57\cdot10^{-12}$	19	17

4 REFERENCES

Boghammar A., Grundfelt B., Hartley L., 1997. ”Investigation of the large scale regional hydrogeological situation at Ceberg”, SKB Technical report TR 97-21.

Hartley L., Boghammar A., Grundfelt B., 1998. ”Investigation of the large scale regional hydrogeological situation at Beberg”, SKB Technical Report TR 98-24.

Munier R., Sandstedt H., Niland L., ”Förslag till principiella utformningar av förvar enligt KBS-3 för Aberg, Beberg och Ceberg”, SKB rapport R-97-09, 1997.

Appendix 3

Effect of isosaccharinic acid, ISA, on sorption and solubility of radionuclides in SFL 3

Kristina Skagius[1]

Michael Pettersson[1]

Yngve Albinsson[2]

Stellan Holgersson[2]

[1] **Kemakta Konsult AB**

[2] **Dept. of Nuclear Chemistry, CTH**

November 1999

Contents

1 Introduction

Infiltrating water will re-saturate the waste packages after repository closure. There are considerable amounts of concrete in the waste packages, and therefore the pore water will be highly alkaline for a long period of time. Under such conditions, cellulose present in the waste disposed of in SFL 3 will degrade to hydroxycarboxylic acids. These compounds are strong complexing agents at high pH, which may affect the sorption and the solubility of radionuclides.

One example of such a degradation product which is of significance for the repository performance is isosaccharinic acid, ISA. Based on the present knowledge regarding yields of ISA and the effect of ISA on sorption and solubility of elements, distribution coefficients for radionuclide sorption and the solubility of radionuclides under the influence of ISA in SFL 3 are estimated.

2 Studies on alkaline degradation of cellulose and effects on element sorption and solubility

2.1 Overview

The alkaline degradation of cellulose will yield products that may have large effects on solubility as well as on sorption of certain elements. The first reported observations of the enhanced solubility of plutonium in the presence of cellulose at high pH were made in 1986 (Bradshaw *et al.*, 1986, Bradshaw *et al.*, 1987).

Various assumptions have been made concerning the composition of the cellulose degradation products that would account for the observed enhanced solubility of e.g. plutonium. It is known that minor fractions of polyhydroxycarboxylic acids (typically hexose derivatives) can be formed. Several hexose derivatives have been selected as model substances in experimental studies of cellulose degradation effects on radionuclide mobility (Greenfield *et al.*, 1993).

Recent experiments have confirmed that D-glucoisosaccharinic acid is the dominant strong complexing acid that will be formed during alkaline cellulose degradation (Greenfield *et al.,* 1995, Pavasars, 1999), as was previously suggested (Allard and Borén, 1991, Van Loon, 1993).

Since the first reported observations on the enhanced solubility of plutonium in the presence of cellulose at high pH were made in 1986 (Bradshaw *et al.,* 1986, Bradshaw *et al.,* 1987), a number of studies have been performed on the topic. For example, the solubility of Pu, Th, U, Np, Am, Tc, and Sn in the presence of cellulose or hexose derivatives have been investigated (Greenfield *et al.,* 1992). There are a few studies on adsorption of Pu, Am, Th, Ra, Pm and Eu on cement and on minerals at various pH, in the presence of cellulose degradation products or hexose derivatives (D-gluconic acid, D-glucoisosaccharinic acid) (Bradbury and Sarott, 1994, Holgersson *et al.,* 1998, Rai *et al.,* 1998, Wieland *et al.,* 1998). There are also several efforts made to develop models that can be used for the calculation of the effects of cellulose on adsorption.

Considering results reported on the adsorption of Pu, Th, Pm, Sm and Eu on cement and mineral surfaces (Baston *et al.,* 1995, Nordén and Allard, 1994, Bourbon and Toulhout, 1996, Holgersson *et al.,* 1998, Bradbury and Van Loon, 1998, Pavasars, 1999) it can be concluded that:

- The presence of cellulose degradation will enhance the solubility of especially tetravalent elements at high pH.
- The major potential complexing acid that can be formed at substantial yield by the alkaline degradation of cellulose is D-glucoisosaccharinic acid.
- Isosaccharinic acid shows strong affinity for sorption on cementitious materials

- The presence of cellulose degradation products at equilibrium concentrations of 20-30 mg/l or above may lead to an initial reduction of the adsorption of trivalent and tetravalent elements on mineral surfaces at high pH (e.g. cement at pH 12).

- The presence of the acidic hexose derivatives D-gluconic acid at equilibrium concentrations above 10^{-4} M and D-glucoisosaccharinic acid (at slightly higher concentrations) would lead to an initial reduction of the adsorption, just as for a real mixture of cellulose degradation products.

- The reduction of adsorption owing to the formation of complexes with hexose derivatives etc cannot be calculated from the corresponding increased solubility.

- Initial effects on adsorption caused by gluconic or isosaccharinic acids decrease with time at pH above 12, particularly for isosaccharinic acid. The effects are only minor after 5-6 months (gluconic acid) and 1-2 months (isosaccharinic acid) at equilibrium concentrations in the mM range.

2.2 Cellulose degradation and yield

The cellulose chain is essentially a linear molecule consisting of a number of glucose units. The number of glucose units represents its degree of polymerisation (DP). The molecule has one reducing and one non-reducing end-group.

The degradation of cellulose is a successive chain depolymerisation mechanism, a peeling-off mechanism, where the reducing end-group is removed from the cellulose chain (Van Loon and Glaus, 1998). The peeling-off mechanism is determined by two competing mechanisms; a propagation reaction which leads to a progressive shortening of the cellulose molecule and a stopping reaction. The propagation reaction can either lead to the formation of ISA, or, by a fragmentation process, to other carboxylic acids.

Under alkaline conditions, the degradation of cellulose is promoted by the cleavage of a glucosidic bond in the cellulose chain. This results in the formation of new reducing end groups that can be transformed into ISA by the peeling off reaction.

The most important parameters in the alkaline degradation process of cellulose are pH, temperature and solution composition. Temperature and pH influence mainly the rate of degradation, but do not influence the type of degradation products formed. The solution composition on the other hand is much more important in this respect (Van Loon and Glaus, 1998).

Based on long-term experiments, carried out under relevant conditions with different types of cellulose materials, Van Loon and Glaus (1998) draw the conclusion that the extent of cellulose degradation mainly depends on the mole fraction of reducing end groups of the cellulose and on its degree of crystallinity (accessibility). Furthermore, their calculations based on these experiments show that about 5 % of the cellulose present in a cementitious repository would degrade by the peeling off reaction during the first 10^4 to 10^5 years.

Recent experiments carried out at the Linköping University has shown that 15 to 20 % of the cellulose was converted to ISA after 3 years with an initial loading of 100 g/l of cellulose powder (Pavasars, 1999). The degradation rate decreased with time and a long-term prediction showed that all cellulose would be degraded after 150 to 550 years assuming a constant pH of 13.4. In an experiment with degradation of sawdust, approximately 3 g of ISA had been generated after 3 years with an initial loading of sawdust of 100 g/l (Pavasars, 1999). Assuming that sawdust contains 50 % cellulose this would mean that 6 % of the cellulose in sawdust was converted to ISA. In contrary to the experiments with cellulose powder, the concentration of ISA seemed to remain constant with time at the end of the experiment after 3 years (Pavasars, 1999).

2.3 Sorption of ISA on cement

The concentration of ISA in cement pore water can be reduced due to sorption of ISA on cement. The sorption isotherm of ISA on crushed cement paste was experimentally determined over an initial concentration range from 10^{-5} to 10^{-2} M (Bradbury and Van Loon, 1998). A Langmuir isotherm for sorption of ISA on cement paste was derived:

$$\{ISA\}_{sorbed} = \frac{K_{ISA} \cdot \{ISA\}_{\max} \cdot C_{eq}}{1 + K_{ISA} \cdot C_{eq}} \qquad (1)$$

where $\{ISA\}_{sorbed}$ = the amount of ISA sorbed on cement (mole/kg)

$\{ISA\}_{max}$ = the maximum sorption capacity of ISA on cement ≈ 0.17 (mole/kg)

K_{ISA} = the sorption-affinity parameter ≈ 690 (litre/mole)

C_{eq} = the aqueous equilibrium concentration of ISA (mole/litre)

With these data, 0.011 mole/kg of ISA is sorbed at an equilibrium concentration of ISA in solution of $1 \cdot 10^{-4}$ M. This corresponds to a sorption distribution coefficient, K_d, of 0.11 m^3/kg for ISA on cement at an equilibrium concentration of $1 \cdot 10^{-4}$ M in solution. A somewhat higher sorption distribution coefficient is obtained at lower equilibrium concentrations of ISA in solution, e.g. K_d = 0.12 m^3/kg at an equilibrium concentration of ISA in solution of $1 \cdot 10^{-5}$ M.

Van Loon and Glaus (1998) confirmed a Langmuir isotherm for the sorption of ISA on cement, but a two-site model with Langmuir adsorption gave better fit to the experimental data. With their two-site Langmuir isotherm the maximum sorption capacity of ISA on cement was determined to be about 0.3 mole/kg. Using their best fit of the Langmuir isotherm gives a sorption distribution coefficient for ISA on cement of 0.15 m^3/kg at an equilibrium concentration of ISA of $1 \cdot 10^{-4}$ M and a sorption distribution coefficient of 0.17 m^3/kg at an equilibrium concentration of $1 \cdot 10^{-5}$ M.

Experiments with batch sorption of ISA on crushed cement have been carried out by Holgersson *et al.* (1999). The initial concentration range of ISA was $5 \cdot 10^{-4}$ - $5 \cdot 10^{-3}$ M and the results could be fitted to a single-site Langmuir isotherm with $\{ISA\}_{max}$ = 0.10 mole/kg and K_{ISA} ≈ 2 300 litre/mole. This gives K_d = 0.19 m^3/kg for ISA at an

equilibrium concentration of $1 \cdot 10^{-4}$ M and $K_d = 0.22$ m^3/kg at an equilibrium concentration of $1 \cdot 10^{-5}$ M.

From an experiment with diffusion of ISA through a concrete disc, the sorption of ISA was evaluated in terms of a K_d (Pavasars, 1999). The K_d was found to be at least $1.73 \cdot 10^{-4}$ m^3/kg at initial ISA concentrations of 19.1 g/l (0.1 M). The diffusion experiment was carried out with an alkaline leachate from pure cellulose that was separated by a concrete disc from another chamber filled with concrete porewater.

2.4 Effect of ISA on sorption

It is well known that ISA may have a negative effect on the sorption of radionuclides. Bradbury and Van Loon (1998) discuss the effect of ISA on sorption of some divalent, trivalent, and tetravalent elements on cement paste. They conclude that:

- There seems to be no effect of ISA on the sorption of the monovalent element Cs and divalent elements Sr and Ni on cement for equilibrium concentrations of ISA up to 10^{-2} M.

- Measured K_d-values for Eu(III) without ISA present are high, $>10^3$ m^3/kg, and there seems to be no effect of ISA on the sorption for equilibrium concentrations of ISA up to 10^{-4} M. Increasing the concentration to 10^{-3} M cause only a minor reduction in sorption. The ISA concentration has to be increased to 10^{-2} M before a significant reduction in K_d is observed. At a concentration of 0.1 M, sorption is reduced by approximately a factor of 100.

- K_d values obtained for Th(IV) are as high as for Eu for equilibrium concentrations of ISA up to 10^{-4} M. At higher ISA concentration K_d decreases with an increase in ISA concentration. For an ISA concentration of 10^{-2} M, K_d is reduced by more than four orders of magnitude, from 10^3 m^3/kg to 10^{-1} m^3/kg.

Results from batch sorption experiments carried out at Chalmers University (Holgersson *et al.*, 1998) indicate that ISA concentrations have to be in the mM range before sorption of Th and Pm on crushed cement is affected.

2.5 Effect of ISA on solubility

The solubility of trivalent and tetravalent elements is strongly affected by the presence of ISA. A compilation of data on the solubility measured in the presence of ISA shows that the solubility of U, Th and Pu increase with a factor of 250, 500 and $2 \cdot 10^5$, respectively, at an ISA concentration of 2 mM (Allard *et al.*, 1995). Different measured values of the solubility of Pu in the presence of ISA show that a major increase in solubility is established at ISA concentrations above 0.1 mM. At an ISA concentration of 1 mM the solubility of Pu is of the order of 10^{-5} M and at an ISA concentration of 5 mM the solubility is of the order of 10^{-4} M (Allard *et al.*, 1995).

Experiments performed with a total ISA concentration of 5 mM (Holgersson *et al.,* 1999), result in an increase in solubility for Th, Pm and Ni with a factor of 14000, 300 and 2, respectively.

A general conclusion that can be made from the experiments carried out is that the presence of ISA will cause a large increase in the solubility of the actinides. This is a reason to use much higher (Th, U, Pm) or disregard (Np, Pu, Pa, Am, and Cm) solubility constraints for the trivalent and the tetravalent radionuclides in a case in which cellulose dehydration products are expected to be present.

3 Estimated effects of ISA on sorption and solubility in SFL 3

The waste to be deposited in SFL 3 may contain some cellulose. The effect of ISA on sorption and solubility of radionuclides seems to depend on the concentration of ISA in solution. The expected ISA concentration in waste packages containing cellulose material is estimated from available information on organic materials in the waste types and material composition and geometry of the waste packages. The concentration of ISA in water inside the waste packages is calculated taking sorption of ISA on cement and concrete into account. Based on this concentration, an assessment is made of possible effects on sorption and solubility due to formation of complex between radionuclides initially present in waste packages and ISA.

3.1 Quantities of organic materials, water and concrete/cement

There are five different waste types in SFL 3 containing wood, paper, textiles and rags and therefore also cellulose (Lindgren *et al.,* 1998). Four of these waste types come from Studsvik and the fifth type is scrap and trash from CLAB and the encapsulation plant. In addition, there are two waste types from Studsvik containing unspecified organic wastes that possibly contain some cellulose. The different waste types are:

- Concrete containers with intermediate level waste from Studsvik (Cont. ILW)
- Concrete containers with plutonium (Cont. Pu)
- Steel drums with refuse and scrap from Studsvik (Drum refuse)
- Concrete boxes with plutonium waste from Studsvik (Box Pu)
- Steel drums with solidified sludge from Studsvik (Drum sludge)
- Steel drums with ashes from Studsvik (Drum ash)
- Concrete containers with metal scrap and trash from CLAB and the encapsulation plant (Cont. scrap CLAB)

The estimated quantities of different material in the different waste types are compiled in Table3-1.

Table3-1 Estimated quantities of cellulose material in SFL 3 (Lindgren *et al.*, 1998).

Waste type	Number of packages	Wood and paper (kg)	Textiles and rags (kg)	Unspecified org. material (kg)
Cont. ILW	400	1 178	2 733	
Cont. Pu	100	222	444	
Drum refuse	2 390	1 759	4 083	
Box Pu	29	129	258	
Drum sludge	1 000			500
Drum ash	556			222
Cont. scrap CLAB	360	1 584	12 960	

The volume of water that primarily is available for cellulose degradation and for the ISA complexes formed is given in Table 3-2. It is assumed that the water volume is the sum of the porosity/void in the waste, voids inside and in between steel drums, voids in between steel drums and outer containers and the porosity of concrete moulds. For waste stabilised in cement ('Drum sludge') it is assumed that the void inside the steel drum is equal to 30 % of the inner volume of the steel drum. For waste stabilised in concrete ('Cont. scrap CLAB') it is assumed that the void inside the concrete container is equal to the unfilled volume plus the porosity of the waste matrix that is assumed to be 15 %. The remaining data on available voids in the packages are from Lindgren *et al.* (1998), except for the porosity of concrete as packaging that is assumed to be 15 %. The amount of concrete and cement in the waste packages are given in Lindgren *et al.* (1998).

Table3-2 Estimated water volumes and amount of concrete in packages in SFL 3.

Waste type	Number of packages	Volume of water (m^3)	Concrete and cement[1)] (tonnes)
Cont. ILW	400	195	1 200
Cont. Pu	100	57	301
Drum refuse	2 390	180	551
Box Pu	29	49	87
Drum sludge	1 000	60	400
Drum ash	556	58	128
Cont. scrap CLAB	360	193	749

[1)] *For the waste type Drum sludge the amount refers to cement*

3.2 Estimated concentrations of ISA

Based on available experimental data on alkaline degradation of cellulose (see 2.2) and the fact that the organic materials in the wastes are not pure cellulose, a yield of 0.1 mole ISA/kg cellulose material is assumed (Allard, pers. com., 1999). Using this yield and the estimated quantities of organic materials (Table 3-1) and water in the waste packages (Table 3-2) the amount of ISA present per volume of water can be calculated.

The highest amount of ISA in the water is obtained for the waste type "Concrete container with metal scrap and trash from CLAB and the encapsulation plant". Assuming degradation of all wood, paper, textiles, and rags results in about 8 mmole ISA/litre. The waste types " Concrete containers with intermediate level waste from Studsvik" and "Steel drums with refuse and scrap from Studsvik" would obtain about 2 to 3 mmole ISA/litre. Degradation of the organic materials in the waste category "Concrete containers with plutonium waste" would result in about 1 mmole ISA/litre and the remaining waste categories in less than 1 mmole ISA/litre.

The actual concentration of ISA in the water will be lower than the figures above due to sorption of ISA on cement in the waste packages. The concentration of ISA in the waste packages is calculated assuming a distribution coefficient of 0.1 m^3/kg. This value of the distribution coefficient will not underestimate the concentration of ISA in the water as long as the equilibrium concentration of ISA is equal to or smaller than $1 \cdot 10^{-4}$ M (see section 2.3). The amount of cement present in the waste packages is given in Table 3-2 for the waste category 'Steel drums with solidified sludge from Studsvik' (Drum sludge). For the other waste categories the amount of cement in the waste packages is calculated assuming 420 kg of cement per m^3 of concrete, which is the cement content in concrete moulds to SFR (Höglund and Bengtsson, 1991). The results are given in Table 3-3.

Table 3-3 Calculated equilibrium concentrations of ISA assuming a degradation yield of 0.1 mole ISA per kg of organic materials and a distribution coefficient of ISA on cement of 0.1 m^3/kg.

Waste type	Organic materials (kg)	Water (m^3)	Cement (kg)	Equilibrium conc. of ISA (M)
Cont. ILW	3 911	195	$2{,}0 \cdot 10^5$	$2.0 \cdot 10^{-5}$
Cont. Pu	666	57	$5.0 \cdot 10^4$	$1.3 \cdot 10^{-5}$
Drum refuse	5 842	180	$1.0 \cdot 10^5$	$5.7 \cdot 10^{-5}$
Box Pu	387	49	$1.6 \cdot 10^4$	$2.4 \cdot 10^{-5}$
Drum sludge	500	60	$4.0 \cdot 10^5$	$1.2 \cdot 10^{-6}$
Drum ash	222	58	$2.4 \cdot 10^4$	$9.2 \cdot 10^{-6}$
Cont. scrap CLAB	14 544	193	$1.4 \cdot 10^5$	$1.0 \cdot 10^{-4}$

Table 3-3 shows that the concrete containers with metal scrap and trash from CLAB and the encapsulation plant give rise to the highest estimated equilibrium concentration of ISA in the packages. However, the estimated concentration of $1 \cdot 10^{-4}$ M is not higher than the upper limit for which the applied distribution coefficient is valid. The quantity

of ISA sorbed on the cement is 0.01 mole/kg. This is well below the maximum sorption capacity of 0.17 to 0.3 mole/kg reported in the literature (see section 2.3).

3.3 Effects on element sorption in SFL 3

Experimental data on element sorption indicates that equilibrium concentrations of ISA has to be larger than 10^{-4} to 10^{-3} M before significant effects on the sorption of trivalent and tetravalent element are expected (see section 2.4). Since the expected equilibrium concentration of ISA in the different waste categories in SFL 3 containing cellulose materials is 10^{-4} M or lower, effects on radionuclide sorption should be negligible.

Similar results were obtained for the Swiss low and intermediate level waste repository. Equilibrium concentrations of ISA in the part of the repository with the highest loading of organic materials (SMA4) were estimated to be at most about 10^{-4} M (Bradbury and van Loon, 1998, Van Loon and Glaus, 1998). The conclusion made was that this expected ISA concentration is too low to significantly affect radionuclide sorption.

3.4 Effects on element solubility

The experimental results available indicate that the presence of ISA may cause a large increase of the solubility of actinides (see section 2.5). In order to display the effects of ISA it is therefore suggested to use much higher or even disregard solubility constraints for the trivalent and the tetravalent radionuclides in some of the calculations. The solubility limits recommended are given in Table 3-4 and are selected based on the experimental results available.

Table 3-4 Recommended solubility limits in concrete water in SFL 3.

Element	Solubility (M)	
	not affected by ISA	affected by ISA
Ni	$1 \cdot 10^{-7}$	$2 \cdot 10^{-7}$
Pm	$9 \cdot 10^{-8}$	$3 \cdot 10^{-5}$
Am, Cm,	$9 \cdot 10^{-8}$	-
Pa, Np, Pu	$5 \cdot 10^{-9}$	-
Th, U	$5 \cdot 10^{-9}$	$7 \cdot 10^{-5}$

References

Allard B, Borén H, 1991. Organic degradation products in SFR and their effects on radionuclide mobility. SKB Report SFR 91-03, Swedish Nuclear Fuel and Waste Management Co, Stockholm, Sweden

Allard B, Borén H, Ephraim J, 1995. Cellulosa i cementsystem. Nedbrytningsprodukter och deras effekter på radionukliders transportegenskaper. SKB Report SFR 95-01, Swedish Nuclear Fuel and Waste Management Co, Stockholm, Sweden (in Swedish).

Allard B, 1999. Personal communication.

Baston G M N, Berry J A, Brownsword M, Heat T G, Tweed C J, Williams S J, 1995. Sorption of Pu and Am on repository, backfill and geological materials relevant to the JFNL low-level radioactive waste repository at Rokkasho-mura. Mat. Res. Soc. Symp. Proc. **353**, p. 957.

Bourbon X, Toulhoat P, 1996. Influence of organic degradation products on the solubilisation of radionuclides in intermediate and low level radioactive wastes. Radiochim Acta **74** p. 315.

Bradbury M H, Sarott F-A, 1994. Sorption Databases for the Cementitious Near-Field of a L/ILW Repository for Performance Assessment. Nagra Technical Report 93-08, Wettingen, Switzerland.

Bradbury M H, Van Loon L R, 1998. Cementitious Near-Field Sorption Data Bases for Performance Assessment of a L/ILW Repository in a Palfris Marl Host Rock (CEM94:UPDATE I, June 1997). PSI Bericht Nr. 98-01, Paul Scherrer Institut, Villigen, Switzerland.

Bradshaw S, Gaudie S C, Greenfield B F, Lyon C E, Rees J H, Spindler M W, Wilkins J D, 1986. Preliminary experimental studies in the chemical and radiation degradation of combustionable plutonium contaminated material.
Report AERE-R12223, AEA Technology, Harwell, UK.

Bradshaw S, Gaudie S C, Greenfield B F, Long S, Spindler M W, Wilkins J D, 1987. Experimental studies on the chemical and radiation decomposition of intermediate-level wastes containing organic materials. Report AERE-R12806, AEA Technology, Harwell, UK.

Greenfield B F, Moreton A D, Spindler M W, Williams S J, Woodwark D R, 1992. The effects of the degradation of organic materials in the near field of a radioactive waste repository. In Scientific Basis for Nuclear Waste Management XV, pp 299-306.

Greenfield B F, Harrison W N, Robertsson G P, Somers P J, Spindler M W, 1993. Mechanistic studies of the alkaline degradation of cellulose in cement. NIREX Report NSS/R272, AEA Technology, Harwell, UK.

Greenfield B F, Spindler M W, Woodwark D, 1993b. Summery of the effects of organic degradation products on near-field radionuclide chemistry. NIREX Report NSS/R298, AEA Technology, Harwell, UK.

Greenfield B F, Holtom, Hurdus M H, O'Kelly N, Pilkington N J, Rosevear A, Spindler M W, Williams S J, 1995. The identification and degradation of isosaccharinic acid, a cellulose degradation product. Mat. Res. Soc. Symp. Proc. **353** p. 1151.

Holgersson S, Albinsson Y, Allard B, Borén H, Pavasars I, Engkvist I, 1998. Effects of Gluco-isosaccharinate on Cs, Ni, Pm and Th sorption onto, and diffusion into cement. Radiochim. Acta, **82**, p 393 – 398.

Holgersson S, Albinsson Y, Allard B, Borén H, Pavasars I, Engkvist I, 1999. Effects of Gluco-isosaccharinate on Cs, Ni, Pm and Th sorption onto and diffusion into cement Part 2. In preparation.

Höglund L O, Bengtsson A, 1991. Some chemical and physical processes related to the long-term performance of the SFR repository. SKB Report SFR 91-06, Swedish Nuclear Fuel and Waste Management Co, Stockholm, Sweden.

Lindgren M, Pers K, Skagius K, Wiborgh M, Brodén K, Carlsson J, Riggare P, Skogsberg M, 1998. Low and Intermediate Level Waste in SFL 3-5: Reference Inventory. Reg. No: 19.41/DL 31, Swedish Nuclear Fuel and Waste Management Co, Stockholm Sweden.

Nordén M, Allard B, 1994. The influence of cellulose and its degradation products on the adsorption of Eu on cement. In Nordén M, The complexation of some radionuclides with natural organics – implications for radioactive waste disposal. Linköping Studies in Arts and Science 103, Linköping University, Sweden. (Diss.)

Pavasars I, 1999. Characterisation of organic substances in waste materials under alkaline conditions. Linköping Studies in Arts and Science 196, Linköping University, Sweden. (Diss.)

Rai D, Linfeng R, Moore D A, 1998. Influence of isosaccharinic acid on the solubility of Np(IV) hydrous oxide. Radiochim. Acta **83,** p.9.

Van Loon L R, 1993. The alkaline degradation of cellulose and cellulose derivatives: Impact on radionuclide speciation. PSI Technical Report TM-43-92-45, Paul Scherrer Institut, Villingen, Switzerland.

Van Loon L R, Glaus M A, 1998. Experimental and Theoretical Studies on Alkaline Degradation of Cellulose and its Impact on the Sorption of Radionuclides. Nagra Technical Report 97-04, Wettingen, Switzerland.

Wieland E, Tits J, Spieler P, Dobler J P, 1998. Interaction of Eu(III) and Th(IV) with sulphate-resisting Portland cement. Mat. Res. Soc. Symp. Proc. **506**, p. 573.

APPENDIX 4

Heat generation in SFL 3-5

Maria Lindgren

Kemakta Konsult AB

August 1999

1 Introduction

Heat will be generated in the waste in SFL 3-5 due to loss of energy as the radionuclides in the waste decays. In an earlier prestudy of the performance of the barriers in SFL 3-5 the heat generation and the resulting increase in temperature in SFL 5 was estimated (Wiborgh, 1995). Since new estimates of the content of radionuclides in the waste have been made and the design of the SFL 3-5 repository has been changed an update of the earlier calculations of heat generation and effects on temperature has been made. These new calculations are described in this appendix.

2 Calculations and data

After closure heat will be generated due to radionuclide decay. In the prestudy (Lindgren and Pers, 1994) the increase in temperature in SFL 5 due to heat generation in the waste was calculated. The calculations were based on an earlier inventory and design. In the earlier design, SFL 5 comprised 3 parallel caverns with a total length of 390 m and a distance between them of 24 m. The increase in temperature 100 years after closure was calculated taking into account heat capacity and conductive transport in the caverns with their content and 12 m of the surrounding rock mass, i.e. half the distance between the caverns. The result showed that the heat transport in the system was fast compared to the heat generation and that the temperature in the waste becomes negligible higher than the average temperature in the system. The average temperature in the system was calculated to be less than 2ºC above the initial temperature, when Co-60 and Ni-63 are taken into account as a source for the heat generation. 99% of the heat generation arise from the decay of these two nuclides.

In the new design, SFL 5 consists of only one, 115 m long cavern with a cross-sectional area larger than in the earlier design. The SFL 5 cavern is parallel to SFL 3 and the distance between them is 40 m. The material conducting heat are the same in both designs. The new estimate of the inventory of Co-60 and Ni-63 in SFL 5 is about 1.5 times higher than in the earlier calculations.

A new estimate of the temperature increase assuming fast heat transport in comparison to the heat generation has been performed. Likewise to the earlier calculations, a cylindrical geometry is assumed for the SFL 5 cavern and the surrounding rock. The centre of the cylinder, representing the waste, is surrounded by two shells where the innermost represents the concrete in the vault and the outermost the rock outside the vault.

The increase in average temperature in the whole cylinder due to radioactive decay during 100 years is calculated as:

$$\Delta T = A_0 \cdot 3.15 \cdot 10^7 \cdot \frac{1}{\lambda}\left(1 - e^{-\lambda \cdot 100}\right)\left(E_\alpha + E_\beta + E_\gamma\right) \cdot Z \cdot \frac{1}{L} \cdot \frac{1}{CAPT}$$

where:

ΔT	is the average increase in temperature in the studied area (K)
A_0	is the activity of nuclide at year 2040 (Bq), (decay·s^{-1})
λ	is the decay constant (yr^{-1})
E_α	is the alpha energy per transformation of the nuclide (MeV·$decay^{-1}$)
E_β	is the beta energy per transformation of the nuclide (MeV·$decay^{-1}$)
E_γ	is the gamma energy per transformation of the nuclide (MeV·$decay^{-1}$)
Z	is the transformation factor ($1.60219 \cdot 10^{-13}$ J·MeV^{-1})
L	is the length of the repository (m)
CAPT	is the specific heat per metre repository (kJ·K^{-1}·m^{-1}) (Volume per metre·Density·Heat capacity, see Table A4-1.

Material data used in the calculations are given in Table A4-1 and radionuclide data are given in Table A4-2. To check whether the extent of water saturation has any impact on the results, calculations were performed assuming either that the porosity in SFL 5 is filled with air (unsaturated) or filled with water (saturated).

Table A4-1 Material data used in the heat generation calculations for SFL 5.

		Volume per metre vault (m^3/m)	Density (kg/$m^{3)}$	Heat capacity (kJ/kg,K)	Specific heat content per metre, CAPT (kJ/K,m)
Waste -	steel	4	7800	0.46	$1.32 \cdot 10^4$
	water	14	1000	4.2	$5.77 \cdot 10^4$
	air	14	1.3	1.0	18.2
Concrete		108	2400	1	$2.58 \cdot 10^5$
Gravel -	rock	128	2700	0.8	$2.76 \cdot 10^5$
	water	55	1000	4.2	$2.30 \cdot 10^5$
	air	55	1.3	1.0	71.2
Rock		2388	2700	0.8	$5.16 \cdot 10^6$
Total saturated					$5.99 \cdot 10^6$
Total unsaturated					$5.70 \cdot 10^6$

Table A4-2 Radionuclide data used in the heat generation calculations for SFL 5.

Radionuclide	Half-life (yr)	Decay constant (yr^{-1})	Activity (Bq)	Alpha (MeV)	Beta (MeV)	Gamma (MeV)
Co-60	5.3	0.132	$8.1 \cdot 10^{15}$	0	0.0965	2.5
Ni-63	96	$7.22 \cdot 10^{-3}$	$1.2 \cdot 10^{17}$	0	0.0171	0

3 Results

The calculations show that the increase in average temperature in the repository and 20 m out in the rock is 2.3˚C after 100 years if saturated conditions prevail and when Co-60 and Ni-63 are considered as the source for the heat generation. If the repository is not yet saturated the calculations show a negligibly higher temperature increase, 2.4˚C, after 100 years. Compared to the earlier design both the heat generation and the specific heat of the system are higher. Since both of them are higher they cancel each other out and the resulting temperature increase is about the same.

This type of calculation does not give any information on how the temperature increase is distributed within the system, since it assumes that the heat transport in the system is fast. A comparison of the dimensions of the earlier design and the new design shows that the new system is larger. The rock volume that can be accounted for is larger, since the distance between the caverns is larger in the new design, 40 m compared to 24 m. The earlier calculations show that the heat transport is fast enough to level out the temperature in that system (Lindgren and Pers, 1995). Based on this and the fact that the design differences are rather small this should also be valid for the new system. Consequently, the increase in temperature inside the waste should be negligibly higher than the average temperature in the repository and surrounding rock.

The heat generation in the other two repository parts, SFL 3 and SFL 4, are about 10 % of the heat generation in SFL 5 and hence the influence from them is negligible.

The conclusions is that the increase in temperature is small and the influence on the long-term properties of the barriers and the water flow is negligible and does not need to be considered in the radionuclide transport calculations.

References

Lindgren M and Pers K, 1995. Radionuclide release from the near-field of SFL 3-5. A preliminary study. SKB AR 94-54, Swedish Nuclear Fuel and Waste Management Co.

Wiborgh M (editor), 1995. Prestudy of final disposal of long-lived low and intermediate level waste. SKB Technical Report 95-03. Swedish Nuclear Fuel and Waste Management Co.